uOttawa

L'Université canadienne
Canada's university

FACULTÉ DES ÉTUDES SUPÉRIEURES ET POSTOCTORALES

uOttawa

L'Université canadienne
Canada's university

FACULTY OF GRADUATE AND POSDOCTORAL STUDIES

Lukxmi Balathasan

AUTEUR DE LA THÈSE / AUTHOR OF THESIS

M.Sc. (Microbiology and Immunology)

GRADE / DEGREE

Department of Microbiology and Immunology

FACULTÉ, ÉCOLE, DÉPARTEMENT / FACULTY, SCHOOL, DEPARTMENT

Characterizing the CNS Protection Induced by Systemic Administration of the Oncolytic Mutant Virus ΔM51-VSV

TITRE DE LA THÈSE / TITLE OF THESIS

Dr. Robert Korneluk

DIRECTEUR (DIRECTRICE) DE LA THÈSE / THESIS SUPERVISOR

Dr. David Stojdl

CO-DIRECTEUR (CO-DIRECTRICE) DE LA THÈSE / THESIS CO-SUPERVISOR

EXAMINATEURS (EXAMINATRICES) DE LA THÈSE / THESIS EXAMINERS

Dr. E. Brown

Dr. S. Sad

Gary W. Slater

Le Doyen de la Faculté des études supérieures et postdoctorales / Dean of the Faculty of Graduate and Postdoctoral Studies

Characterizing the CNS protection induced by systemic administration of the oncolytic mutant virus ΔM51-VSV

By

Lukxmi Balathasan

A thesis submitted in partial fulfillment of the
requirements for the degree of Masters of Science

University of Ottawa

Faculty of Medicine

September 21, 2006

Your file Votre référence
ISBN: 978-0-494-25742-5
Our file Notre référence
ISBN: 978-0-494-25742-5

Characterizing the CNS Protection induced by systemic administration of the oncolytic mutant virus ΔM51-VSV

By

Lukxmi Balathasan

Chairpersons of the Supervisory Committee: Dr Robert G Korneluk[1] and Dr. David F Stojdl[2]
[1]Professor, Department of Biochemistry, Microbiology and Immunology, University of Ottawa
[2]Adjunct Professor, Department of Paediatrics, University of Ottawa

ABSTRACT

Direct brain infection with VSV in mice, including the attenuated ΔM51 strain, results in widespread viral replication, leading to irreversible and often fatal damage. When ΔM51-VSV is administered i.v., a trace amount of the virus is found within the brain, but is eventually cleared leaving the animal physically undamaged. In response to a peripheral infection, it seems that the host is able to mount an antiviral state in the CNS. Here, I show that by "priming" the host with mutant VSV prior to direct injection of VSV into the CNS, the host is able to send "warnings" in the form of cellular messengers and/or chemical signals preparing the brain to protect itself by any means possible against VSV. I used *in vivo* imaging techniques coupled with direct labelling of brain tissue sections to assess the effects of priming and CNS protection. My experiments indicate that priming mice with the interferon inducing mutant VSV, ΔM51-VSV, is in fact CNS protective. Priming limits VSV spread in the brain not by preventing infection of neurons, but by rapid induction of apoptosis in either infected cells or cells neighbouring areas of active infection. Further investigation into the factor(s) or mechanism(s) mediating viral clearance and CNS protection indicates that the innate immune system is able to control and clear ΔM51-VSV from the CNS before an adaptive response is required.

DEDICATION

To Amma, Appa and Sauce for their continued love and support

ACKNOWLEDGMENTS

First, I would like to acknowledge my department supervisor Dr. Robert G Korneluk and my research supervisor Dr. David F Stojdl for giving me the opportunity to be a part of an amazing project and for their encouragement and guidance. I would like to thank my Thesis Advisory Committee; Dr. Steffany Bennett and Dr. Jonathan Angel for their support and constructive feedback. For their technical assistance in performing all the tail vein animal injections, I would like to thank Jennifer Sparling and Teresa Falls. To my past and current lab mates, Micale Prevost and Waigin Fong, I thank you for your patience, advice and much appreciated company. From The Apoptosis Research Centre (ARC), I would like to thank all staff and students for making this an enjoyable experience. I would especially like to thank Dr. Peter Liston and Dr. Herman Cheung for their motivation, guidance and most of all, humour. I am most grateful to all those friends I have made outside my "lab" life who have collectively made the past two years a memorable and cherished journey. For my amazing friend Sonia, who always believed in me and kept me motivated. Bina, Priya and Janine, I don't think I would have made it this far without you guys in my life. Thank you.

TABLE OF CONTENTS

List of Figures

List of Tables

List of Abbreviations

BBB: blood brain barrier

CNS: central nervous system

CSF: cerebrospinal fluid

CTL: cytotoxic T lymphocyte

DC: dendritic cell

dsRNA: double stranded ribonucleic acid

EC50: Effective concentration that is required for 50% desired effect

ELISA: enzyme-linked immunosorbent assay

FLuc: Firefly luciferase

G-CSF: Granulocyte colony stimulating factor

GFP: green fluorescent protein

GM-CSF: Granulocyte macrophage colony stimulating factor

HLP: hind limb paralysis

i.c.: intra-cranial

ICAM-1: Intra cellular adhesion molecule -1

IFN: Interferon

IL: Interleukin

i.n..: intra-nasal

i.p.: intra-peritoneal

i.v.: intra-venous

IVIS: *in vivo* imaging system

kb: kilo base-pairs

LIF: Leukemia inhibitory factor

LPS: Lipopolysaccharide

MCP-1: Monocyte chemotactic protein-1

M-CSF: Macrophage colony stimulating factor

MHC: Major histocompatibility complex

mRNA: messenger ribonucleic acid

NGF: Nerve growth factor

NMDA: N-methyl-D-aspartatic acid

NO: Nitric oxide

NOS: Nitric oxide synthase

OB: olfactory bulb

PBS: phosphate buffered saline

PDGF: Platelet derived growth factor

PFA: paraformaldehyde

Pfu: plaque forming units

PKR: Protein kinase RNA

PS: phosphatidylserine

Reovirus: Respiratory enteric orphan virus

RNA: ribonucleic acid

ROI: region of interest

SDF-1: Stromal derived factor -1

sub-cu.: sub-cutaneous

TGF: Tumour growth factor

TNF: Tumour necrosis factor

TUNEL: TdT (terminal deoxynucleotidyl transferase)-mediated dUTP nick end labeling

UV: ultra-violet

WT: wild-type

VSV: Vesicular stomatitis virus

CHAPTER 1: INTRODUCTION

1.1 Vesicular Stomatitis Virus (VSV)

Vesicular stomatitis virus (VSV) is an arthropod borne insect virus belonging to the Rhabdoviridae family of viruses under the genus, Vesiculovirus [1]. Thus far, 28 Vesiculoviruses have been discovered that infect vertebrates and invertebrates, including two serotypes of VSV, VSV Indiana and VSV New Jersey [1, 2]. In animals, especially livestock, VSV causes a self-limiting disease characterized by ulceration of the tongue, oral tissues, feet, and teats [3]. VSV is highly cytopathic and can illicit a strong humoral and cellular immune response. In most cases animals recovered from infection [2, 4]. In man, VSV infection causes a temporarily distressing disease characterized by mild flu-like symptoms and only one case of viral induced encephalitis has been reported in a young boy [2]. VSV infections have been endemic in southeastern United States and northern South America in the agriculture population and still remain problematic [5].

VSV carries an 11kb single-stranded negative sense RNA genome that encodes five viral proteins: nucleocapsid (N), phosphoprotein (P), matrix (M), glycoprotein (G), and polymerase or "large" protein (L) [9] (*Figure 1.1*). VSV infects its host by using the G protein to bind phosphatidylserine (PS) molecules found on the host cell's outer membrane and makes its way into the cell via endosome mediated entry [6, 8]. The low pH environment within the endosome mediates viral release into the cytoplasm where viral transcription and replication occurs. The viral polymerase, composed of the L and P proteins and host factors, produces a 47 nucleotide leader RNA sequence along with five monocistronic mRNAs that correspond to the five viral proteins [9, 10]. The N protein is responsible for coating and protecting the viral genome, while the G protein

coats the outer membrane of the bullet-shaped capsule encasing the viral genome. The M protein mediates interaction between the nucleocapsids and the cytoplasmic tails of the G protein molecules. The M protein is also fundamental for cytopathology. It is involved in host gene-expression shut-off thereby allowing viral genes to be expressed and translated. Furthermore, this prevents host action against VSV because the host can no longer express proteins that counteract viral infection, the most important of which is the cytokine interferon (IFN). IFN is the first line of host defence against VSV. Therefore, virus mediated host shut down not only exclusively allows for viral replication, it allows the virus to further spread and infect. The M protein prevents host gene expression through several mechanisms including interfering with host polymerases [11], inhibiting nuclear export of host mRNAs [12] and by inhibiting host translation [13, 14]. This quickly leads to the induction of caspase-dependent cell death (apoptosis) [15]. The M protein also assists in the breakdown of the cytoskeleton as part of the apoptotic process [16]. These events lead to rapid tissue destruction and allow viral progeny to be released into the extra-cellular environment.

Figure 1.1: Schematic representation of VSV particles and genomic organization

The bullet-shaped virion encompasses an 11 kb negative sense RNA genome which codes for five viral products. The diagram of the VSV genome depicts the non-transcribed leader (l), and five consecutively transcribed mRNAs blocks. Gene order dictates the quantity of each protein produced with N being made most abundantly. Each letter refers to the proteins and numbers below each block represents the lengths in nucleotides of the genes. Adapted from J. Patterson

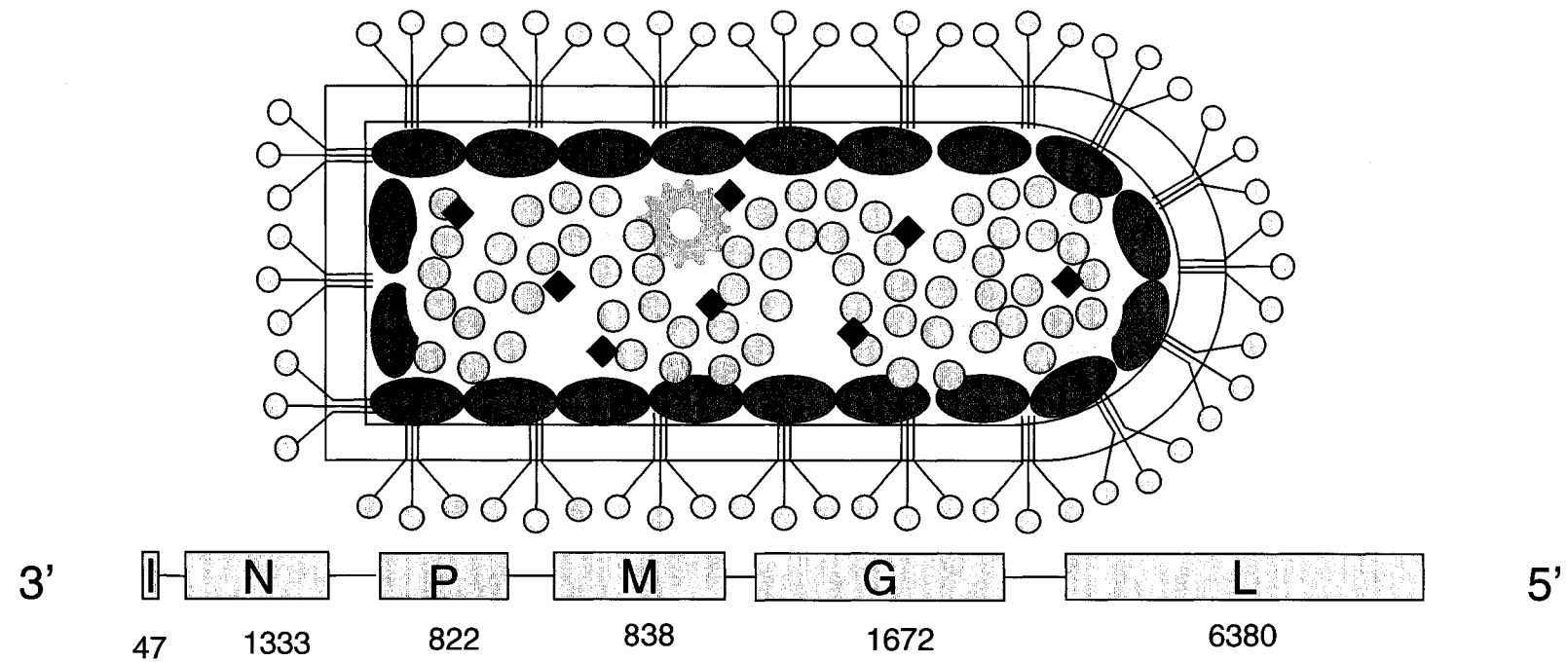
3'
I
N
P
M
G
L
5'
47
1333
822
838
1672
6380
11 kb (-) sense RNA
Polymerase (L)
Glycoprotein (G)
Phosphoprotein (P)
Nucleocapsid (N)
Matrix Protein (M)

1.2 VSV and Neurotropism

Experimental VSV infections in murine models have been studied extensively in order to understand host-virus relationships. Infections in neonatal mice are generally fatal. However, in adult mice the disease depends not only on the type of Vesiculovirus, but also on dose and route of infection [17, 18]. Systemic low grade VSV infection is limited by the host immune system and the virus is eventually cleared, leaving the host intact. However, VSV has been shown to be neurotropic when the virus enters the central nervous system (CNS) [19]and systemic delivery can lead to infection of specific sites in the brain if the immune system fails to clear the virus [20, 21]. *Sabin* had initially characterized VSV infection of the CNS and had reported that upon intra-nasal (i.n.) instillation, this virus invades the CNS along the olfactory pathway. Initial infection of the olfactory receptor neurons, if not cleared by host mechanisms, results in subsequent spread of VSV into the olfactory bulb (OB) and caudally through periglomerular and granule cells to the ventricluar zone [19, 20]. VSV spreads deeply into the CNS via mature olfactory neurons but can also infect basal cells and other non-neuronal cells. VSV is thus able to use trans-neuronal, non-neuronal and cerebrospinal fluid (CSF) routes for entry and spread [20, 21]. The i.n. infection results in encephalitis, ventriculitis, and total overt necrosis of grey matter leading to hind limb paralysis (HLP) between 6-8 days post-infection followed by death [19, 20, 22].

1.3 VSV: A Naturally Occurring Oncolytic Virus

VSV is an important virus for science and many crucial observations made in immunology and virology are credited to information obtained by studying this virus. It is in fact used as the standard virus when titrating IFN levels due to its exquisite sensitivity to IFN [52]. Much of the research carried out by others has thus far focused on using VSV for vaccine development. However, our group and others are interested in the potential use of VSV as a cancer therapeutic.

When viruses infect their host organism, the host responds by activating its defensive mechanisms to protect itself from uncontrolled viral infection. Tumour cell types generally lack the ability to produce or respond to such protective mechanisms since these anti-viral factors are often accompanied by anti-proliferative properties. Oncolytic viruses are defined as those viruses that infect and replicate preferentially in cancer cells specifically, leaving the normal cells unaffected [53]. These viruses take advantage of the defects in the antiviral responses of tumour cell types thereby causing widespread destruction of the tumour. Defects in the ability to produce or respond to IFN are a frequent finding in a vast array of transformed cell types [54]. IFN not only has anti-viral properties, but it is also pro-apoptotic as well as anti-proliferative – two factors that are not conducive to tumour formation and survival. Therefore, many tumour cell lines have evolved defects in their IFN signalling pathway allowing them to grow and spread unchecked (*Table 1.2*). With a defective IFN system and thus lacking any anti-viral potential, these tumour types are a perfect niche for viruses to replicate unabated.

Being extremely sensitive to the antiviral effects of IFN makes VSV a naturally occurring oncolytic virus. Armed with this knowledge, preliminary studies have shown that VSV-Indiana, while relatively non-infectious in normal cell types, replicates freely in tumour cell lines [53, 55]. Any replication taking place in normal cells can be prevented by pre-treatment with exogenous IFN. *In*

vivo testing with human xenograft tumour models in thymus deficient nude mice also shows VSV to be a highly selective and effective killer of tumours. Although defects in nude mice are known to make them more susceptible to VSV, pre-treatment of tumour bearing nude mice with IFN, allowed for selective killing of the cancerous mass while enabling the mice to survive [55].

Taking the natural backbone of a virus with oncolytic potential and manipulating its simple genome enables us to engineer superior viruses with a greater therapeutic window. Improving the therapeutic window involves providing better tumour killing potential yet maintaining the non-permissive character of normal cells. Naturally occurring mutants of VSV exist and are not only effective oncolytic agents, but also potent inducers of IFN [56, 57]. The AV1 mutant has a single amino acid switch at position 51 (methionine to arginine – M51R), while the AV2 mutant has two amino acid substitutions (V221F and S226R). Mutations of the M protein prevents viral mediated shut-down of host mRNA, therefore allowing the cell to initiate an antiviral response and protect surrounding uninfected cells. Both of these mutant viruses can be delivered at higher doses *in vivo* to specifically target cancer cells while leaving host cells intact without the need for exogenous IFN treatment. To account for potentially lethal revertants, a genetically engineered version of AV1, termed AV3 was constructed by deleting the amino acid at position 51 of the M protein. AV3 (more commonly referred to as ΔM51) has subsequently been shown to be a safe yet efficacious oncolytic virus *in vitro* as well as *in vivo* against a vast panel of tumour cell lines [56].

Table 1.1: The majority of cell lines in the NCI 60 panel show defects in IFN signalling

Cell lines of commonly occurring cancers from the NCI 60 panel were tested for their ability to respond to either IFN-α or IFN-β pre-treatment. Cell lines were deemed unresponsive if IFN pre-treatment was unable to significantly affect (< 10 fold) the EC50 of cells infected with WT VSV (Indiana serotype) for 48h. Data courtesy of J. Bell Laboratory.

Table 1.2

Cancer Cell Line	Type 1 IFN Defects
Leukemia	100%
NSC Lung	71%
Colon Cancer	100%
CNS	75%
Melanoma	85%
Ovarian Carcinoma	67%
Renal Carcinoma	75%
Prostate	100%
Breast	60%

1.4 VSV and Brain Cancers

The therapeutic potential of VSV in treating many forms of cancer in the periphery is highly promising. However problems arise when attempting to use VSV to treat cancers of the brain. Primary brain tumours, defined as cancers originating in the CNS, account for 1.5 percent of all cancers in the US adult population but can be as high as 20-25 percent in the paediatric population [58]. Individuals with benign forms of brain tumours can survive for several years but in cases such as glioblastoma multiforme, the most aggressive type of primary astrocytoma, the survival time is limited to a few months [59, 60]. Therapeutic options for primary tumours are currently limited to surgical removal of as much of the mass as possible, followed by radiation or chemotherapy. In most instances recurrence of the tumour is likely due to residual cancer cells after surgery. Metastatic brain cancer is defined by cancerous cells from the periphery that make their way into the CNS and are more prevalent than primary tumours. Furthermore, metastatic brain disease is generally more difficult to control and treat. Given the frequency and prognosis of brain cancers, there is clearly a great need for a better therapeutic intervention and the use of oncolytic viruses might prove to be a useful tool.

In vitro experiments using ΔM51-VSV have shown its capability in infecting and killing a wide range of brain tumour cell lines [62]. Whitt's group has also shown that in organotypic brain tissue slice – glioma co-cultures, VSV replicates well in the glioma but however does cause some damage to normal neurons [61]. *In vivo*, our group in collaboration with others had shown that ΔM51-VSV was capable of targeting human gliomas implanted in the brains of nude mice. A green fluorescent protein (GFP) expressing recombinant ΔM51-VSV delivered i.v. was able to reach the site of the primary tumour as well as smaller metastatic sites as seen by GFP expression in these tumour cells. Normal brain tissue appears to have been unaffected, since no detectable

GFP signal was found when brains were examined post-mortem (unpublished data). Although systemic administration of ΔM51-VSV was capable of selective replication in the glioma, only 25 percent of all treated mice were cured of their disease. The fatality seen here was not due to the neuropathogenic nature of VSV but a result of inefficient viral delivery to the tumour, allowing for continued tumour expansion. In hopes of attaining maximal virus replication in the tumour, we attempted local delivery of virus via intra-cranial injection (i.c.). However, i.c. injection results in complete fatality (unpublished results). Even in immunocompetent, cancer-free Balb/c mice, low doses of ΔM51-VSV (<100 pfu) injected into the brain results in viral induced pathology that manifests itself as hind limb paralysis. The IFN-inducing mutant VSV still targets neurons but only when delivered directly to the brain. However, indirect delivery of virus to the brain via the circulatory system is able to set-up an antiviral state in the brain prior to the appearance of VSV in the CNS. A system is in place that this mutant virus is not able to shut down which signals to the CNS when virus is first detected in the periphery. The local immune response is then triggered in the CNS, which prepares it to combat a potential viral attack and effectively limits ΔM51-VSV infection of normal brain tissue. VSV that encodes wild-type (wt) M protein blocks this response and thus does not possess this therapeutic window.

1.5 Host Defense against VSV

The host defense against VSV has been examined *in vitro* and in experimental *in vivo* infections and is attributed to both the innate and adaptive arms of the immune system. Infections outside of the CNS in immunocompetent mice generally do not equate to disease and the host is able to mount a robust and long-lasting immunity. The host response starts with rapid virus-induced type 1 interferon (IFN) production, leading then to a specific cytotoxic T-lymphocyte

(CTL) response and antibody production. When a systemic infection finds its way into the CNS, or due to direct i.n. inoculation, most of the infected animals will succumb due to VSV-induced encephalitis. Mortality is seen in immunocompromised mice lacking T-cells (nude), B-cells or type I IFN regardless of route of infection (*Table 1.1*).

1.5.1 Interferon

Interferon, an inducible cytokine, belongs to a multigene family and is the first line of defence against VSV. Initially characterized as an antiviral protein, IFN is now known to have a plethora of effects including regulation of cell growth, differentiation, apoptosis and modulation of the immune response against a pathogen [25]. There are two types of IFN: "antiviral" or type I IFN and "immune" or type II IFN. IFN-α, IFN-β and the lesser known IFN-ω are classified as type I IFN. IFN-α is produced by all leukocytes while IFN-β is produced by fibroblasts. Type 2 IFN consists of IFN-γ and is produced by natural killer (NK) cells, CD4+ T helper 1 cells (Th1), and CD8+ cytotoxic T suppressor cells [23, 24]. Type I IFN is a key component of host innate defences, whereas type II IFN-γ plays a role in both innate and adaptive immunity. RNA viruses, such as VSV, trigger the IFN response when cells detect double-stranded RNA (dsRNA). Production of IFN turns on a cascade of events that stimulate the production of IFN-inducible proteins within the infected cell and in surrounding cells (reviewed in [25]). The subsequent antiviral protein systems stimulated by IFN act to limit and clear the viral infection by various means including mRNA translation inhibition, RNA degradation and/or editing and induction of cell death. Since virtually all viruses trigger the IFN response upon infection, many have evolved mechanisms that evade this antiviral response. Such is the case with the M protein coded by VSV which prevents nuclear export of host mRNA resulting in general shut-off of host gene-expression.

Table 1.2: Outcome of VSV i.n. infection in various strains of wild-type and immune deficient mice

Outcome of VSV-Indiana infection in different strains of wild-type mice and mice with genetic defects in specific immune responses have been characterized. I.n. infection of wild-type mice is lethal half of the time but is completely fatal in mice that lack T-cells (nude), B-cells or both (SCID) and in mice that lack a functional Type I IFN receptor. Adapted from [21]

Table 1.2

Mouse strain	Defect(s)	Outcome of infection (percent survival)
Balb/c	None	50%
C57BL/6	None	50%
A/J	complement	0%
GKO	IFN-γ	50%
NOS-1 -/-	Neuronal NO	25%
NOS-3 -/-	Endothelial cell NO	50%
Nude	T cells	0%
SCID	Tcells + B cells	0%
Type I IFN -/-	IFN-α, β	0%
B-cell deficient	B-cells	0%

Spread of VSV infections *in vitro* is arrested by IFN-mediated antiviral activity. *In vitro*, freshly harvested mouse peritoneal macrophages have been shown to be resistant to VSV infection due to the presence of low levels of IFN [26, 27]. This protection can be transferred to other cells lines grown on top of these macrophages [28]. Longer times in culture render these macrophage cultures susceptible to VSV due to loss of endogenous IFN. *In vivo*, IFNα/β receptor knock-out mice quickly succumb to a systemic VSV infection indicating that type 1 IFNs are essential for host survival [29]. *Stojdl et al* have also shown the importance of the Protein Kinase RNA (PKR) antiviral system in limiting VSV infection [30]. IFN produced by infected cells is able to exert its effects on surrounding cells to prepare surrounding uninfected cells for viral infection by inducing large amounts of the antiviral PKR. PKR inhibits translation initiation within the cell through the phosphorylation of protein synthesis initiation factor eIF-2α upon stimulation by dsRNA [31]. This leads to inhibition of viral replication within the infected cell.

Although these observations suggest that type I IFN is critical for host recovery from peripheral VSV infections, IFN does not seem to be sufficient for protection against CNS infections. Treatment of immunocompetent mice with exogenous type I IFN results in increased survival or a delay in pathological outcome compared to untreated, VSV infected mice [32, 33]. Outcome slightly improved when mice were treated with polyriboinosinic polyribocytidylic acid (poly(I:C)), a synthetic polymer that resembles double stranded RNA and is used to stimulate the immune system to produce IFN. This stimulation of macrophages to induce IFN endogenously increased protection from VSV induced CNS pathology but over half of the animals still succumbed to virus induced encephalitis [32, 34]. In separate experiments, macrophage depletion studies indicate that elimination of certain subsets of macrophages renders these mice permissive to VSV infection even when high titres of IFN are present [35]. Therefore, with infections of the CNS, even with an intact IFN system, half of the experimentally infected animals will succumb to

the virus. Although type II IFN (IFN-γ) may be important in limiting peripheral infections, it is not essential for protection against neuronal infection[36-38]. As with many host responses to a pathogen, it seems likely that the IFN antiviral response is not the only participant in eliciting protection against VSV in the CNS and is likely part of a co-operative effect.

1.5.2 Nitric Oxide Synthases (NOS) and Nitric Oxide (NO)

Nitric oxide synthases (NOS) are a group of enzymes that convert L-arginine into nitric oxide (NO) and citrulline [39]. NO is an important biological signalling molecule and plays a role in a variety of biological functions including neurotransmission, vessel dilation and the antiviral response. Small amounts of NO are constitutively expressed by neurons through NOS-1 and endothelial cells via NOS-3. Much greater amounts can be produced by inducible NOS (iNOS/NOS-2). iNOS is expressed by many cells in the periphery including macrophages, and in the CNS by activated astrocytes and microglia [40, 41]. These cell types produce NO upon stimulation with lipopolysaccharide (LPS), IFN-γ or tumour necrosis factor α (TNF-α) [40]. NO is an important part of innate immunity in the CNS and has been shown to inhibit VSV *in vitro*. Pretreatment of NBH1A3 neuroblastoma cell lines before VSV infection with S-nitrosyl-acetylpenicillamine (SNAP), a NO donor or N-methyl-D-aspartate (NMDA), an activator of NOS, increases cell survival [42]. The protective effect of NMDA was reversed by treatment of the cell line with the competitive NOS inhibitor NG-monomethyl-L-arginine (L-NMMA) but not by pre-treatment with haemoglobin, a NO binding protein. Since NMDA is able to diffuse into the cell whereas haemoglobin cannot, the protective response is most likely taking place within the NO producing cell.

In vivo, iNOS is seen 3 days after an i.n. infection with VSV in the OB and in the hippocampus by day 4. The majority of NO is produced by microglial cells and is concentrated

around areas of VSV infection [42]. Knock-out studies in mice for each type of NOS have shown that NOS-1 production of NO is important for surviving i.n. infection with VSV while NOS-2 synthesized NO further exasperated the pathological effects [43]. Thus far, NO produced via NOS-1 within neurons is hypothesized to be the most important factor of CNS innate immunity against VSV infection of neurons and may lead to non-cytolytic clearance.

1.5.3 Apoptosis

Apoptosis is an active, gene dependent program of cell death [44]. It is a carefully orchestrated biological process that is necessary to maintain homeostasis within an organism. Too much cell death can lead to host malfunction while too little results in cancerous cell growth. Apoptotic cells detach from surrounding cells and contain a compact shrunken cytoplasm and nucleus. The chromatin condenses and is marginalized to the periphery of the nuclear membrane and the DNA gets cleaved into regular fragments at late stages. The cell shrinks, with the plasma membrane forming blebs. These little vesicles or apoptotic bodies are cleared by scavenger cells by phagocytosis and do not trigger an inflammatory response.

VSV is known to trigger apoptosis and two mechanisms have been characterized. One mechanism is solely dependent on the inhibition of host gene transcription mediated by the M protein and occurs through the intrinsic caspase-dependent apoptotic pathway that is associated with the mitochondria [15, 16, 45]. The other mechanism involves a pathway distinct from the first, and is attributed to other viral proteins not yet determined. This second mechanism is hypothesized to act via the extrinsic death receptor mediated pathway and is a characteristic of the AV1 mutant strain of VSV [15, 46]. This mutant is replication competent but in certain cell types shows slower kinetics of apoptosis induction. As previously mentioned, the AV1 mutation prevents VSV M

protein form shutting down host gene expression and therefore allows IFN to be expressed by the host. The extrinsic apoptotic pathway is typically activated when IFN is induced by dsRNA [46].

In vivo, neurological damage has been attributed to the induction of apoptosis by either direct or indirect mechanisms [47-49]. *In situ* hybridization and terminal transferase dUTP nick end labelling (TUNEL) studies looking at VSV infected and apoptotic cells in the CNS show that in certain areas such as the brain stem, the extent of the VSV RNA positive area is equivalent to the amount of apoptosis detected by TUNEL. In other areas, there is considerably more cells infected with VSV than apoptotic cells. This may be due to the difference in susceptibility of neurons, glial cells and inflammatory cells to the effects of infection and apoptosis [49]. In general, the majority of CNS cells are not double labelled for VSV RNA and apoptosis suggesting that uninfected cells either die due to a cytokine-dependent pathway induced by inflammatory cells. Alternatively, TUNEL positive apoptotic cells may have already degraded or altered cytoplasmic viral RNA, are therefore, underestimated by experimental methods [49].

1.5.4 Adaptive Immune response

Although the type 1 IFN response is required to prevent an active and robust viral replication in the periphery [29], the absence of a functional adaptive immune response can also allow VSV to reach the CNS [50, 51]. Experiments in which splenic cell populations are transferred to nude mice indicate that cell mediated immunity is not sufficient to prevent VSV spread to the CNS and subsequent death [38, 51]. Immune serum harvested from mice infected with VSV for 5 days contains neutralizing IgM antibodies. Transfer of this day 5 serum delays the onset of disease progression in B-cell deficient mice but is still fatal. However, day 14 serum containing neutralizing IgG antibodies significantly improves survival [38]. The IgM antibody response to VSV is T-cell independent. IgM is able to delay the spread of VSV to the brain but an IgG response is

needed for effective control and prevention of spread to the CNS. Thus a delay in the onset of morbidity only requires B-cell production of antibodies, but long term survival depends on the interaction of B-cells with CD4+ T helper cells [38].

1.6 The CNS response to Viral Infections

The CNS consists of the lepto-meninges, brain and spinal cord and is anatomically well protected. It is comprised of highly complex tissue whose demise is detrimental to the host. The cell types found within this protected area are the neurons and the neuroglia. Neurons are non-dividing terminally differentiated cells and are the structural and functional units of the nervous tissue. Neurons consist of a cell body (soma) with extended processes (axons and dendrites) used to perform sophisticated functions such as conduction of electrical signals and to communicate with each other and their surroundings through synaptic connections. The non-neuronal supporting cells of the CNS are collectively called neuroglia and include oligodendrocytes, astrocytes, microglia, and ependymal cells. Oligodendrocytes are found in grey and white matter. They function to form the myelin sheaths around multiple axons. Microglia are also found in both grey and white matter regions of the CNS and are the main phagocytic cell population. In response to tissue damage, these cells migrate to the site, proliferate, and become reactive in order to phagocytose dead or foreign tissue. Astrocytes are found attached to capillary endothelial cells and neurons and support metabolic exchange between the two. Ependymal cells are special epithelial cells that line the ventricles of the brain and the central canal of the spinal cord. Ependymal cells contain cilia that assist in CSF movement throughout the CNS. The CSF is a clear colourless fluid that bathes the brain and spinal cord not only to cushion and protect against

physical injuries but also provides an optimal chemical environment for neuronal function. Small vascular cells covered by epithelium called the choroids plexus, extend into the ventricles and secrete CSF continuously in the lateral, third and fourth ventricles.

The CNS is isolated from the rest of the host by the blood-brain barrier (BBB) and the brain-CSF barrier. The BBB is made of tightly joined endothelial cells surrounded by astrocyte foot processes and the basal lamina while the CSF barrier is found at the choroids plexus and consists of endothelium with fenestrations and tightly joined choroid plexus epithelial cells. Even with this tight seal, microbes are still able to find ways into the CNS mainly though blood vessels, nerves and local invasions through sinuses. Penetration of the BBB or brain-CSF barrier occurs when microbes infect cells that make up the barrier, by passive transport in intracellular vacuoles, or can be carried across by infected white blood cells. Blood-borne invasion across the BBB results in encephalitis while across the CSF barrier results in meningitis.

1.6.1 *Local Immune Response in the CNS*

Microglia, the resident macrophages found throughout the CNS are the first cell type to respond to a variety of CNS injuries [75]. When the BBB is compromised during encephalitis, this allows for an increase in microglia from blood-borne monocytes [76]. Astrocytes and other cells of the BBB produce the chemokine monocyte chemoattractant protein (MCP-1) in the parenchyma that directs the migration of monocytes to the brain [77, 78]. Once inside the CNS, the monocytes quickly take on microglia like properties [76]. In the normal brain, microglia are in a resting state and are referred to as ramified microglia and possess many processes. In the injured brain, the processes retract, the cells increase in volume and become reactive microglia. These activated microglia do not always act as phagocytes. This role is only possessed when cell death occurs and microglia are needed to engulf and dispose of the dead cell and residual debris.

Microglia only acquire antigen presenting qualities once the brain is in a state of pathology. CD200 expression by neurons suppresses microglia from becoming antigen presenting cells (APCs), but maturation of microglia occurs upon stimulation by certain cytokines (GM-CSF, IFN-γ) and co-stimulatory signals [79]. Therefore, activation of microglia involves up-regulation of MHC class II antigens, converting them into antigen-presenting cells capable of releasing a slew of potential neurotoxins, including NO, superoxide, platelet activating factor (PAF), pro-inflammatory cytokines and cysteine [80]. Activation is amplified by the autocrine effects of TNF-α and at later stages by IFN-γ which is released by activated lymphocytes [81]. This inflammatory response is also amplified by cytokines secreted by activated microglia and some have neurotoxic potential. On the other hand, microglia can also produce neuroprotective factors and cytokines. The response depends on the type on injury and the signals emitted from injured neurons or activated astrocytes.

1.6.1.a Local Cytokine Response

Although there is not the same breadth of knowledge about CNS cells and the soluble factors they secrete and respond to, it is becoming increasingly clear that soluble factors have important implications for viral infections in the CNS. Cytokines mediate communication between cells of the peripheral immune system and CNS immune cells allowing them to work in concert to defend the host against a pathogen (*Figure 1.2*). Infected cells, CNS immune cells and infiltrating lymphomononuclear cells can secrete cytokines within the CNS to act on surrounding brain tissue as well as the cells of the immune system [82]. As with cell-mediated immunity, cytokines can be a double-edged sword. They are important factors in stimulating humoural and cell-mediated responses leading to host antiviral immune responses but in many instances propagate CNS pathogenesis instigated by infection. Cytokines induce antiviral proteins such as

Mx and up regulate cell surface molecules like MHC antigens [82]. The early presence of the immunoregulatory molecule, MHC II, on astrocytes and microglial cells due to infection function in protection but can also lead to pathology and disease when MHC II is expressed days or weeks post infection [83]. MHC I expression is usually absent or expressed at low levels on neurons but can be up-regulated in order for efficient cell-mediated defence against brain pathogens.

Interferon

As described previously, the IFN family of cytokines is usually the first line of defence against viral infections. Although IFN made in the periphery can diffuse into the CNS, local production of IFN within the CNS has been noted [84-86]. Receptors for both types of IFN are expressed by astrocytes, microglia and oligodendrocytes and they respond by inhibiting a pro-inflammatory cytokine response, inducing IL-10 as well as suppressing matrix metalloproteinases [87]. Type I IFNs have been detected in the brain and CSF of mammals during viral infections of the CNS and has been reported to be beneficial against neurotropic viruses. However, over-expression of Type I IFN has been shown to be detrimental due to inflammation and neurodegeneration [88]. More recently, it has become evident that infected neurons produce IFN-β in response to infection by some but not all viruses [84, 85]. IFN-β is preferentially produced locally in the CNS over IFN-α because IFN-β possesses neuroprotective roles while IFN-α may be neuro-toxic [68].

IFN-γ is predominantly pro-inflammatory in nature and is secreted by Th1 cells for Th1 mediated immune responses. IFN-γ does have a protective effect against neurotropic viruses, but can also produce detrimental effects including post-infection encephalitis and autoimmue diseases. IFN-γ expression in the brain leads to infiltration of NK, CD8+ T –cells and Th1 type T-cells and induces antimicrobial, cytotoxic, and antigen-presenting functions of microglia [29, 89].

Astrocytes and Schwann cells express MHC and adhesion molecules in response to IFN-γ[36]. Combined with the cytokines IL-1β and/or TNF, IFN-γ also induces the production of NO in these cells, which allows for killing of intracellular pathogens [90, 40]. Some CNS inflammatory inhibition properties are exhibited by IFN-γ due to the induction of apoptosis in encephalitogenic T cells and microglia [82].

Interleukin-10 (IL-10) belongs to the IFN family and is made in the CNS by astrocytes and microglia and these cells also carry the IL-10 receptor. IL-10 receptor is constitutively expressed in the brain and following infection the IL-10 protein is made by infiltrating monocytes/macrophage and resident cells [87]. In the CNS, stimulation of IL-10 promotes cell survival and has both an immunosuppressive and an anti-inflammatory role which act to inhibit expression of the pro-inflammatory cytokines TNF-α, IL-1β, IFN-γ, IL-6 and IL-12 [91]. By inhibiting expression of MHC II, CD40 and B7 expression on cells, IL-10 also inhibits the T-cell response within the CNS. Astrocyte expression of IL-10 prevents intracellular adhesion molecule (ICAM-1) and tumour necrosis factor alpha (TNF-α) expression and inhibits microglia from cytokine and chemokine expression [82, 92]. In addition, oligodendrocytes produce IL-10 to protect against LPS/IFN-γ induced cytotoxicity [91].

Other key cytokines and chemokines in the CNS

It is becoming increasingly evident that a rapid innate local response plays an important role in controlling brain infections. Studies with several neurotropic viruses indicate that specific cytokines/chemokines are quickly up-regulated in the CNS in response to infections. Thus far a number of soluble factors have been catalogued that are produced by local immune cells and by neurons. These factors can have both inflammatory and anti-inflammatory properties that serve to contain the infection or in some cases propagate viral induced destruction.

The IL family of cytokines have long been known to be important signalling molecules involved in the peripheral immune response and it is becoming increasingly evident that they are also critical in the CNS. IL-1α and IL-1β are considered to be master pro-inflammatory cytokines and are made predominately by macrophages and microglia. IL-1β is seen in many viral infections of the CNS and mediates the inflammatory response by inducing the expression of cell adhesion molecules and production of chemokines that recruit neutrophils, monocytes and macrophages [91]. The infiltration of these cell types exacerbates neuronal damage because they function to release noxious substances. Astrocytes and Schwann cells also express IL-1β in pathological conditions and can act on these cells alone or with the aid of TNF-α and IFN-γ to induce the expression of inflammatory genes and neurotrophic factors [93]. Microglia also produce IL-1ra, an IL-1 receptor antagonist that has anti-inflammatory functions and is neuroprotective [81].

The IL-6 receptor is expressed on neurons and astrocytes and expression increases in an inflammatory setting. Astrocytes secrete IL-6 during a viral infection and copious amounts are seen in culture [93]. After infection is detected in the CNS, IL-6 activates a quick pro-inflammatory response allowing the immune mediated clearance of virus and promotes leukocyte recruitment. The levels and source of IL-6 are critical in determining the outcome of infection. IL-6 produced by astrocytes results in CNS inflammation and neurodegeneration, but when expressed by neurons results in microgliosis and astrogliosis but does not cause neuronal damage [94]. IL-6 also possesses anti-inflammatory properties because it can act to inhibit other pro-inflammatory cytokines and induce the secretion of IL-1ra which acts to decrease inflammation [82].

The IL-12 family of cytokines (IL-12, 15, 18) helps develop both the innate and adaptive immune response and regulate IFN-γ production. Secretion of IL-12 in the brain by infiltrating macrophages and microglia favours inflammation and acts to recruit and activate T-cells [83]. Microglia also express the IL-12 receptor, which upon stimulation activates these cells to

produce NO [41]. The expression IL-15 receptor on microglia also stimulates the production of NO[41]. IL-18 mRNA is detected in the normal brain although it is predominately made by macrophages and DCs [91]. It induces IFN-γ and promotes IL-12 induced Th1 response and plays a role in the clearance of neurotropic viruses [68].

Along with the IL family of cytokines, several other families of soluble signalling molecules play a role in the CNS. The ones that have been studied in relation to viral infections of the CNS include the Colony Stimulating Factors (CSF), Transforming Growth Factors β family (TGF-β) and the Tumour Necrosis Factor (TNF) family. CSFs are haematopoietic cytokines and include IL-3, macrophage CSF (M-CSF), granulocyte macrophage CSF (GM-CSF), and granulocyte CSF (G-CSF). All of these are produced in the CNS and their common theme includes proliferation and activation of microglia [93]. TGF-β1, is the most studied member of the TGF-β family in relation to the nervous system. It is expressed by both neurons and glia and functions to regulate responses to injury and inflammation by modulating several activities including astrocyte proliferation, extracellular matrix synthesis, vascular changes, maintenance of macrophage, microglia activation and leukocyte recruitment to the CNS [91]. TGF-β1 is classified as a neurotrophic cytokine that suppresses apoptosis and is neuroprotective [95]. TGF-β1 acts on astrocytes to increase proliferation and activates them to increase production of IL-6, leukemia inhibitory factor (LIF), nerve growth factor (NGF), platelet derived growth factor (PDGF) and monocyte chemo-attractant protein-1(MCP-1/CCL2) [95]. Both TNF Family members, TNF-α and TNF-β (lymphotaxin) have pleotropic actions and are mainly secreted by activated macrophages and microglia. The receptors for these ligands (TNFR1, TNFR2) are co-expressed on neurons, glia and cerebrovascular endothelial cells. Both cytokines play a key role in the regulation of neuro-inflammation [93].

Chemokines, as the name suggests, are small proteins that direct the movement of nearby cells in accordance to environmental signals and are important mediators that connect the peripheral and CNS immune systems. They can be released by many different cell types and serve to guide leukocytes (monocytes and neutrophils) of the innate immune system and also the lymphocytes to sites of infection. Chemokines are made in the CNS by neurons and glia and all neurons express chemokine receptors [93]. Constitutive chemokines in the brain include stromal derived factor (SDF-1/CXCL12), and fractalkine/CX3CL1 [93]. MCP-1/CCL2 is made by astrocytes in response to a pathological condition and acts to recruit monocytes/macrophages into the brain during infection [96].

1.6.1b Apoptosis in the CNS

Effective elimination of the invading virus may sometimes only be achieved after host cell death. Apoptosis is an altruistic approach to infection in which the cell sacrifices itself for its neighbours in order to limit viral spread. Cell suicide can be an effective first line of defence against a viral infection in the periphery but cannot be applied to neurons due to the fact that they are virtually irreplaceable and vital to host survival. To prevent compromising the survival of the whole organism, it is preferable to have infected, live neurons than dead ones. Neurons are likely not programmed to trigger a suicide response since they lack expression of MHC I, preventing surveillance of infection and death induction by cytotoxic T-cells [66]. However, the consequence of neuronal resistance to cytotoxic T-cells is viral persistence, neuronal dysfunction and disease.

Experimental virus infection *in vivo* shows that in the developing rodent CNS, neurotropic viral infection results in widespread apoptosis [69]. In contrast to the developing brain, virally induced apoptosis of the mature CNS seems to depend on the virus strain and cell type [47, 48, 69-74]. As neurons mature and reach post-mitotic status, they increase their resistance to apoptosis

but this varies depending on the neuronal population because of distinct cell type expression pattern of regulatory proteins and their expression levels. OB neurons are formed late in development and are still renewed throughout adult life either as a need for neuronal plasticity or because the olfactory nerve has direct access to the CNS from the outside environment. Most natural CNS viral infections occur via the nasal passages and, therefore, the cells of the OB may remain susceptible to apoptosis in order to help prevent spread of the virus. Once access is gained past the OB, many viruses can still induce apoptosis in the adult brain as seen with the TE strain of Sindbis virus, F strain of Herpes Simplex Virus and with VSV [69]. Potentially, neuronal death may be due to the ability of the virus to overcome endogenous cell factors that keep the cell alive in order to allow the virus to spread or the infection exceeds the threshold needed to cause apoptosis.

1.6.2 *The Systemic Immune Response in the CNS*

Unlike systemic viral infections where tissue can be sacrificed and later replaced by stem cells, the CNS has a limited regeneration capacity, thus rendering neuronal populations essentially irreplaceable. Immune responses within the CNS are thus unique and distinct from those of the periphery. The CNS is an immune privileged site because induction of cell-mediated immunity is kept to a minimum. Lymphatic drainage is scarce, and there is a lack of constitutive major histocompatibility complex (MHC) expression [63]. Lack of class II and to a lesser extent even class I MHC expression ensures protection from the systemic immune system[93]. Activated T-cells enter the CNS to perform surveillance duties, but in the absence of a specific threat, T-cells leave the CNS or are induced to die [64-66]. Although the CNS contains its own immune system consisting of the macroglia that serve as antigen-presenting cells and immunomodulatory cells during CNS insult, in response to a viral insult, a local protective response is unlikely without the participation

of the peripheral immune system. The CNS does not have a proper lymphatic drainage system, but interstitial fluid and CSF proteins can make their way into the cervical lymph nodes, thereby connecting the CNS to the periphery [63]. When danger is detected in the CNS, the BBB is often compromised, allowing for an increase in leukocyte traffic. Antigen-specific immune response ensues and activated T-cells traffic into the CNS [65]. Antibody is produced locally in the CNS by plasma cells since only minute amounts of antibody are available from the blood [67, 68]. These immune reactions are aimed at eliminating the infection but due to the delicate nature of the CNS, these actions can often cause more harm than benefit.

In most well characterized CNS viral infections, control depends on the generation of a humoral and cell-mediated immunity that leads to viral clearance (reviewed in [67]). Humoral immunity involves antibody formation which primarily attacks extra-cellular particles to limit virus spread. If CNS infection occurs concomitantly with an acute peripheral infection, there can be a rapid recruitment of pre-existing virus-specific antibody-secreting plasma cells into the brain. However, if this is not the case, the immune response needs to be initiated in the peripheral lymphatic system via the cervical lymph nodes thus giving the virus more time to replicate within the CNS until humoral effector cells gain access [67]. A late non-specific humoral immunity leads to viral spread within the CNS and destruction of important neuronal cells.

Antibody mediated action against viral CNS infections or cell surface molecules acts without compromising cell integrity. In contrast, T-cell protection is mediated by cell destruction that often leads to pathology. If the T-cell response encounters a site of limited infection, the benefits are usually outweighed by pathological costs to the host. A robust and vigorous response that is beneficial outside the CNS is highly destructive within the CNS. The balance of kinetics of response and virus-host interactions is vital to the outcome and depends on the type of neuronal cell infected. A CD4+ helper T–cell response is predominant over a cytotoxic CD8+ response in

the CNS [67]. Outside the CNS, the opposite holds true. Acute and chronic viral infections of the periphery are fought with a cytotoxic MHC I restricted CD8+ T-cell attack in hopes of protecting the whole organism through destruction of infected or otherwise dangerous cells. Although each virus-host relationship differs, in the CNS the antiviral cell-mediated activity is largely dependent on CD4+ T-cells [66].

Figure 1.2: Cytokine mediated interaction of the peripheral and CNS immune cells

Cytokines secreted from peripheral immune cells (macrophages, T-cells, B-cells) can act on each other and distally on the immune cells of the CNS (astrocytes, microglia, oligodendrocytes). The same interaction is observed with CNS cells which secrete soluble factors to stimulate surrounding local cells and to communicate with peripheral immune cells. Solid arrows (black) indicate effects mediated by cells of the systemic immune system while stippled (grey) arrows indicate cytokine effects mediated by CNS cells. Adapted from [91].

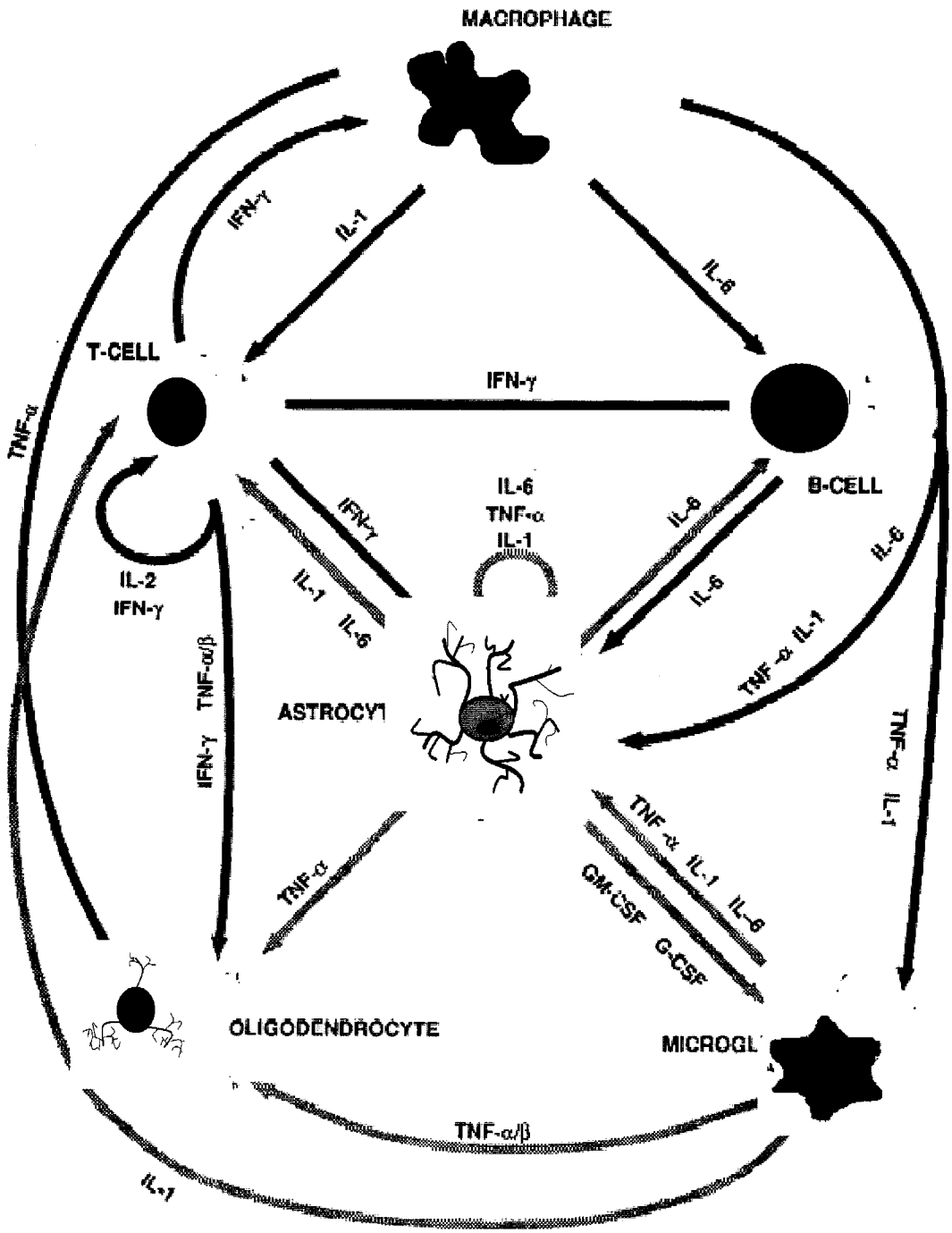
MACROPHAGE
IFN-γ
IL-1
IL-6
T-CELL
IFN-γ
B-CELL
TNF-α
IL-6
TNF-α
IL-1
IL-2
IFN-γ
IFN-γ
IL-1
IL-6
IL-6
TNF-α
IL-6
IL-6
TNF-α
IL-1
IFN-γ
TNF-α/β
ASTROCYT
TNF-α
IL-1
TNF-α
IL-1
IL-6
GM-CSF
G-CSF
OLIGODENDROCYTE
MICROGL
TNF-α/β
IL-1

1.7 Rationale for Experiments and Objectives

VSV is a potent oncolytic agent with promising therapeutic potential as demonstrated by studies in mouse models of peripheral cancers. The "IFN inducing" mutant ΔM51-VSV provides superior clinical value because this mutant is restricted from replicating in normal host cells. However, this restriction does not apply to neurons, since the ΔM51-VSV strain maintains its neurotropic potential and infection in the CNS is detrimental to the host. Previous data indicates that systemic infections proceed to the CNS to preferentially replicate in implanted CNS tumours while leaving normal neurons intact. In contrast, virus directly injected into the brain is lethal. We thus propose that prior exposure to the virus in the periphery sets up a protective state in the brain. Since virus traveling through the host to find its way to the CNS is relatively harmless, we hope to prevent fatality in mouse models of VSV infection by pre-infecting mice with a substantial dose of ΔM51-VSV systemically (herein called the "priming" dose) prior to challenging mice intra-cranially with the same mutant virus. **The first objective of this thesis was to assess whether or not systemic priming induces CNS protection against a subsequent i.c. dose of ΔM51-VSV.** We employed the recombinant ΔM51-VSV expressing both green fluorescent protein (GFP) and firefly luciferase (FLuc) reporter genes allowing *in vivo* imaging (IVIS, Xenogen Corp.) and tracking of virus replication in a non-invasive fashion in the same animal over the time-course of infection.

Host immune response to wt VSV infection of the periphery has been characterized in detail. However information is limited with respect to host defence mechanisms in the CNS against wt or the ΔM51 mutant VSV. Thus far, it is known that type I IFN is critical for immediate action against VSV and infection of IFN α/β receptor knock-out mice is fatal [29, 51].

However, active immunization with VSV immune serum provides complete protection against VSV induced fatality in IFNα/β receptor knock-out mice [51]. Neutralizing antibodies are effective in limiting infection in peripheral organs and preventing spread to the CNS, but once the virus makes its way to this site, antibodies cannot provide sufficient protection to prevent lethal encephalitis [38, 51, 22]. Immunocompetent mice produce a cytotoxic T-cell (CTL) response which peaks at 6 days post infection and T-cells are seen in the CNS after i.n. infection with VSV [97]. As is the case in the periphery, cytokines, chemokines, and growth factors work in concert to influence survival, proliferation, and functional activity of all cell types in the CNS. Thus far type I IFN is the only cytokine implicated in protecting the entire host against VSV [98, 99]. In terms of other key soluble factors, TNF-α, IFN-γ, IL-1a, IL-12, and IL-6 may be important in defending the CNS against VSV since the mRNAs for these cytokines have been detected soon after neurotropic infections with a number of difference viruses [68]. Although others are actively characterizing host responses to mutant VSV in the periphery, little is known about ΔM51-VSV and CNS infections. Therefore, **the second objective of this thesis is to study the host response to ΔM51-VSV infection of the CNS**. This will not only allow us to understand a fundamental host-virus relationship, but we can then exploit this knowledge to improve VSV based therapy for cancers of the brain.

CHAPER 2: MATERIALS AND METHOD

2.1 Viral Maintenance and Titration

The ΔM51-VSV GFP (Indiana serotype) and ΔM51-VSV GFP Firefly luciferase (FLuc) were constructed and provided courtesy of the John Bell laboratory. Stocks were maintained by viral propagation on VERO cells lines. Briefly, each mutant VSV was used to infect confluent 150mm dishes of VERO cells at an multiplicity of infection (MOI) of 0.1 plaque forming units (PFU) and incubated for 45 minutes at 37°C in a tissue culture incubator, after which 20ml of complete (10% fetal bovine serum (FBS) + 1% L-glutamine) α-MEM was added to each plate and left to incubate overnight. The supernatant was then spun down to remove residual VERO cells and then filtered through the 22μM Nalgene filters. Filtered supernatant was spun at 30,000 x g for 1.5 h. The resulting pellet was re-suspended in sterile PBS and stored at -80°C. Virus titres were determined by standard plaque assay as described in [104].

2.2 Animal Experiments

6 to 8 week old Balb/c, C57BL/6, FVBN, CD-1 nude and IFN-γ knock-out mice (Jackson Laboratories) were housed at the Apoptosis Research Centre. Animal use protocols were approved by the University of Ottawa committee on the Use of Live Animals in Teaching and Research. Mice were kept in sterile isolation cages with sterile food, water and bedding on a daily 12h day-night cycle and were handled in compliance with all institutional guidelines for the humane treatment of experimental animals. Unless otherwise stated, all mice were primed by tail vein injection with $1x10^8$ pfu of ΔM51-VSV-GFP in 100ul of sterile PBS or mock primed with just 100ul of PBS. All mice were challenged i.c. with $2x10^7$ pfu ΔM51 VSV-GFP-FLuc 24h after receiving the priming dose. Mice were weighed daily and given fluids when required until endpoint was reached (hind limb paralysis or loss of more than 20% of initial body weight).

2.3 IVIS Imaging

D-luciferin, potassium salt (Molecular Imaging Products) was dissolved in sterile PBS to obtain a concentration of 20mg/ml. Weekly stocks were made and stored at 4°C or long term stocks were stored at -80°C. Mice were injected i.p.. with 4 mg of luciferin and maintained under isofluorane anesthesia for 5 minutes prior to imaging (*Figure 2.1*). All mice were imaged using a cooled CCD camera (Xenogen IVIS 200). D-luciferin dependent photon flux was produced from cells infected with the luciferase encoding VSV, and thus serves as a quantitative surrogate marker of virus replication. Images were collected and integrated for a period of 3 minutes unless otherwise stated. Images were processed using Living Image software (Xenogen). To quantify the measured light, IGOR image analysis software (WaveMetrics) was used to draw regions of interest (ROI) over the head and/or spine area showing light signal, and maximum photons/sec/cm^2/steridian (sr) were obtained. Background photon levels were determined by drawing equivalent ROIs over areas devoid of luminescence.

2.4 Interferon α, β, γ ELISA

Blood samples were collected by exsanguinations of heavily anaesthetized mice via cardiac puncture. In cases where CSF was also required, mice were anaesthetized with Euthansol and the scalp was cut to expose the skull. About 5-10ul of CSF was collected from the cisterna magna using a pipette and stored in eppendorf tubes on dry ice. After CSF collection, blood was quickly collected via exsanguinations and heart blood was collected in lithium heparin treated Microvette CB 300LH tubes kept on ice. All blood samples were spun at 10,000 x g for 10 minutes and the top plasma layer was collected and stored at -80°C. Individual enzyme linked immunosorbent assay (ELISA) for detection of interferon α, β, and γ (PBL Biomedical Laboratories) were performed in triplicate to detect levels of these proteins in the CSF and blood using the manufactures recommended procedure. A Spectramax 340 PC (Molecular Devices) automated

plate reader was used to measure the optical density at 450 nm. For some assays, the readings were also taken at 550 nm to correct for imperfections in the 96 well plates. Data was acquired using Softmax Pro version 4.7.1 (Molecular Devices).

2.5 Plaque Reduction Assay

Blood was collected from mice and plasma was separated and stored at -80°C as described above. In order to determine the plaque reduction ability of plasma collected at various times after priming or mock priming, plasma was diluted 1:100 and incubated with various serial dilutions of either ΔM51-VSV-GFP or AV1 mutant viruses at 37°C. After 45-60 minutes, 65mm dishes of confluent VERO cells were infected with the plasma-virus mixture. Negative controls consisted of virus incubated with α-MEM media in place of plasma while positive controls included virus incubated with plasma taken from mice known to contain neutralizing antibodies against VSV. After infection of VERO cells for 60 minutes at 37°C, a 1:1 mixture of 2x α-MEM containing 20% FBS and agarose overlay was placed over the cells and left overnight in a tissue culture incubator at 37°C. Plaque count was determined the next day.

Figure 2.1: Schematic of experimental set-up for imaging of ΔM51-VSV infected mice

In vivo imaging techniques (IVIS 200, Xenogen Corp.) were utilized in order to detect and quantify viral replication taking place after the i.c. challenge dose of ΔM51-VSV. Mice were either primed or mock primed and challenged i.c. a day after priming using the indicated viral doses. The challenge virus encoded the luciferase gene allowing photon flux to be collected from only virus injected into the brain. Imaging always commenced 24h after the challenge dose. D-luciferin was administered i.p.. 5 minutes prior to imaging. All images and photons were collected using identical parameters within an experiment with the IGOR Pro software. Photon flux was quantified using Living Image software.

IVIS – Experimental Setup

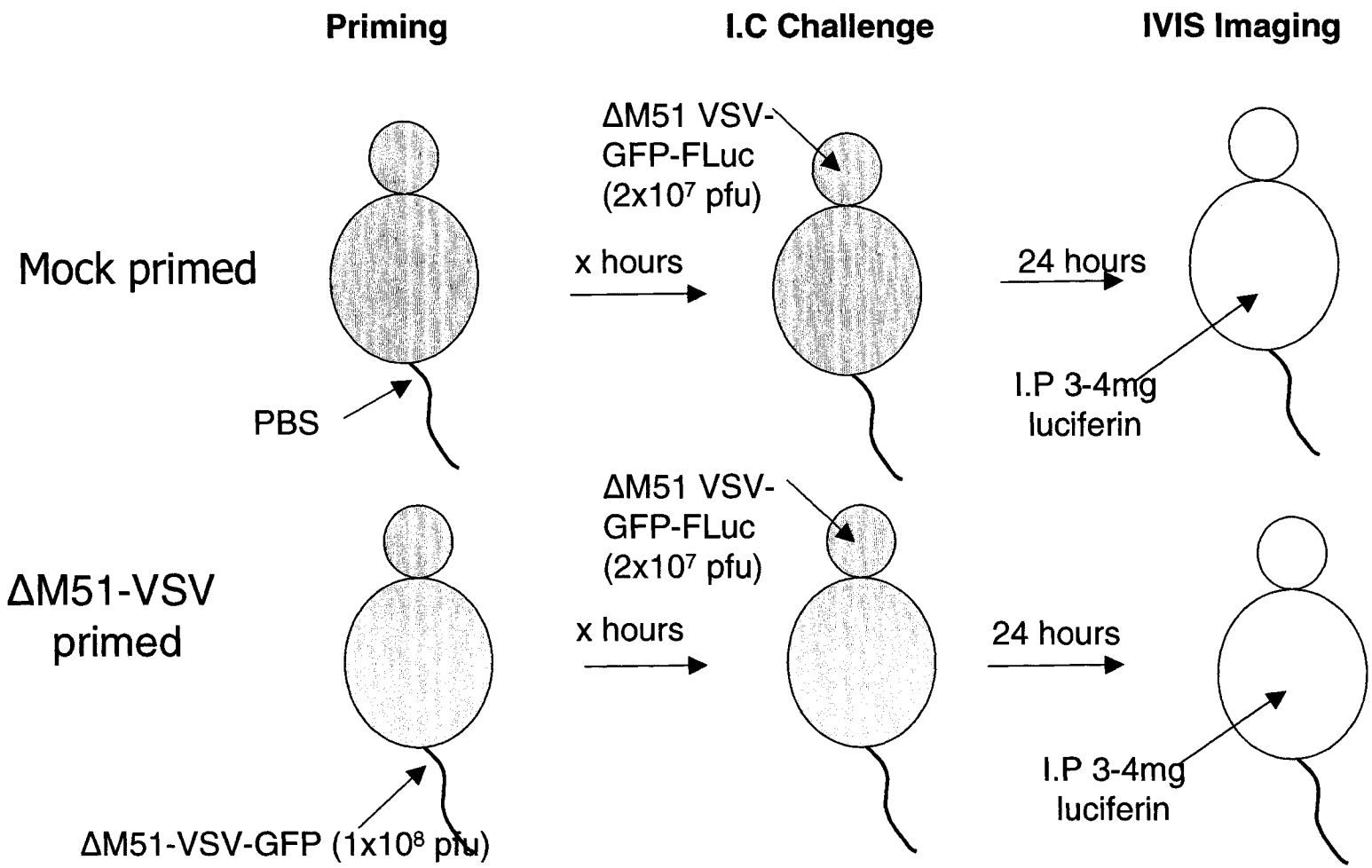

2.6 Immunohistochemistry (IHC), immunoflorescence (IF), microscopy

Tissue preparation. Mice were anaesthetized using Euthansol and trans-cardially perfused with 60 ml of sterile PBS and then with 4% paraformaldehyde (PFA) made fresh weekly. Brains were dissected from the skull and placed in 4% PFA overnight at 4°C. The next day, brains were washed in 5-6 changes of 20% sucrose for five minutes each and then left for 24-48h in 20% sucrose at 4°C. After equilibration in sucrose solution, brains were flash frozen in isopentane on dry ice and stored at -80°C. 10-micrometer (μm) thick horizontal or sagittal sections were cut using Micromax HM 500 OM microtome cryostat set at -20 to 25°C. Sections were mounted on Superfrost Plus (Fisher Scientific) glass slides with 4-5 sections per slide giving a representative view of either the entire brain (horizontal sections) or of one hemisphere (sagittal sections). Slides were stored at -20°C.

Immunohistochemistry. Slide mounted sections were removed from the freezer, incubated at 37°C for 30 minutes, and immersed in 4% PFA for 20 minutes. Sections were rinsed with PBS for 5 minutes (3 times) then incubated with 3% hydrogen peroxide in PBS for 15 minutes to block endogenous peroxidase activity. Sections were then rinsed 3 minutes (3 times) in PBS, then each slide was wiped clean of residual PBS and incubated in 1.5% normal goat serum in PBS for 1 hour. Sections were incubated with avidin for 15 minutes and then biotin for another 15 minutes in order to block endogenous biotin (Vector Laboratories). Sections were then incubated with the primary antibody (*Table 2.1*) diluted in 1.5% normal goat serum (Vector Laboratories) for 2 hours, rinsed 3 times in PBS for 3 minutes, and incubated with a biotinylated secondary antibody (*Table 2.1*) corresponding to the primary. As a negative control for each antibody, normal goat serum rather than primary antibody was added on parallel slides. Sections were rinsed again for 3 minutes, 3 times each, and incubated in avidin-biotin-peroxidase complex (ABC Kit, Vector

Laboratories) according to the manufacture's protocol. Sections were then rinsed 4 times for 3 minutes each, and DAB (KLP Laboratories) mixture was added to each section for 2 minutes each. DAB reaction was performed according to the manufacture's protocol. The reaction was stopped by immersing the sections in distilled water. Sections were rinsed three times for three minutes each in PBS, counterstained with hemotoxylin, rinsed with acid alcohol, dehydrated in decreasing grades of ethanol and xylene and coverslipped.

Immunofluorescence Frozen slides were thawed at 37°C for 30 minutes and then each section on the slide was partitioned off with a PAP hydrophobic marker (ESBE Scientific). Thawed sections were rinsed in PBS (pH 7.4) and then incubated in 4% PFA for 20 minutes. The sections were rinsed again and washed 3x 5 minutes in PBS. Non-specific interactions were blocked using serum from the same animal species the secondary was raised against for one hour at room temperature. The primary antibody (*Table 2.1*) was then added for 2 hours at room temperature or at 4°C overnight. For negative controls, primary antibody was omitted and the sections were kept in normal blocking serum. Antibodies were diluted in PBS containing 0.03% Triton X-100 or commercially available antibody diluent (BD PharMingen). The sections were washed 3x 5mins in PBS and then the secondary antibody was applied for 30 minutes to an hour at room temperature. Counter-staining was done to visualize all nuclei using Hoechst 33258 stain at a 1/1 000 000 dilution in PBS for 1 minute followed by 3 washes in PBS for 5 minutes each. The slides were then mounted using anti-fade fluorescent mounting medium (Vector Laboratories), cover-slipped and stored in the dark at 4°C.

For double labelling the first primary (if multi labelling with anti-VSV, the anti-VSV antibody was always added first) was applied after blocking with normal goat serum for 2 hours and then rinsed before the corresponding secondary was added for 30 minutes. The secondary was then washed off with PBS 3x 5 minutes, after which the second primary was added diluted in

antibody diluent for 3h. After washing off the second primary, the corresponding secondary was added. Hoechst 33258 counter staining was performed as described prior to cover-slipping the sections. TUNEL staining was performed using the ApopTag Plus *In Situ* Apoptosis detection Kit (Chemicon International) according to the manufacture's instructions. TUNEL was always performed prior to any other antigen labelling.

Microscopy: Sections were viewed using Zeiss axioskop 2 mot plus epi-fluorescence microscope (Carl Zeiss Canada) fitted with a QICAM digital CCD camera (QImaging,). Northern Eclipse software (EMPIX Imaging Inc.) was used to acquire all images.

Table 2.1: Primary and secondary antibodies used in IHC and IF experiments

IHC was used to detect T-cells, B-cells or VSV infected cells in the CNS using the indicated antibodies at the appropriate dilution. Fluorescent labelling of brain sections was carried out to detect CNS glial cells astrocytes and microglia and also to detect neurons. IF was done when co-labelling was required with the CNS cell markers and VSV or TUNEL to detect apoptotic cells.

Table 2.1

Cell Type/virus	Primary Antibody (source)	Primary dilution	Secondary Antibody (source)	Secondary dilution
T-cells	hamster anti-mouse CD-3ε (BD Pharmingen)	1:50	biotin conjugated mouse anti-hamster (BD Pharmingen)	1:50
B-cells	rat anti-mouse CD45R/B220 (BD Pharmingen)	1:100	biotin conjugated mouse anti-rat Ig, κ light chain (BD Pharmingen)	1:100
Astrocytes	1) rabbit polyclonal anti GFAP (Abcam) 2) chicken polyclonal anti-GFAP(Abcam)	1) pre-diluted 2)1:100	1) goat anti-rabbit Alexa-488; goat anti-rabbit Cy3(BD Biosciences) 2) goat anti-chicken IgY H&L Texas red (Abcam)	1) 1:400; 1:800 2) 1:100
Microglia	biotinylated Ricinus Communis Agglutinin 1 (Vector Laboratories)	1:1000	Texas red streptavidin (Vector Laboratories)	1:200
Neurons	mouse anti-neuronal nuclei (NeuN) (Chemicon International)	1:100	1) goat anti-mouse Alexa 488 (BD Bioscience) 2) goat anti-mouse rhodamine (Abcam)	1) 1:400 2)1:100
VSV	rabbit anti-mouse (Dr. Earl Brown, University of Ottawa)	1:5000	1) goat anti rabbitAlexa 488 (BD Biosciences) 2) goat anti rabbit Cy3 (BD Biosciences)	1) 1:400 2)1:800

CHAPTER 3: RESULTS – CHARACTERIZING THE PRIMING PHENOMENON

3.1 Intravenous priming with ΔM51-VSV induces an anti-viral state in the CNS

To assess whether injecting mice in the periphery with the ΔM51 mutant VSV prior to challenging i.c. is CNS protective, six to eight week old female Balb/c mice were i.v. injected or "primed" with 100ul of 1 x 10^9 pfu/ml ΔM51-VSV-GFP. Control groups were mock primed with 100ul PBS. Twenty-four hours after priming, all mice were i.c. challenged with 5ul of 4 x 10^9 pfu/ml of ΔM51-VSV-GFP. Mice were weighed daily and assessed for activity levels, status of fur, and ability to walk. End point was established to be when the animal had lost 20% of its initial body weight or had developed hind limb paralysis (HLP). All mice primed with ΔM51-VSV-GFP initially lost some weight and showed signs of pilo-erection. However, by 48h after the challenge dose, these mice recovered to a healthy status. Mock primed mice rapidly lost weight, became inactive, never recovered from pilo-erection and developed HLP within 6-8 days after i.c. challenge. These initial experiments were based on phenotypic observations using ΔM51-VSV-GFP as the priming virus and the challenge virus.

Previously, we had constructed the mutant virus, ΔM51-VSV to not only express GFP but also encode for firefly luciferase (FLuc). Coupled with the *in vivo* imaging system (IVIS, Xenogen Corp.), the ΔM51-VSV-GFP-FLuc was used as the challenge virus allowing us to track the i.c. challenge dose of the virus in the same mouse in a non-invasive fashion over time. This technique therefore enabled us to not only assess priming based on survival but also in terms of replication and/or spread of VSV in a living animal. IVIS imaging commenced 24h after the i.c. challenge and continued everyday until either luminescence

signal diminished to near background levels, or the mice had reached endpoint (*Figure 3.1*). Images were taken using Igor Pro software (Xenogen Corp.) using the same capture parameters throughout the experiment. In mock injected Balb/c mice, luminescence was detected within 24h after challenge in the brain, and seen in the spinal cord within 72h (*Figure 3.1 A*). By 120h post i.c. challenge, all mock primed mice had reached endpoint. In contrast, ΔM51-VSV-GFP primed mice initially emitted luminescence from within the head, but by 72h after challenge, signal diminished from the head and minimal luminescence, if any, was seen in the spine of most mice. All primed mice recovered from initial weight loss and survived past 15 days.

In order to determine if priming is strain specific, parallel experiments were performed in the C57Bl/6 strain of mice. Signal strength was generally lower in C57Bl/6 mice, probably due to the dark colour of their fur which absorbed most of the luminescence. However, difference in signal was evident between the mock primed and the VSV primed cases and the final outcome was consistent with Balb/c mice (*Figure 3.1 B*). Although signal was not detected in the spine of the mock primed C57Bl/6 mice, all of them developed HLP by 120h post i.c. challenge. As expected, primed C57Bl/6 mice survived the i.c. challenge.

The possibility of gender influence was addressed in a similar experiment using groups of male and female FVB/N mice. As seen in *figure 3.1 C*, no gender differences were observed in that virus primed mice survive an i.c. challenge with virus while mock primed mice develop HLP. These experiments indicate that CNS protection induced by priming is not strain or sex specific. Due to the optimal signal detected with white haired mice, female Balb/c mice were chosen as the model strain for further characterization.

Figure 3.1: Priming induced CNS protection is not strain or sex specific

Balb/c (A) or C57Bl/6 (B) strains of mice were either mock primed (i.v.. injected with 100ul PBS – top row) or primed with $1x10^8$ pfu/100ul ΔM51-VSV-GFP (bottom row). 24h after priming, mice were i.c. challenged with ΔM51-VSV-GFP –FLuc at a dose of $2x10^7$ pfu/5ul. IVIS imaging commenced 24 hours after the i.c. challenge. Each mouse was injected i.p. with 3mg of luciferin (in 200ul PBS) just prior to imaging. Photons were integrated for 3 minutes at medium resolution for all images. Only images taken at 24h and 72h after i.c. challenge are shown. (C) Survival curves for the various strains (Balb/c, C57Bl/6 – top graph) and sexes (FVBN strain – bottom graph) are shown. Mock or ΔM51-VSV-GFP primed mice were challenged 24h after with ΔM51-VSV-GFP –FLuc. Endpoint was determined to be when the mouse either developed HLP or death. (F) female; (M) male

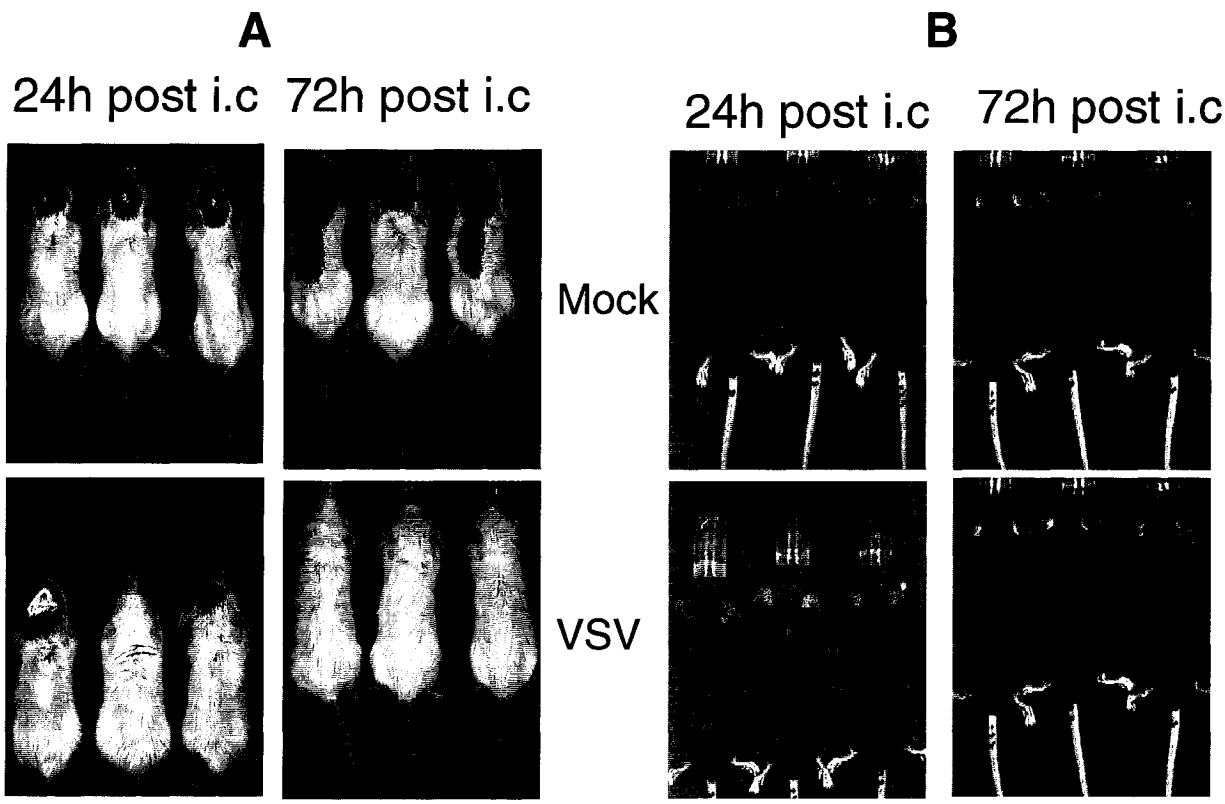
A
B
24h post i.c
72h post i.c
24h post i.c
72h post i.c
Mock
VSV

C

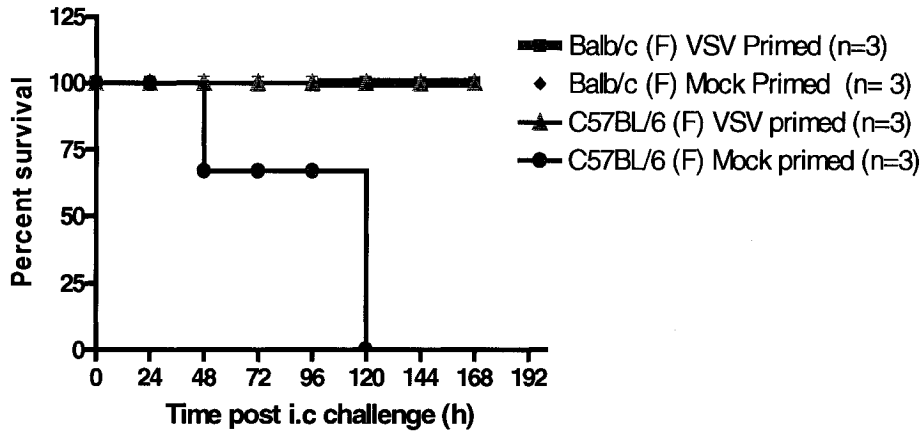
Percent survival
125
100
75
50
25
0
0 24 48 72 96 120 144 168 192
Time post i.c challenge (h)
Balb/c (F) VSV Primed (n=3)
Balb/c (F) Mock Primed (n= 3)
C57BL/6 (F) VSV primed (n=3)
C57BL/6 (F) Mock primed (n=3)

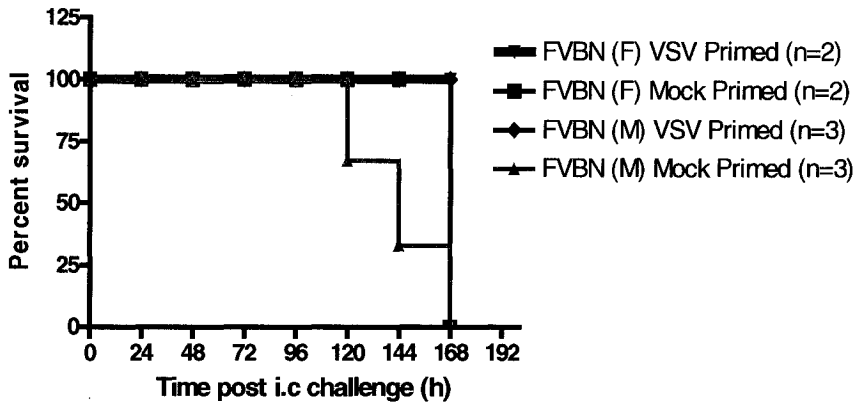
Percent survival
125
100
75
50
25
0
0 24 48 72 96 120 144 168 192
Time post i.c challenge (h)
FVBN (F) VSV Primed (n=2)
FVBN (F) Mock Primed (n=2)
FVBN (M) VSV Primed (n=3)
FVBN (M) Mock Primed (n=3)

3.2 Correlation of photon flux with viral titre

In order to validate the use of the IVIS as a quantitative tool to measure replicating virus, brains were harvested after imaging to compare the quantity of photons emitted from the brain to actual viral titres. Balb/c female mice were primed with ΔM51-VSV-GFP and another set were mock primed with PBS. Both groups of mice were challenged i.c. with ΔM51-VSV-GFP-FLuc 24h after priming. Three mice from each group were imaged 24h post i.c. challenge, euthanized and brains were collected. During imaging, photons were collected and integrated for 3 minutes per each set of mice. Two brains from each group were weighed and frozen in PBS while one brain was flash frozen in isopentane for IHC studies. This was repeated with the remaining mice at 72h and 120h post i.c. challenge (three mice per group per time point). *Figure 3.2 A* depicts the images taken each day indicated before the mice were euthanized. Total amount of photons emitted from the head were measured using Living Image software from all six mice at each time point, but only data from the mice euthanized for viral titration was plotted (2 of 3 animals) since the third animal was used for IHC studies. To quantify the detected luminescence, regions of interest (ROI) were either drawn manually over areas of the head region showing luminescence or were automatically generated by the software and the maximum photons/sec/cm^2/sr was obtained. No significant difference in values was noted when luminescence was detected using regions of interest (ROI) created manually versus automatically plotted by the program. The ROIs shown in *figure 3.2 A* are the result of contours generated by the Living Image program and software generated photon values. ROI log values taken from the two mice whose brains were titrated were plotted against time post i.c. challenge (*Figure 3.2 B*). Log values of viral titres in the brain, as determined by standard plaque assay, plotted against time post i.c. challenge are shown in *Figure 3.2 C*. *Figure 3.2 B* indicates that within 24h post i.c. challenge there is a two-log decrease in

viral replication when mice are primed. There is a slight increase in luminescence later in infection, but by 5 days post challenge, the signal in the head reaches background levels. Background luminescence was quantified by creating ROIs in areas where the signal is not present or by imaging mice without administering D-luciferin. Mock primed mice maintained a high level of luminescence and all mice showed spread of virus to the spine by 72h post i.c. challenge. At the time when primed mice showed clearance of virus from the CNS (120h), mock primed individuals still emitted two-log more photons from the head and two of three mice showed signs of HLP. ΔM51-VSV primed mice were at a healthy weight at time of sacrifice and displayed normal activity levels.

To validate the fact that luminescence is representative of actual viral replication, we plotted the total amount of photons quantified from each mouse against actual viral titre as determined by the plaque assay. Values from VSV primed mice at 120 hours post i.c. were omitted because photon values were at background levels and therefore negligible. Plotting total amount of photons emitted from the head region using software created ROIs versus viral titres produces a correlation value of 0.95 and manually created ROI values produce a correlation of 0.938. Therefore, luminescence detected using the IVIS is a quantitative measure of replicating VSV in living mice.

Figure 3.2: IVIS data correlated with viral titres

A) Mice were i.v. primed with either $1x10^8$pfu/ 100ul Δ51VSV-GFP or mock primed with 100ul of sterile PBS. 24h after priming, both groups were i.c. challenged with $2x10^7$pfu of Δ51VSV-GFP-FLuc in 5ul of sterile PBS. Three mice from each priming group were imaged using the IVIS at different times post i.c. challenge as indicated in the figure and then euthanized. The brains were isolated and homogenates were titered on VERO cells using a standard plaque assay. Regions of interest were drawn over luminescent areas of the head were quantified using Living Image software. The scale bar on the left indicates the quantity of photons emitted from the mice according to the colour code.

B) Luminescence emitted from each mouse quantified using Living Image software is plotted against time post i.c. challenge. Background indicates the average amount of luminescence captured from non-luminescent areas on the mice. Each data point is the average taken from three mice.

C) Actual viral titres from primed and mock brains imaged in (A) are plotted against time post challenge. Each data point represents the average titre from two mice per time-point.

D) Photons emitted from the head are plotted against viral titres from the same mouse. The data point for primed mice imaged 120h after challenge was omitted due to negligible viral titres and IVIS signal. Total photons emitted correlates with actual viral titre in the head.

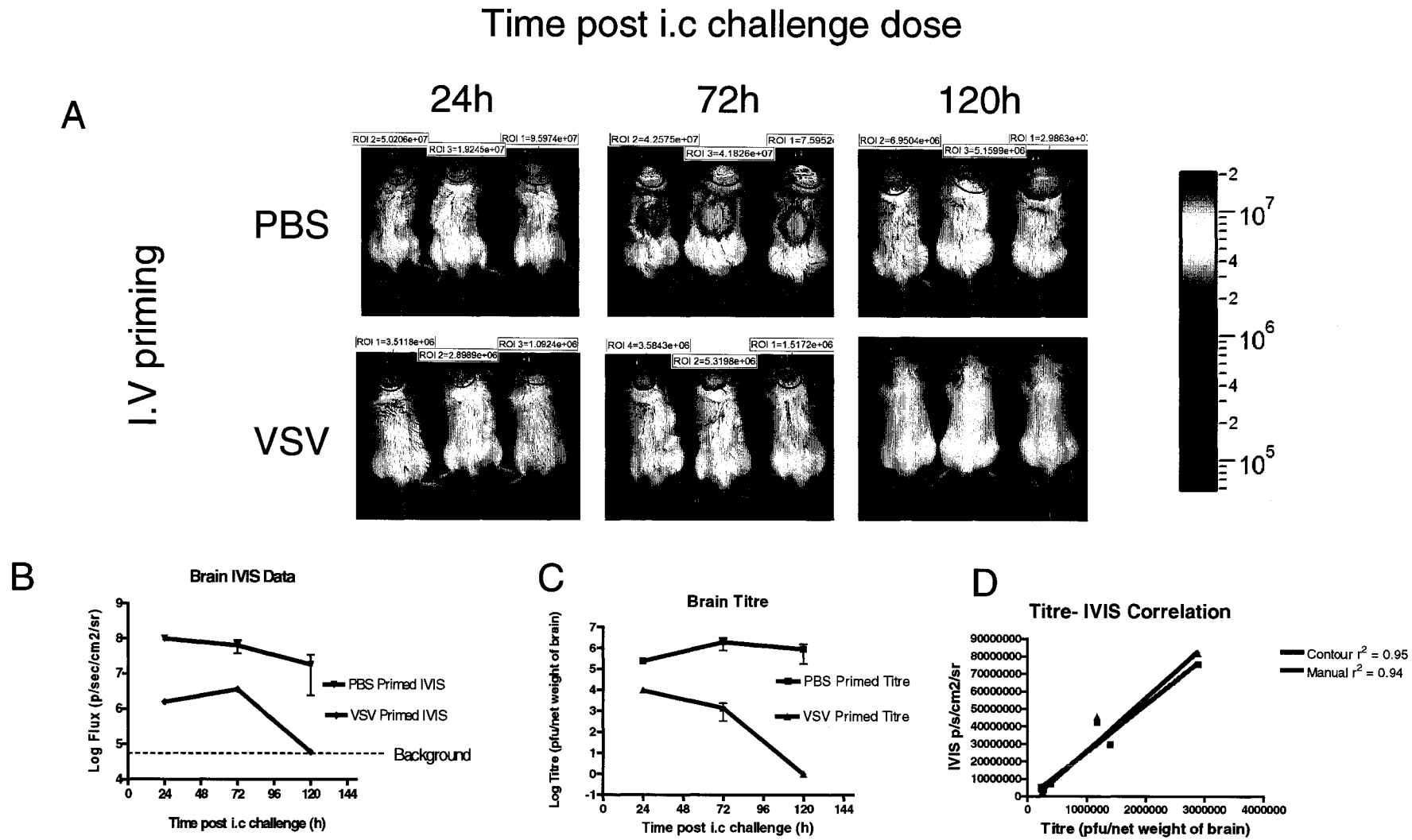
Time post i.c challenge dose
A
24h
72h
120h
I.V priming
PBS
VSV
ROI 2=5.0206e+07
ROI 1=9.5974e+07
ROI 3=1.9245e+07
ROI 2=4.2575e+07
ROI 1=7.5952
ROI 3=4.1826e+07
ROI 2=6.9504e+06
ROI 1=2.9863e+0
ROI 3=5.1599e+06
ROI 1=3.5118e+06
ROI 3=1.0924e+06
ROI 2=2.8989e+06
ROI 4=3.5843e+06
ROI 1=1.5172e+06
ROI 2=5.3198e+06
10^7
10^6
10^5
B
Brain IVIS Data
Log Flux (p/sec/cm2/sr)
PBS Primed IVIS
VSV Primed IVIS
Background
Time post i.c challenge (h)
C
Brain Titre
Log Titre (pfu/net weight of brain)
PBS Primed Titre
VSV Primed Titre
Time post i.c challenge (h)
D
Titre- IVIS Correlation
IVIS p/s/cm2/sr
Contour r^2 = 0.95
Manual r^2 = 0.94
Titre (pfu/net weight of brain)

3.3 Kinetics of priming

We have shown that priming 24h prior to i.c. challenging is effective at protecting the host, but we wanted to determine the exact onset and duration of protection. Balb/c mice were primed with ΔM51-VSV-GFP and at various time points, mice were i.c. injected with the challenge dose of ΔM51-VSV-GFP-FLuc. Again, mice were imaged starting 24h after the challenge dose. The times chosen to challenge were 12h, 24h, 48h, 72h, and 96h after priming. Past 96h, it is known that a robust antibody response is initiated by the host to limit VSV infection of the periphery and also by this time point, primed mice have recovered [51, 97]. Visual comparison of the amount of light emitted from the heads of the mice indicated that the longer the challenge dose was delayed after priming, the less viral replication was seen in the head (*Figure 3.3*). Viral challenge at 12h or 24h after priming still allowed for virus to replicate extensively in the brain and then eventually spread to the spine. However, in these mice the signal eventually cleared and all mice survived. Waiting past 96h produced the best result, minimizing the initial amount of replication taking place in the brain. *Figure 3.4* quantitatively compares viral replication at the various challenge times. When compared to signal emitted from mock primed mice, it was evident that even as early as 12h, there was a substantial decrease in the amount of replicating virus in the brain. The greatest drop in signal occurred 96h after the priming dose, regardless of when the mice were challenged. This is evident from *figure 3.3*, where the mice challenged after 96h emit signal just above background and were clear 48h post i.c. challenge. From these results, it was apparent that protection commenced as early as 12h but the strength of the protective response increased the longer the challenge dose was delayed.

Figure 3.3: Kinetics of Priming

15 mice were primed i.v. with $1x10^8$pfu/100ul ΔM51VSV-GFP. At different times (12h, 24h, 48h, 72h, 96h) after priming, 3 mice were challenged i.c. with $2x10^7$pfu/5ul Δ51VSV-GFP-FLuc. Imaging commenced for each set 24h after the i.c. challenge and continued each day until signal diminished or mice reached end-point. All images were collected with Igor Pro software (Xenogen Corp.) using the same parameters. The images shown are taken after 24h and 72h hours post i.c. and are normalized to the same minimum and maximum values. All Δ51VSV-GFP primed mice survived the i.c. challenge dose indicating protection is induced as early as 12h. Mock primed mice (not shown) all developed HLP by 6 days after i.c. challenge

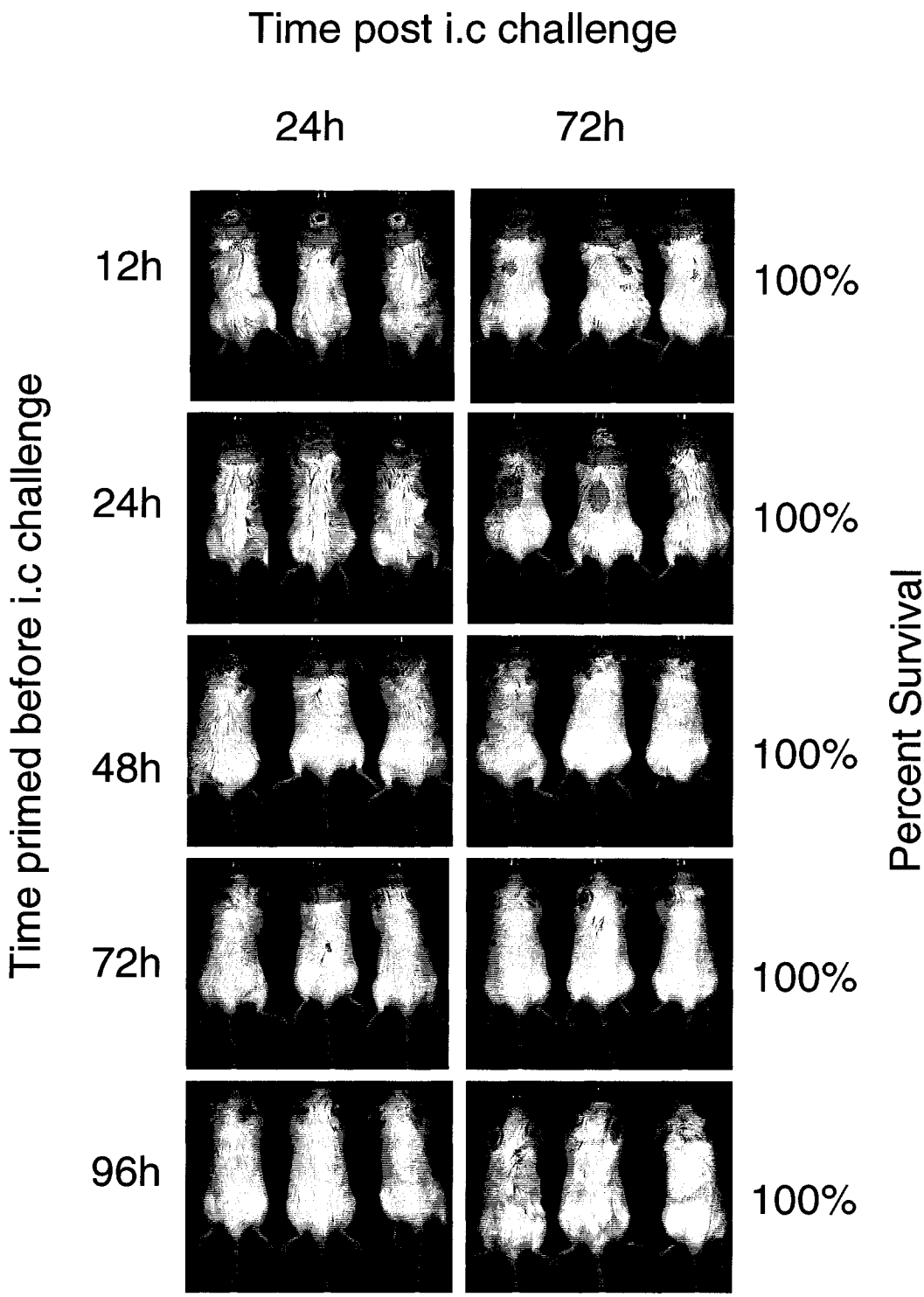
Time post i.c challenge
24h
72h
Time primed before i.c challenge
12h
24h
48h
72h
96h
100%
100%
100%
100%
100%
Percent Survival

Figure 3.4: IVIS quantification of kinetics of priming

Total photons emitted from the head of all mice i.c. challenged at various times after the priming dose is plotted against time post i.c. challenge. The data shown is the average photons from three mice per time-point quantified using Living Image software. The mock primed (PBS) negative control mice were i.c. challenged 24h after priming. All primed mice survived whereas the mock primed all succumbed to HLP. IVIS data indicates that the longer the i.c. challenge is delayed after priming, the less replication takes place in the head and virus is cleared at an accelerated rate.

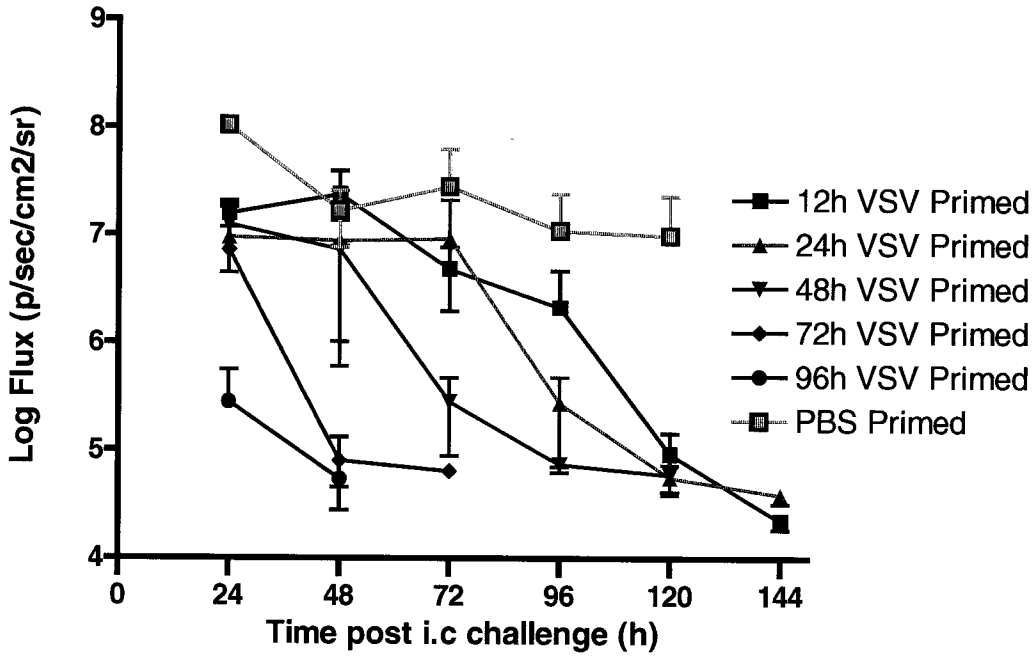
Log Flux (p/sec/cm2/sr)
9
8
7
6
5
4
0
24
48
72
96
120
144
Time post i.c challenge (h)
12h VSV Primed
24h VSV Primed
48h VSV Primed
72h VSV Primed
96h VSV Primed
PBS Primed

3.4 Route of priming

To determine if CNS protection can be altered depending on how the virus is initially introduced into the periphery, different routes of priming were attempted. Mice were primed with ΔM51-VSV-GFP via intra-peritoneal (i.p.), intra-muscular (i.m.), or sub-cutaneous (sub.cu.) injection. Mock primed and positive controls were primed via the i.v. route. All mice were i.c. challenged 48h post priming and were imaged commencing 24h post i.c. challenge. As expected, mock primed mice demonstrated 1-2 log more viral replication in the head in comparison to all VSV primed mice and replication remained high throughout the experiment (*Figure 3.5 A*). No data points are shown for these mock primed mice at the last time point because by 120h post challenge, one mouse had died and the other mouse had developed HLP. All ΔM51-VSV-GFP primed animals survived except the sub-cu. primed group where only one mouse survived. Examination of the luminescent signal emitted from the heads of these mice revealed that i.p. priming is the most effective route, because at 24h post i.c., this route of priming resulted in the least amount of signal in the head and the virus cleared from the mice at an accelerated rate. By 48h post i.c., there was more than 1-log decrease in signal detected in the head from mice primed i.p. in comparison to all other routes. By 96h post i.c., i.p. primed mice had cleared VSV from the head whereas some luminescence was detected in the heads of mice primed by other routes. This experiment was repeated just comparing the i.v. and i.p. routes but challenging the mice 24h post priming. *Figure 3.5 B* compares these two routes of priming at the various challenge times. Challenging 24h after priming via the i.p. route still resulted in a decrease of viral replication in the head and quicker clearance of signal when compared to i.v. priming. In terms of outcome, both routes of priming were effective in protecting the CNS.

Figure 3.5: Influence of priming route on viral replication in the brain

A) Mice were primed with $1x10^8$ pfu/100ul Δ51VSV-GFP via 4 different routes: intra-muscular (i.m), intra-venous (i.v.), subcutaneous (sub.cu.) and intra-peritoneal (i.p.). Three mice were included in each group and two mice were included for the PBS i.v. mock primed negative controls. 48h after priming, mice were challenged i.c. with $2x10^7$ pfu/5ul Δ51VSV-GFP-FLuc and imaging commenced 24h post i.c. challenge. Photons were integrated for 3 minutes and images were taken at high resolution. The photons emitted in the head region of each mouse was quantified and plotted vs. time post i.c. challenge. All primed mice survived the challenge dose except the sub-cu. primed mice where only one survived (indicated in legend). I.p. priming was the most effective in restricting VSV replication in the head and enabled quicker clearance of virus from mice. One mock primed mouse succumbed to the virus at 120h post i.c. and the other developed HLP.

B) The above experiment was repeated but mice were challenged 24h after priming via the i.v. and i.p. routes only (n=3). Again, all primed mice survived. The graph compares signal in the heads of mice challenged via the two different routes at 48h (data from A) and at 24h after priming.

A

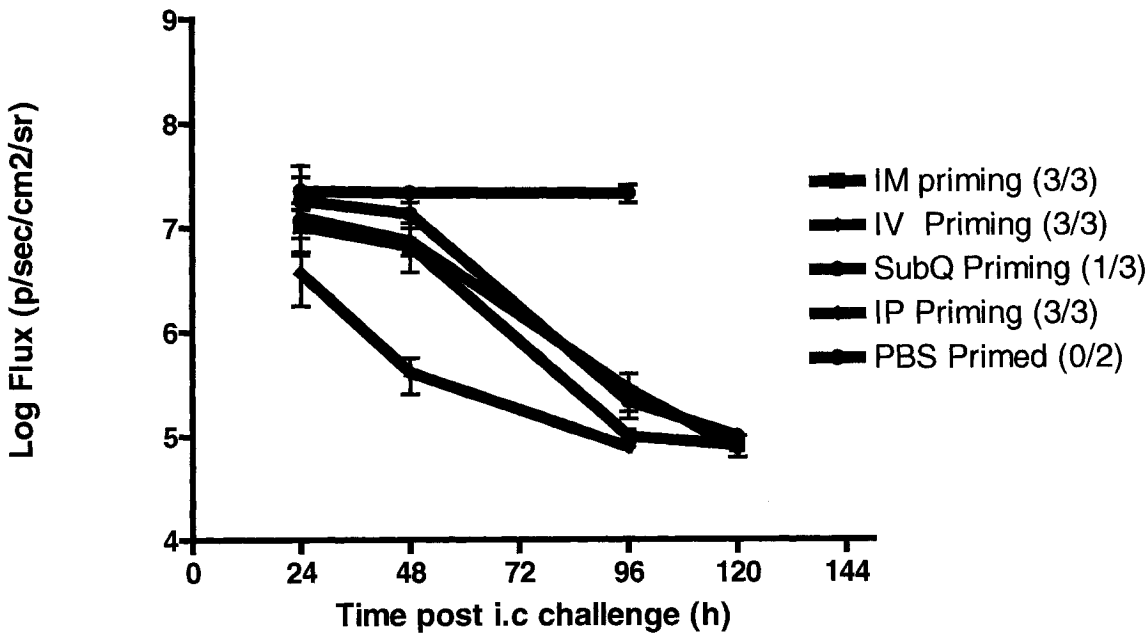
Log Flux (p/sec/cm2/sr)
9
8
7
6
5
4
0
24
48
72
96
120
144
Time post i.c challenge (h)
IM priming (3/3)
IV Priming (3/3)
SubQ Priming (1/3)
IP Priming (3/3)
PBS Primed (0/2)

B

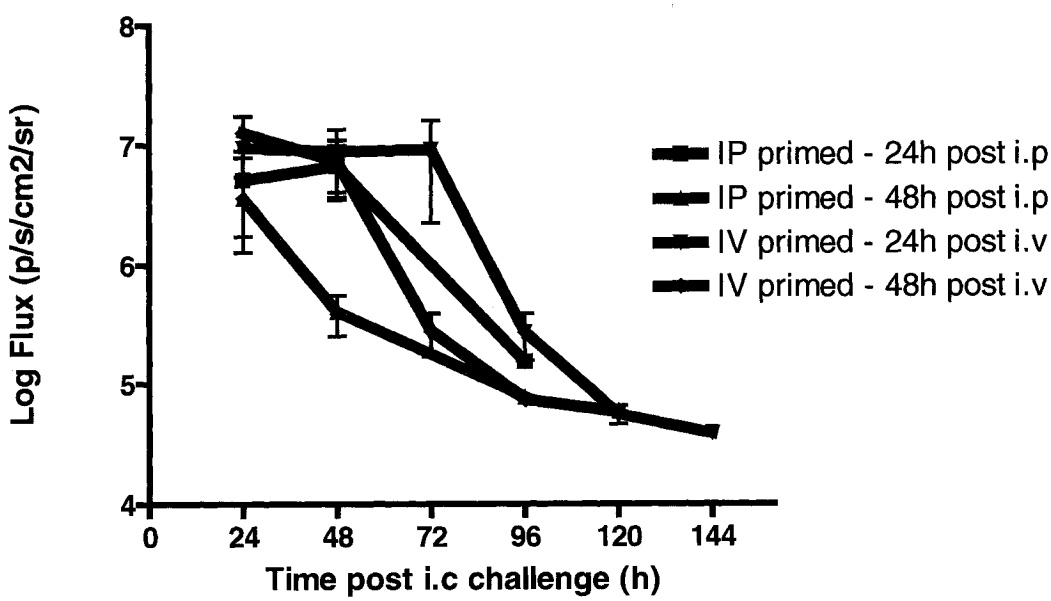
Log Flux (p/s/cm2/sr)
8
7
6
5
4
0
24
48
72
96
120
144
Time post i.c challenge (h)
IP primed - 24h post i.p
IP primed - 48h post i.p
IV primed - 24h post i.v
IV primed - 48h post i.v

3.5 Priming restricts viral replication in the CNS

IVIS imaging allows for a global view of viral replication within a living animal, but can not resolve specific regions of infection. To determine the areas of the brain that are infected by VSV, IHC studies were performed looking for VSV antigen in mouse brain tissue sections. *Figure 3.6* compares various areas of the brain at different time points after i.c. challenge from primed and mock primed mice. The mice were imaged prior to extracting the brains (*Figure 3.2*), therefore, we expected to detect virus in these brain tissue sections.

The sections shown in *figure 3.6 A* are from mice that were i.v. primed with ΔM51-VSV-GFP or PBS and i.c. challenged 24h after priming with ΔM51-VSV-GFP-FLuc. VSV antigen was detected using antibody against the VSV G protein using the standard IHC technique. The brown areas are indicative of VSV antigen positive areas. Hemotoxylin counterstaining was used to stain all nuclei blue. Horizontal sections of the brains were taken at 24h post i.c. and sagittal sections are shown at 72 and 96h post i.c.. In mock primed brains, VSV antigen was seen at 24h post i.c. challenge around the ventricles and in the hippocampus. At the same time-point, in primed brains, VSV antigen was only detected around the ventricles.

At 72h, sagittal sections taken approximately 2.5-2.8 mm lateral to the midline were analyzed for both the mock primed and VSV primed scenarios. In the mock primed section, VSV positive staining was seen around the midsection near the lateral ventricle (LV) and spread extensively around the hippocampus. In the primed brain section at 72h, staining was restricted to areas around the LV and there was some infection of the hippocampus. It was evident that VSV infected the same type of cells (hippocampal cells) at this time point whether the mice were primed or not, but there was significant differences in the extent of viral spread. Priming via the i.p. route (*Figure 3.6 B*) resulted in the same pattern of infection where the hippocampus was

infected but with much more spread along the ventricles and along the entire hippocampus when mice were mock primed.

Comparable sagittal sections are shown for brains harvested at 96h post i.c.. Extensive VSV positive staining is seen in the mock primed section around the dorsal third ventricle (D3V) and third ventricle (3V). The hippocampus was positive for VSV as well as the caudate, thalamus and OB. VSV was seen also by the fourth ventricle (4V) at this later time point. Primed brain sections were only positive for VSV around the 3V and D3V and were also concentrated in the granule cell layer of the OB but staining was not seen in the 4V.

Comparing the images taken from VSV primed and mock primed brains, it was clear that viral priming restricted VSV spread to the area around the ventricles. Without priming, VSV spread from the LV, 3V and D3V specifically to the hippocampus, thalamus, and striatum, eventually making its way to the 4V where it then spread to the spinal cord. VSV i.c. infection had a specific route of spread and did not differ whether the mice were primed or not. The hippocampus was always targeted but there was a difference in the extent of viral replication and spread. No differences in infection pattern were detected from brains of mice primed via the i.p. route but there was a decrease in the extent of VSV positive areas. As shown by IVIS imaging, i.p. priming resulted in less viral replication, therefore, less viral antigen was expected in these brain sections.

Figure 3.6: Priming restricts ΔM51-VSV spread through the mouse brain

A) Brains taken after i.c. infection of mice either i.v. primed 24h prior with ΔM51-VSV-GFP or mock primed. IHC analysis was carried out to detect VSV antigen using antibody against the G protein and is shown as the dark brown staining on the sections. All nuclei were counterstained blue with hemotoxylin. Horizontal sections are shown at 24h post i.c. challenge and sagittal brain sections are shown at 72 and 96h post i.c. challenge. At each time point, relatively similar areas of the brains are presented for each route of priming. 24h after i.c. challenge, very little VSV antigen is detected in primed brains and are restricted to the ventricles. More VSV positive areas are seen when mock primed at 24h post i.c. and are seen by the ventricles and at distal sites. Whereas, primed sections showed less VSV positive areas over time, mock primed brains showed an increase in VSV infection. All images were scanned using the UMAX Astra 1220S scanner and VistaScan32 version 3.55 software

B) 10x image of brain tissue section around the hippocampus labelled for VSV antigen (brown) and counterstained with hemotoxylin (blue). Mice were primed i.p. 24h before i.c. challenge. The images shown here are from primed and mock primed brains taken 72h after i.c. challenge. Images were taken with Zeiss Axioskop 2 mot plus microscope using Northern Eclipse software.

A

	Time post i.c challenge		
	24h	72h	96h
PBS i.v			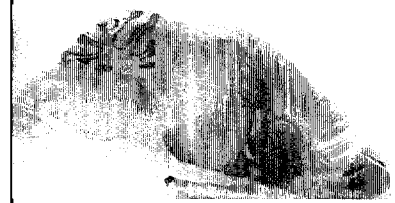
VSV i.v	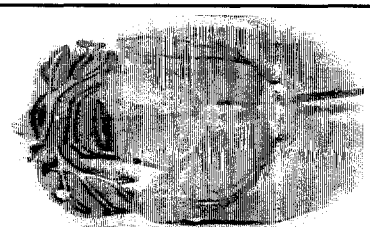	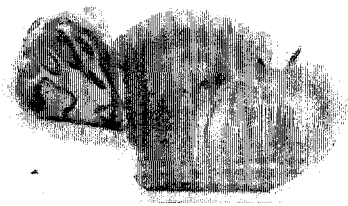	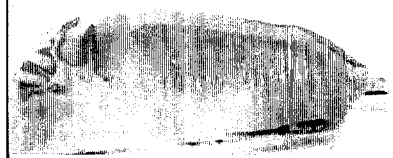

B

72h post i.c (5x)	
PBS i.p	VSV i.p
	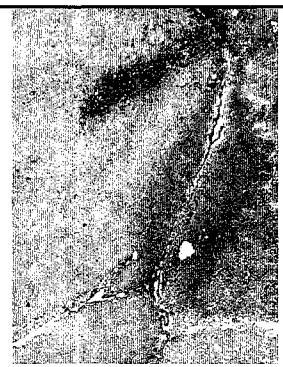

3.6 VSV infection of CNS cells

When wt VSV finds its way to the CNS, it has specific affinity for neurons and is neuropathogenic [17]and this property was not altered with the ΔM51-VSV virus. However, we documented that priming allowed mice to survive and this may be due to restricting infection of neurons. To determine if priming changed the type of cells that are infected by VSV, a double labelling immuno-fluorescence (IF) technique was used. The cell types tested were astrocytes/ependymal cells, microglial cells and neurons. *Figure 3.7* compares primed and mock primed brains at 72h post i.c. challenge that are double labelled for either VSV and anti- glial fibrillary acidic protein (GFAP) or VSV and ricinus communis agglutinin-1 (RCA-1). GFAP is a member of the intermediate filament family and provides support and strength to cells. Several molecules of GFAP oligomerize to form the main intermediate filaments in astroglial/ependymal cells [105]. RCA-1 is a lectin that binds to β –D-galactose residues and labels microglial cells and endothelial cells [106]. GFAP positive staining was seen around areas of VSV infection but did not directly overlap with VSV positive cells. GFAP expression was not seen in areas where there was no viral infection. RCA-1 positive cells were also not positive for VSV antigen indicating that these cells were also not the primary target of a VSV infection. As a negative control, primary antibody was omitted and confirmed that there was little or no non-specific binding taking place with either marker.

Figure 3.8 depicts double IF labelling of VSV and anti-NeuN. Anti-NeuN stains neuronal nuclei and some reactivity is also seen in the cytoplasm, dendrites and axon [105]. It reacts with most neuronal cell types except for Purkinje, mitral and photoreceptor cells [105]. As shown with IHC images, VSV infection was primarily seen around the hippocampus at 72h post i.c.. The

overlay of the individual stains indicated that VSV infected cells are also positive for NeuN in both the primed and mock primed brain sections. The 40x zoomed image of the CA1 region of the hippocampus (*Figure 3.8 B*) clearly showed an overlap of VSV positive cells and NeuN positive cells. From these images it was clear that although priming significantly reduces replication in neurons, it however does not alter neuronal targeting by ΔM51-VSV.

Figure 3.7: VSV does not infect neuroglia cells

10μm mouse brain sections were co-labelled for the astrocyte marker GFAP (red) and VSV antigen (Alexa 488 - green) or for the microglia and endothelial cell marker, RCA-1 (red) and VSV (green). Texas red fluorescent secondary antibody was used to label the cells while Alexa-488 secondary was used to label VSV. Hoechst counter-staining stains all nuclei blue. In both the VSV primed case (A – 10x) and the mock primed brains (B – 20x), no VSV positive staining was seen in astrocytes at anytime during brain infections. VSV also does not infect endothelial cells or microglial cells. All images were captured using the same parameters using the Zeiss Axioskop 2 mot plus epi-fluorescent microscope and Northern Eclipse software. No background staining is seen when the primary antibody is omitted ©.

	GFAP	RCA-1
A		
B		
C	 10x	 5x

Figure 3.8: Priming reduces but does not prevent VSV replication in neurons

10μm thick brain sections were taken from primed or mock primed mice 72h after i.c. infection with ΔM51-VSV-GFF-FLuc. Fluorescence antigen labelling of the brain sections were used to detect neurons (anti-NeuN) using Alexa-488 secondary antibody (green) and VSV antigen using Cy3 secondary antibody (red). Hoechst counter-stains all nuclei of every cell type blue. (A) Comparison of equivalent areas of infection in primed and mock primed brains. In the ΔM51-VSV primed case, VSV antigen staining overlaps with NeuN positive cells of the hippocampus indicating priming does not prevent VSV infection of neurons. As expected, in the mock primed case VSV positive cells also overlaps with neuronal cells. Therefore priming acts to restrict infection but does not prevent infection of neurons. PBS mock i.c. challenged mice show no VSV positive staining (lower left) and no background is seen when all primary antibodies are omitted (lower right) (B) depicts a 40x zoom of the hippocampus where it can be clearly seen that neurons are infected by VSV in both primed and mock primed brain sections. All images were initially captured using the identical parameters for each colour at the same magnification using a Zeiss axioskop 2 mot plus microscope and Northern Eclipse software.

A – 72h post i.c

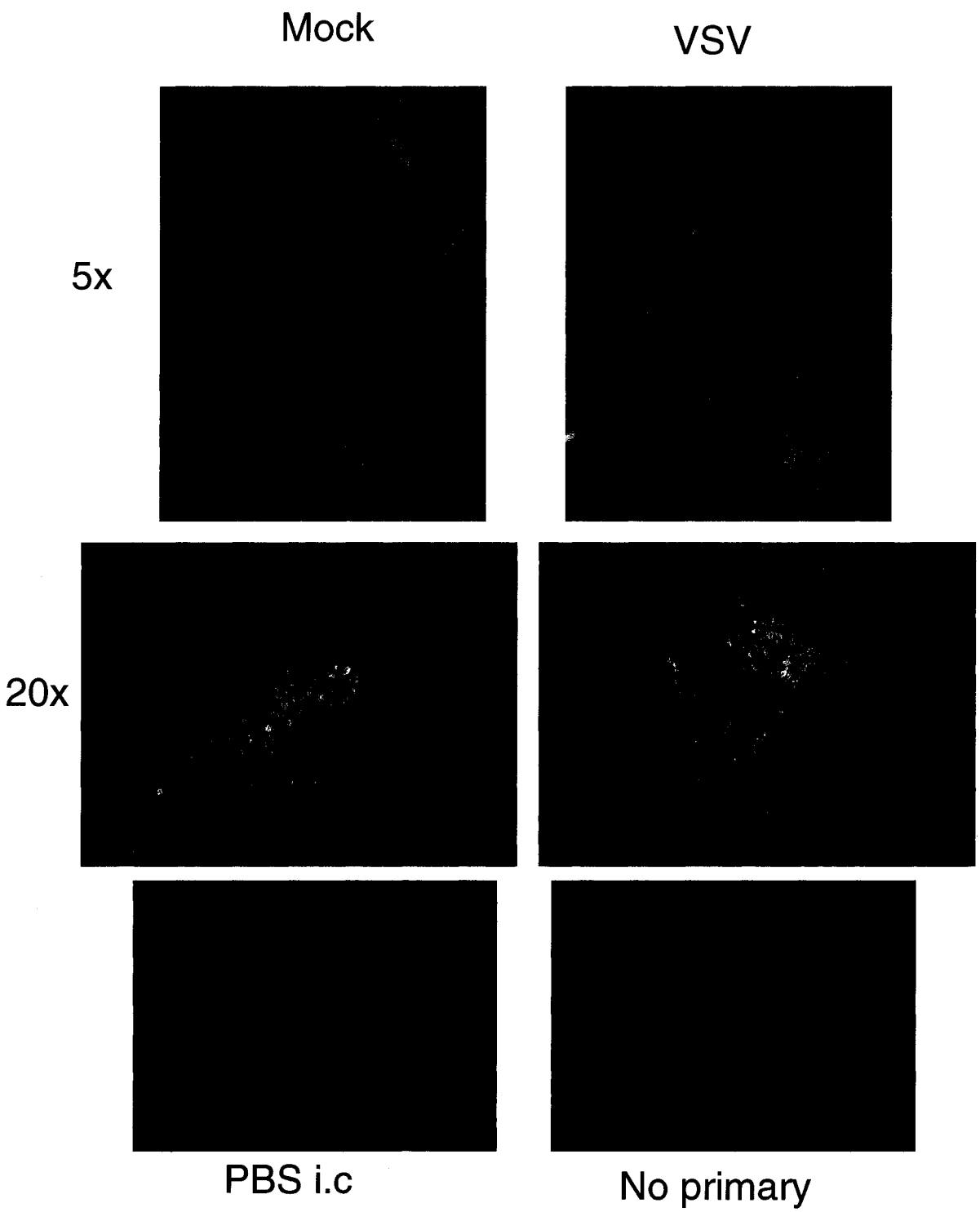

B

	anti-VSV	anti - NeuN	Hoescht	Overlay 40x
Primed	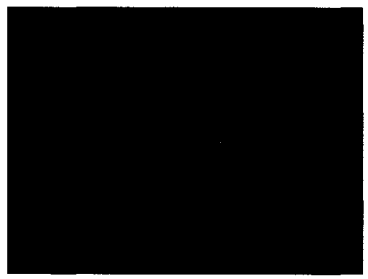		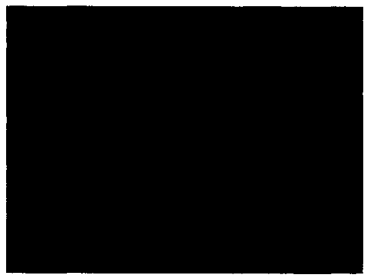	
Mock		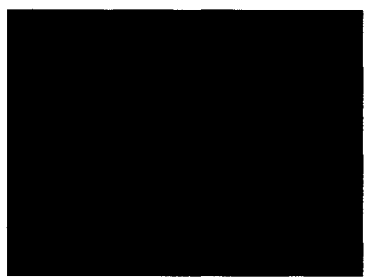		

3.7 Priming sensitizes the CNS to undergo apoptosis

Given the difference in outcome seen when mice were primed, we were interested to determine if priming affected VSV's ability to induce apoptosis of infected neurons. Brain sections from primed and mock primed mice were assayed by *in situ* fluorescent labelling of DNA breaks (TUNEL assay), a marker of apoptosis, and co-labelled with anti-VSV. At 24h, TUNEL positive cells were evident in primed but were even more abundant in the mock primed brain section (*Figure 3.9 A*). In both cases, apoptosis occurred predominately in cells of the ventricles, and at this snapshot in time, apoptotic cells did not overlap with VSV positive cells. In mock primed brains, extensive VSV infection was evident in the parenchyma near areas of apoptosis. Not many VSV infected areas were seen in primed brains and were concentrated in and around ventricles. However, by 72h post i.c. challenge, there were more apoptotic cells than VSV infected cells in the VSV primed brains (*Figure 3.9 B*). Apoptosis was only evident around areas of VSV infection and was not widespread throughout the section. On the other hand, mock primed brains still contained more VSV positive cells than apoptotic cells. Again, the majority of the TUNEL positive cells at this time point did not overlap with VSV infected cells. *Figure 3.9 C* compares the hippocampus and hypothalamus of primed and mock primed mice at 96h post i.c.. Here, apoptosis started to increase in mock primed brains whereas VSV infection decreased significantly in primed brains. In the hippocampus, very little VSV antigen was present in primed brains but apoptotic cells were still spread around the area of infection. In mock primed brain tissue, apoptosis was more evident in comparison to earlier time points but there continued to be a significant number of infected cells.

Figure 3.9: Priming induces more apoptosis around sites of infection

Brain sections (10μm) were taken from brains 24h, 72h and 96h after i.c. challenge with ΔM51-VSV-GFP-FLuc. All mice were i.p. primed with the standard priming dose of ΔM51-VSV-GFP or PBS. Sections were co-labelled for TUNEL (rhodamine - red) and anti-VSV (Alexa-488 - green). (A) shows that by 24h after i.c. challenge, there was intense VSV positive staining seen in the hippocampus (above left image) in mock primed brains with few spots of apoptosis in and around the ventricles (bottom left image). Not much VSV staining was seen in primed brains at this time point and only a few spots of apoptosis were seen. By 72h post i.c. challenge (B), more apoptosis was evident in the parenchyma of primed brains. In mock primed brains, apoptosis was still restricted to the ventricles and there were less apoptotic cells than VSV positive cells. 96h after challenge (C), the number of apoptotic cells increased in the mock primed sections while it decreased in primed brains. All images were taken with Zeiss Axioskop 2 mot plus using Northern Eclipse software using the same parameters.

A- 24h post i.c. challenge

VSV primed

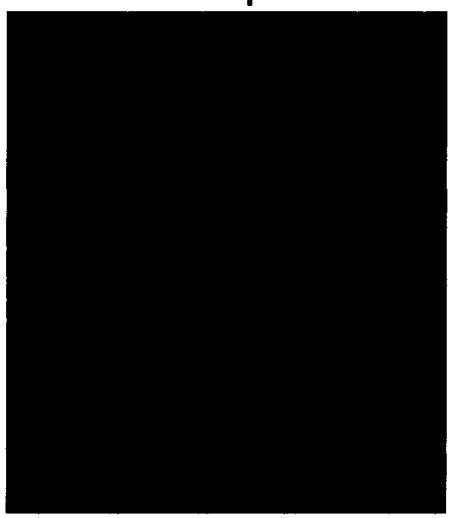

Mock primed

10x hippocampus

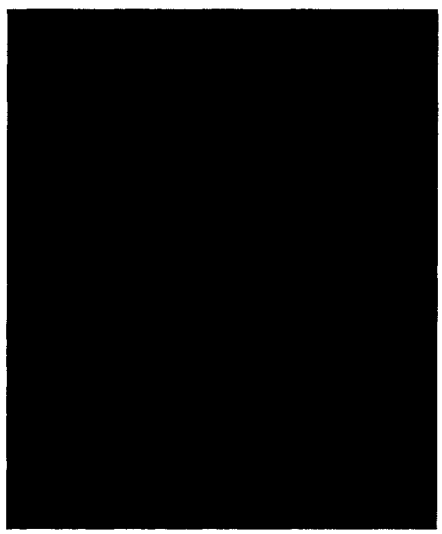

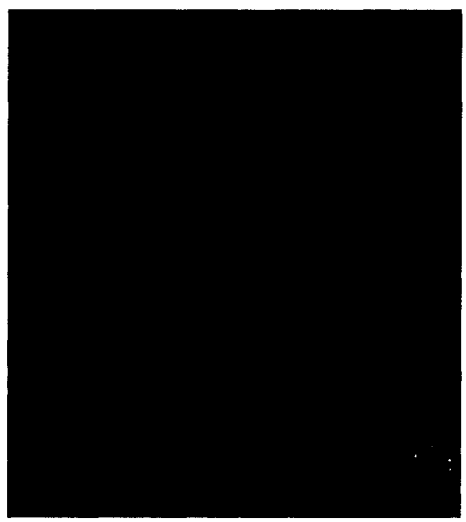

20x near ventricle

B – 72h post i.c. challenge

VSV primed

Mock primed

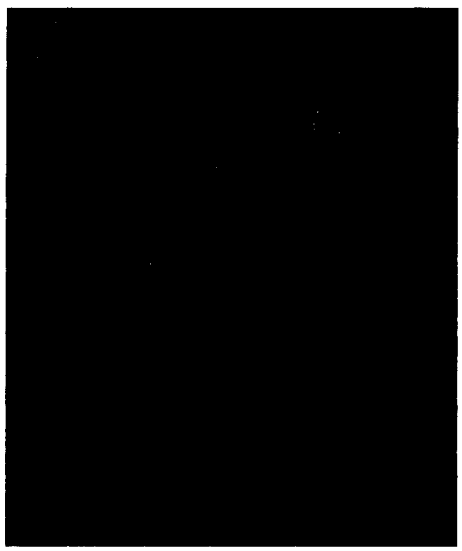

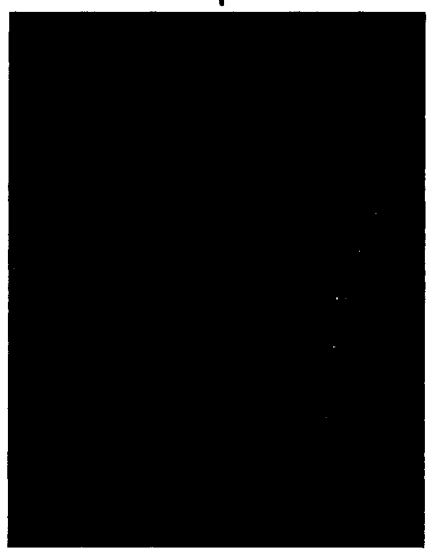

10x hippocampus

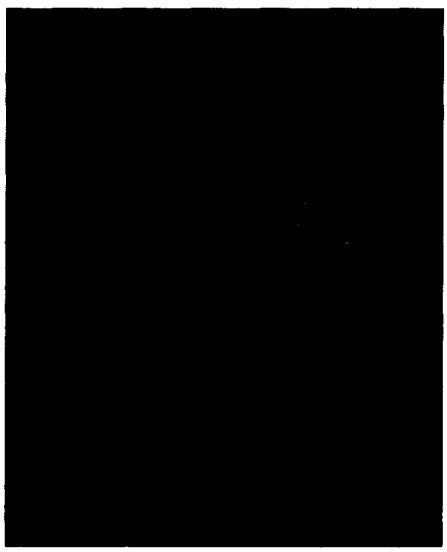

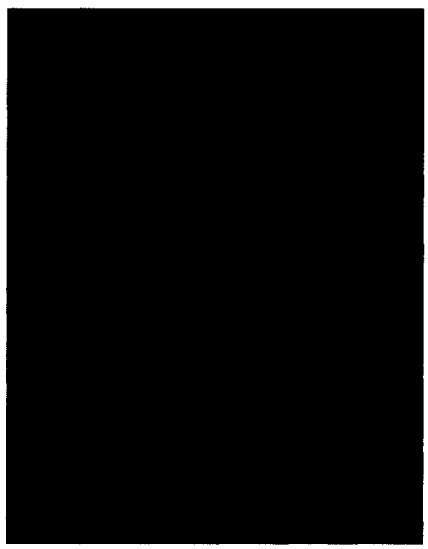

20x hippocampus

C – 96h post i.c. challenge

VSV primed

Mock primed

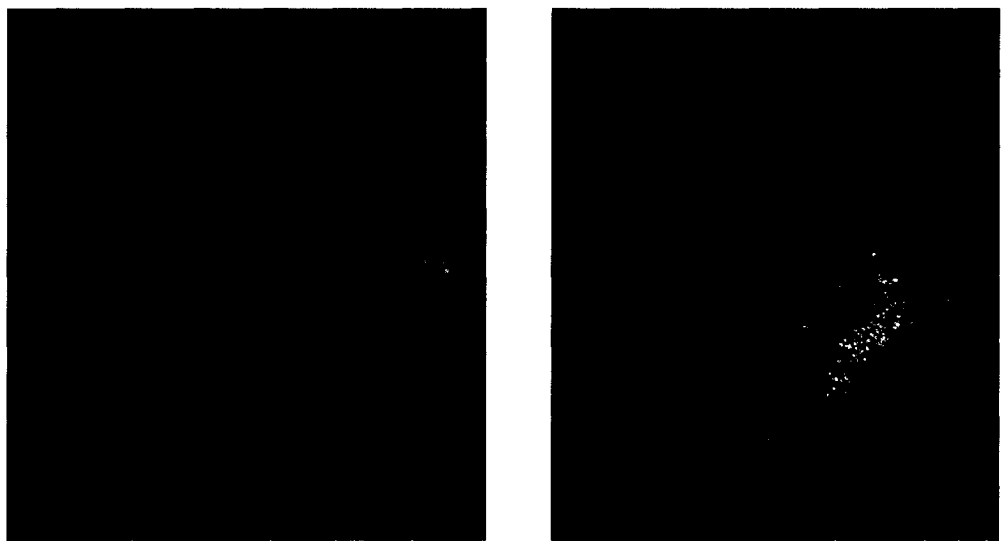

10x hippocampus

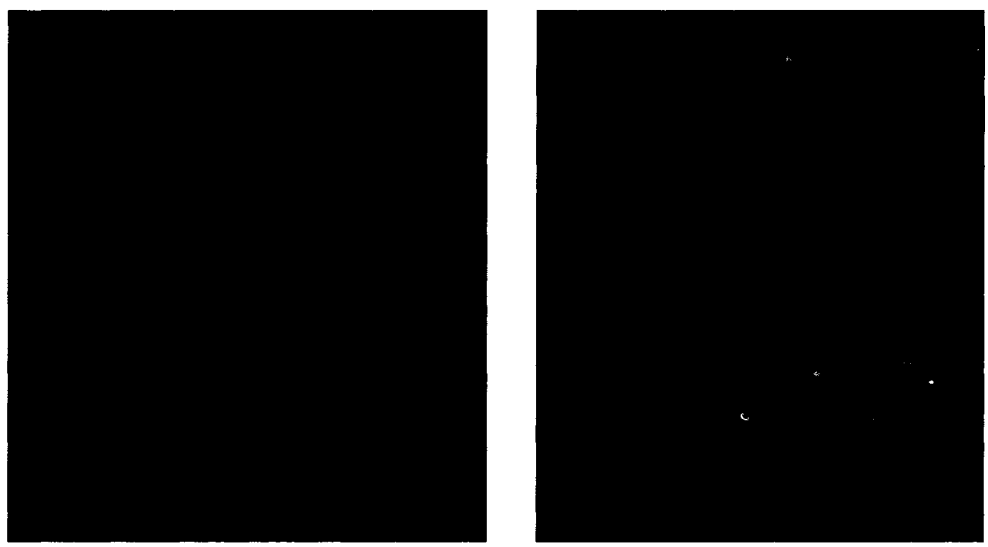

20x hypothalamus

Figure 3.10: VSV infected cells do not overlap with apoptotic cells

Images were taken of fluorescently labelled mouse brains that were i.c. challenged 96h after ΔM51-VSV-GFP primed or PBS mock primed via the i.v.. route. VSV positive cells were labelled using anti-VSV-G protein primary and Alexafluor-488 secondary antibody (green). TUNEL staining technique was used to label apoptotic cells using rhodamine (red). A) 20x section from a mouse brain mock primed with PBS. There were more cells positive for VSV antigen then apoptotic cells and there were only a few apoptotic cells that overlap with VSV staining (shown by the arrow). B) 20x section from a mouse brain VSV primed. There were significantly more areas that were apoptotic then infected with VSV. All the infected cells were not positive for apoptosis. In A and B, the pictures to the right are a zoomed view of what is outlined in the boxes. C) Negative control where VSV primed mice were i.c. challenged with PBS. There was no positive staining for apoptosis or VSV. D) VSV primed mouse, i.c. challenged with VSV where the primary antibody for VSV and the TUNEL TdT enzyme was omitted from the experimental setup. No background staining was seen. All images were taken with Zeiss Axioskop 2 mot plus using Northern Eclipse software using the same parameters for each fluorescent filter.

96h post i.c challenge

A Mock

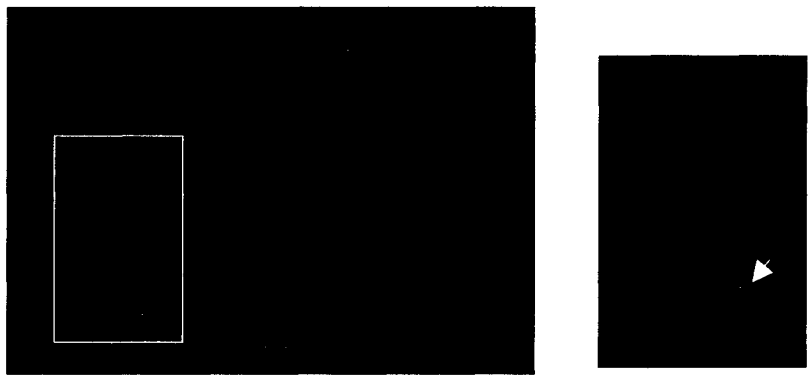

B Primed

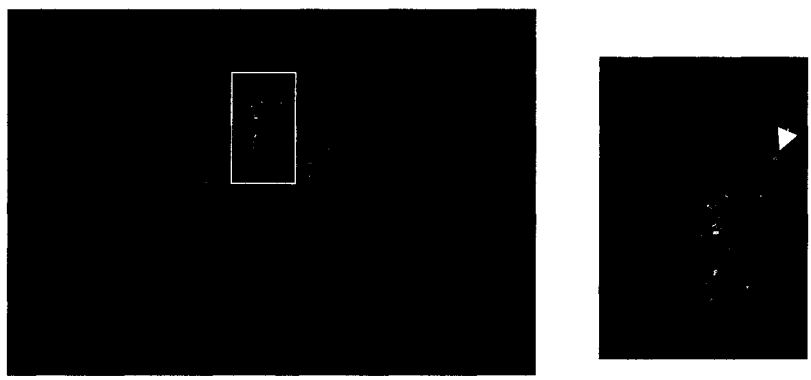

C

PBS i.c challenge

D

No Primary

Figure 3.10 also shows images taken at 96h post i.c. challenge but after i.v. priming. In this figure it was also seen that apoptosis was occurring in VSV rich areas in mock primed brains (*figure 3.10 A*), but again when looking at the primed section, TUNEL positive cells outnumbered VSV positive cells. Magnification of infected cells indicated that most of these cells were not undergoing cell death at that time but apoptosis was occurring in neighbouring cells not positive for VSV. There were some instances where in both mock primed and VSV primed brains, some infected cells were also apoptotic (see *figure 3.10* inserts), but these double positive cells were in the minority. From all sections examined at various time points past 24h post i.c. challenge, VSV primed brain sections always correspond with more apoptotic cells near the area of infection, whereas mock primed brains show a higher ratio of VSV infected cells than to apoptotic cells. PBS i.c. challenged mice were used as controls and show no indication of apoptosis (*figure 3.10 C*).

3.8 VSV brain infection, apoptosis, and resident CNS cells

As with determining the type of CNS cells infected by VSV, the type of cells undergoing apoptosis was also analyzed. TUNEL and the individual cell markers for astrocytes, microglia/endothelial cells and neurons were assayed. *Figures 3.9* and *3.10* illustrate that initially at 24h post i.c., TUNEL positive cells were seen in the ventricle areas where VSV infection was first found and by 96h post i.c. challenge, apoptosis was more evident in the parenchyma when primed. Apoptosis in the parenchyma was not as extensive in mock primed brains at later time points. The top panel of *figure 3.11* indicates that TUNEL positive cells did not overlap with GFAP staining but GFAP expression was predominantly seen surrounding areas of apoptosis. The bottom panel is a 20x image taken of an RCA-1 and TUNEL co-labelled section. Microglia

were also not undergoing apoptosis at this time-point. Negative control slides (no primary antibody) indicate that non-specific binding was minimal.

Figure 3.12 A and *3.12 B* are representative images of brains primed i.p. either with PBS or VSV and labelled with anti-NeuN and TUNEL. Again, more apoptosis was seen in sections where the mice were primed with virus and was more evident in areas away from the ventricle. Mock primed section only had apoptotic cells within the ventricle. *Figure 3.12 B* illustrates a 40x zoom of areas of apoptosis from primed and mock primed mice. The image taken for the mock primed section is of an apoptotic area near the ventricle. The hippocampus is shown for the VSV primed section. From the overlay, it seems that the TUNEL positive red cells did not overlap with the NeuN positive green cells. The TUNEL positive cells were shrunken and also stained very weakly for Hoechst, a DNA binding fluorescent molecule.

Figure 3.11 Apoptosis of CNS glial cells

I.v. Primed or mock primed brain sections were assayed for apoptosis (TUNEL- green) and co-labelled for astrocytes or microglia cells. Astrocytes were detected using the anti-GFAP primary and using Cy3 (red) as the secondary. Microglia were detected using biotin conjugated RCA-1 primary antibody coupled with a streptavidin conjugated Texas red secondary. The images shown were from primed brain sections taken 96h after i.c. challenge. There was no overlap seen with GFAP positive cells or RCA-1 positive cells and TUNEL positive apoptotic cells. GFAP positive astrocytes were seen predominately surrounding areas of apoptosis whereas RCA-1 positive microglia cells were detected in areas of cell death. Negative control sections where the primary antibody or the TUNEL Tdt enzyme was omitted indicated that there was minimal non-specific background staining.

96h post i.c. challenge

GFAP + TUNEL 20x

No primary

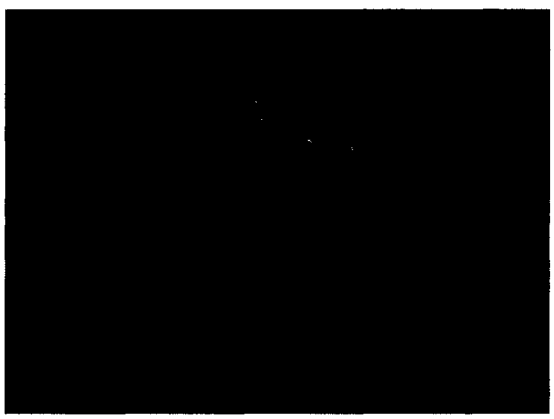

RCA-1 + TUNEL 20x

No primary

Figure 3.12: Apoptosis of neurons

72h after i.c. challenge of i.p. primed or mock primed mice, brain sections were co-labelled for apoptosis (red) using the TUNEL assay and neurons using anti-NeuN and Alexafluor 488 secondary antibody (green). A) 20x image of hippocampus area where VSV infection was usually seen. In mock primed brains apoptosis was seen predominately in the ventricles but was evident in the parenchyma as well as the ventricles in primed brain section. TUNEL positive cells were not seen with PBS mock i.c. challenged brain sections (lower right image) and there was no non-specific staining seen when primary antibody was omitted (lower left image). B) 40x zoom of the ventricle area of mock primed section and of the hippocampus for the primed section. There is no overlap of apoptotic cells and NeuN positive cells. All images were taken using the Zeiss Axioskop 2 mot plus epi-fluorescent microscope using Northern Eclipse software.

A – 72h post i.c. challenge

VSV primed

Mock primed

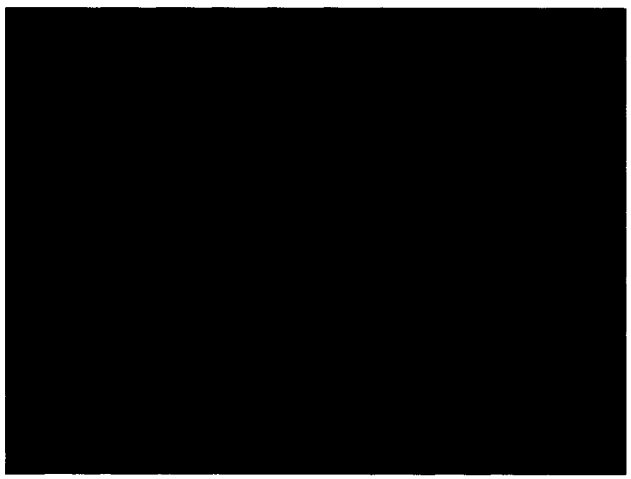

No primary

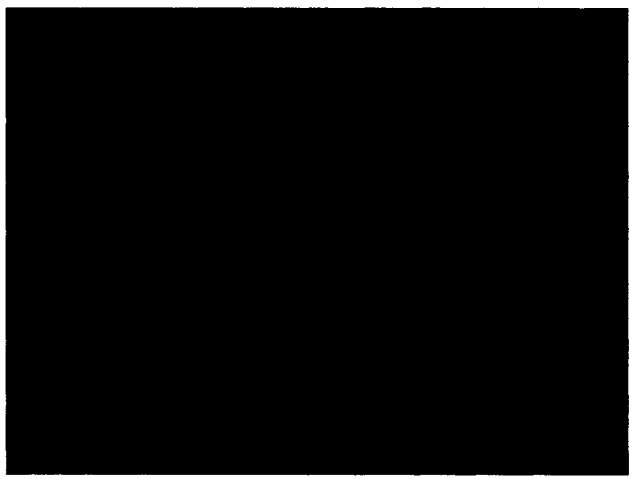

Mock challenged

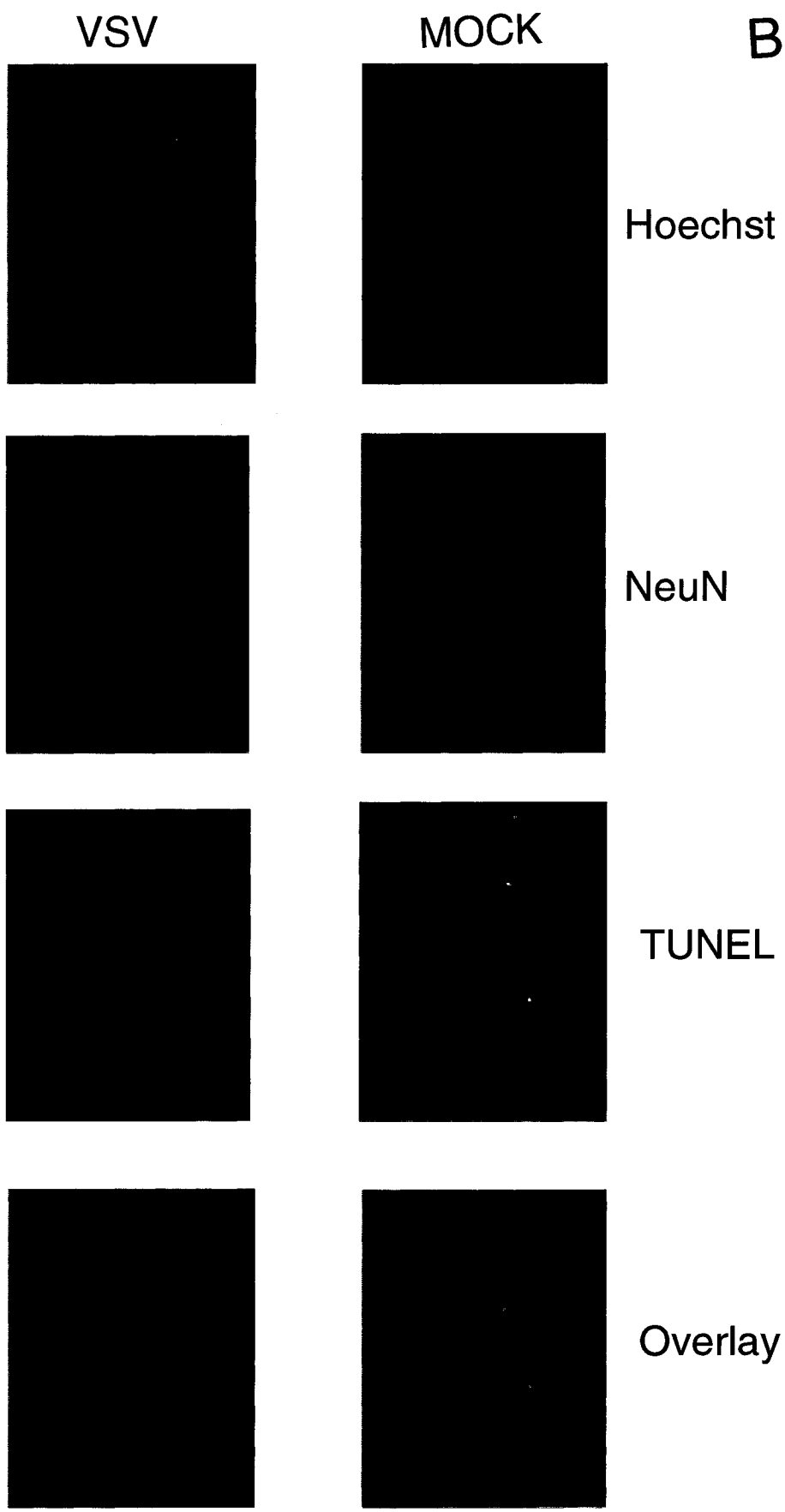
VSV
MOCK
B
Hoechst
NeuN
TUNEL
Overlay

CHAPTER 4: RESULTS - FACTORS INVOLVED IN PRIMING INDUCED PROTECTION

Our initial work focused on assessing priming induced CNS protection. Although the neuro-pathogenic nature of VSV has previously been described, we have shown that priming mice prior to a brain infection does in fact protect the brain from viral induced fatality. Although priming does not alter VSV's affinity for neurons, it accelerates the rate and amount of cell death occurring at the site of infection. Another fundamental result was the kinetics of protection. Others have put importance in the adaptive immune system in preventing VSV induced encephalitis, but we have shown that with our mutant ΔM51-VSV that priming induces CNS protection as early as 12h. At this early time, it seems unlikely that the adaptive immune response is solely responsible for immune mediated clearance of virus from the CNS. This leaves us with a fundamental question – what are the host factors involved in clearing the CNS of ΔM51-VSV infection and therefore preventing fatality?

4.1 Infiltrating immune cells are not involved in CNS protection or pathology

Experiments characterizing wt VSV infection in the CNS via an i.n. challenge indicate that B-cells are not seen in CNS until day 14 post infection. At this time, surviving mice are recovering from the infection and viral antigen is not detected in these brains [97]. It has also been established that neutralizing early IgM (induced by day 3 post infection) or late IgG antibody response are only effective in preventing viral spread to the CNS but is not effective in protecting mice once virus has already gained access to neural tissue [38].

Figure 4.1: IHC to detect infiltrating immune cells into the brain

Mice were i.c. challenged with ΔM51-VSV-GFP-FLuc 24h after i.v. priming with ΔM51-VSV-GPB or PBS. Brains were harvested over a time course after i.c. challenge and processed for IHC analysis. The images shown here are from sections assayed for the presence of T-cells (anti-CD3 ε) and for B-cells (anti CD45 receptor) from brains taken at 6 days post i.c. challenge. Control sections where mice were mock challenged with PBS after priming showed that B-cells or T-cells are not seen in brains that are not virally infected (20x images). B-cells were also not seen in primed or mock primed brains that were challenged with VSV at this time (20x images). However, T-cells were present in both primed and mock primed brains 6 days after VSV i.c. challenge (40x images). T-cells were not seen in the brain prior to this time (not shown). The positive control (spleen) indicates that the antibody we use here was able to detect B and T cells (10x). All images were taken using Zeiss Axioskop 2 mot plus and Northern Eclipse software using the same parameters.

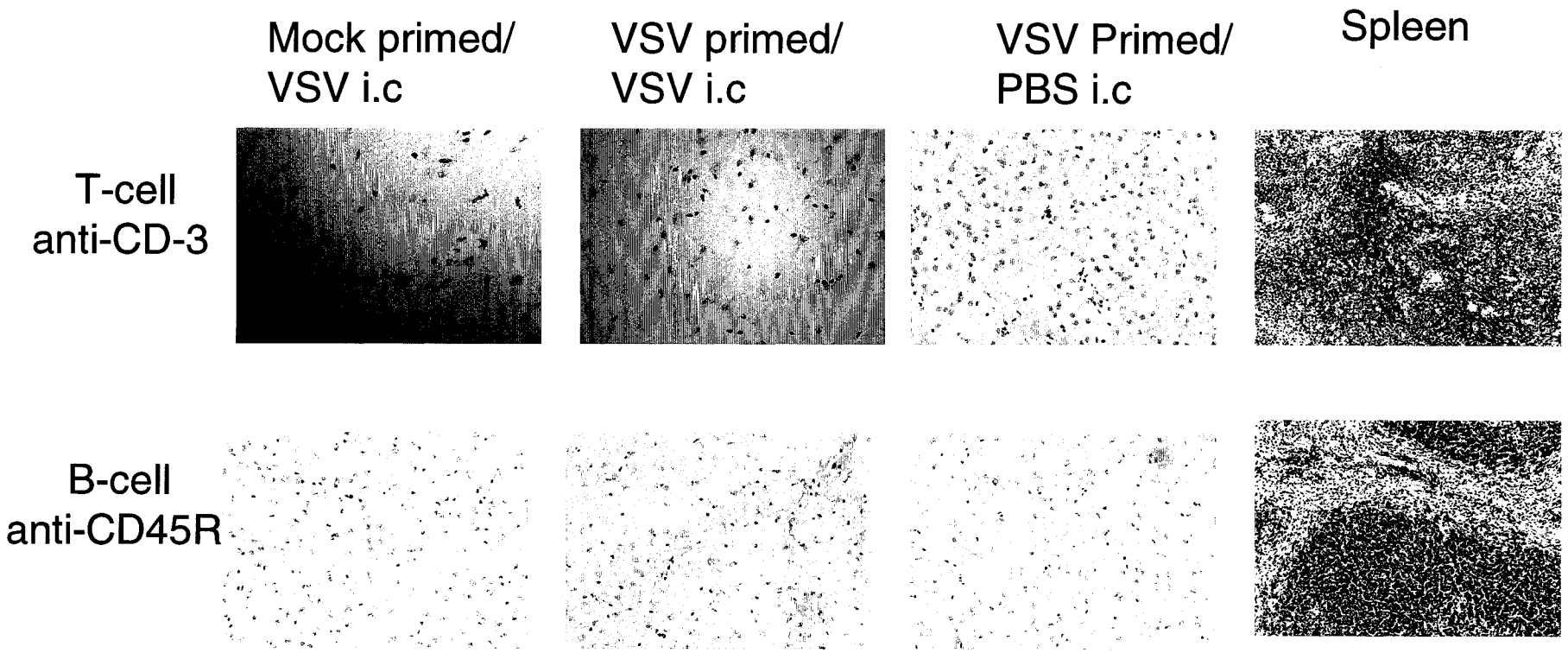
Mock primed/
VSV i.c
VSV primed/
VSV i.c
VSV Primed/
PBS i.c
Spleen
T-cell
anti-CD-3
B-cell
anti-CD45R

Priming experiments with wild-type virus three days prior to an i.c. challenge with 1000 pfu of wt VSV have shown that although a robust antibody response is detected in the serum, the mice still succumb to lethal encephalitis [38]. We therefore wanted to determine if there was a role for B-cells in our model of CNS infection and priming. Brains and spleen were harvested from primed or mock primed mice and processed for IHC analysis to detect CD45R positive cells. CD45R is a surface molecule and that is mainly expressed by the B-cell lineage. *Figure 4.1* (bottom row) indicates that CD45R immunoreactivity is not detected in any of the brain sections by day six of infection, but was detected in the spleen (positive control). Priming did not cause B-cells to infiltrate into the CNS during our time course of infection and thus local antibody production is an unlikely mechanism induced in explaining the limited VSV infection of the CNS.

Previous data has shown that CD8+ T cells are seen in the OB as soon as 1 day after i.n. challenge with VSV and CD4+ T-cells soon follow [97]. We looked for T-cells in the brains of mice to see if we could detect similar patterns of infiltration with ΔM51-VSV. *Figure 4.1* reveals that CD3, a pan T-cell marker, was detected in the brains of both mock primed and virally primed mice only six days after i.c. challenge. T-cell immunoreactivity was never seen prior to this time point in any of the sections examined (data not shown). By the sixth day of infection, primed mice had cleared the virus while mock primed animals had either developed HLP or were close to paralysis. CD3+ cells were not detected in control PBS i.c. challenged mice but were detected in the spleen (positive control).

4.2 Factors in serum neutralize VSV *in vitro*

Although B-cells were not detected in the brain after an i.c. infection with ΔM51-VSV, peripheral antibody production can have effects in the CNS. Blood was collected 24h after priming and tested for the ability to neutralize VSV *in vitro*. Mock primed mouse blood was also collected 24h after PBS priming to serve as the antibody-free negative control. Blood that was known to have antibodies against VSV was obtained from mice that had previously survived a priming experiment (2 month survivors). Plasma samples were collected from three mice from each group (primed, mock primed, positive control) and were incubated with serial dilutions of ΔM51-VSV-GFP or media (α-MEM). All plasma samples were diluted 100-fold in α-MEM. The virus-plasma/control mixture was incubated on VERO cells overnight and plaques were counted the next day. Normal mouse plasma did not neutralize the VSV (177 plaques) and neither did VSV primed plasma at 24 hour post priming (178 plaques) (*Table 4.1 B*). This same result was obtained from mice that were i.v. primed (*Table 4.1 A*). The positive control serum incubated with VSV resulted in no plaque formation indicating that mice that had previously survived an i.c. infection carried factors in their plasma that were able to neutralize VSV. Therefore, at the time of the challenge (24h post priming), there were no factors present in the blood capable of neutralizing VSV.

Table 4.2 summarizes the plaque reduction ability of primed and mock primed plasma obtained 24h and 48h post i.c. challenge. This corresponds to plasma at 48 and 72 hours post priming. At 24h post i.c. (48h post priming), the mock primed plasma plaque value is comparable to VSV incubated with α-MEM or normal mouse plasma (both at about 400 plaques).

Table 4.1: There are no factors in the blood within 24h after priming that neutralizes VSV

Plasma collected from mice 24h after priming with ΔM51-VSV-GFP or PBS was incubated with different dilutions of stock ΔM51-VSV-GFP. These mice were never i.c. challenged. The virus – plasma mixture was incubated on VERO cells overnight and plaques formed were counted the next day and shown here. Virus was also incubated with sham media to serve as the negative control. Plasma obtained from mice who had previously survived a priming-challenge experiment was used as the positive control since they should carry neutralizing antibody against VSV. Table A indicates the average plaque counts (n= 2) from virus incubated with plasma taken from mice i.v. primed and table B shows the plaque counts from mice i.p. primed (n= 2) and incubated with AV1 VSV. While no plaques were seen when the virus was incubated with positive serum (contains VSV neutralizing antibodies), plasma from 24h primed mice show no VSV neutralizing ability. As expected, mock primed serum also does not neutralize VSV.

* indicates an estimated plaque count

A

	Plaque Counts			
ΔM51 GFP-FLuc Dilution factor	ΔM51 GFP-FLuc + α MEM	ΔM51 GFP-FLuc + 24h post i.v PBS	ΔM51 GFP-FLuc + 24h post i.v ΔM51-VSV	ΔM51 GFP-FLuc + positive serum
10^{-8}	500*	500*	500*	0
10^{-9}	60 ± 11.3	38.0 ± 4.2	55.5 ± 4.9	0
10^{-10}	6.5 ± 3.5	7 ± 2.8	5.5 ± 3.5	0

B

	Plaque Counts		
AV1 Dilution factor	AV1 + 24h post i.p PBS	AV1 + 24h post i.p VSV	M2 + positive serum
10^{-8}	177.0 ± 2.82	178.5 ± 14.9	0
10^{-9}	32.5 ± 2.12	18 ± 2.8	0
10^{-10}	4.0	3.5 ± 0.7	0

Table 4.2: VSV neutralizing factors are present in the blood 48h after virus inoculation

Mice were primed or mock primed i.p. and then i.c. challenged with ΔM51-VSV-GFP-Fluc 24h priming. Mice were sacrificed either at 24h (n= 3) or 48h (n= 3) after challenge and plasma was assayed to test for its ability to neutralize VSV. Plasma was incubated with different dilutions of AV1 VSV. AV1 VSV was also incubated with media, normal plasma from uninfected mice and positive control plasma from previously primed and challenged mice to serve as controls. Plasma or media and virus were incubated together then plated on VERO cell lines overnight and plaques were counted the next day. Positive control serum was able to neutralize AV1 at all dilutions whereas (last column) media and normal mouse plasma had no neutralizing ability (column 2 &3). 24h post i.c., primed plasma had some neutralizing ability that was amplified by 48h. Mock primed plasma has no VSV neutralizing ability 24h after challenge but showed immense plaque reduction 48h after challenge. Regardless of route of infection, neutralizing factors form in the serum 48h after virus infection.
v-v – ΔM51-VSV-GFP primed/ΔM51-VSV-GFP-FLuc i.c. challenge
p-v – PBS primed- ΔM51-VSV-GFP-FLuc i.c. challenged
α-MEM – media
* indicates estimated plaque count

	Plaque Counts						
AV1 Dilution factor	AV1 + α-MEM	AV1 + normal mouse plasma	AV1 + 24h p-v plasma	AV1 + 24h v-v plasma	AV1 + 48 p-v plasma	AV1 + 48 v-v plasma	AV1 + positive plasma
10^{-8}	350-400*	350-400*	350-400*	96.7 ± 47.1	125.7 ± 28.8	17.7 ± 8.7	0
10^{-9}	42.0 ± 11.1	50 ± 7.6	52 ± 8.7	5.0 ± 1.0	11.3 ± 3.2	1.7 ± 0.6	0
10^{-10}	3.7 ± 0.6	2.3 ± 0.6	3.7 ± 2.1	0	0.33 ± 0.6	0	0

However, VSV primed plasma results in a significant reduction in plaque numbers (97 plaques). Neutralizing factors therefore accumulated in the blood 48h after priming with virus. At 48h post i.c. (72h post i.p.) there was an even greater reduction in plaque formation (18 plaques). Mock primed plasma only started to show virus neutralizing properties 48h after i.c. challenge (126 plaques). Comparing the plaque numbers from plasma at 24h post i.c., VSV primed and 48h post i.c., mock primed (97 vs. 126), it indicates that 48h past virus infection in mice, regardless of route (i.p. vs. i.c.), VSV neutralizing factors start to be produced and are carried in the blood.

4.3 T- Cells are not involved in CNS protection or pathology

Although we did not detect T-cells in the brain until 5 days after virus challenge, T-cells can exert effects in the brain from the periphery. To conclusively determine if educated T-cells play a role, nude mice (CD-1 nu/nu) were primed and challenged. Nude mice are born without a thymus and therefore cannot generate mature T-cells but do carry peripheral T-cells. This restricts these mice from producing certain types of immune responses such as antibody formation requiring T helper cells, cell mediated immune responses and killing of virus infected or malignant cells that require CTLs [107]. Nude mice were i.p. primed or mock primed and then i.c. challenged 48h later. Mice were imaged 24h after challenge and visually assessed. IVIS images taken of the mice are shown in *figure 4.2*. The top panel represents ΔM51-VSV primed nude mice. These primed mice showed very little viral replication by 24h post challenge. Although signal increased slightly at 72-120h after challenge, virus replication was never detected in the spine.

Figure 4.2: T-cells are not involved in priming induced CNS protection

CD-1 nude mice were primed i.p. with $2x10^8$ pfu/100ul ΔM51 VSV-GFP (n=3) or 100ul sterile PBS (n=3). 48h after priming, both groups were challenged i.c. with $2x10^7$pfu/5ul ΔM51-VSV-GFP-FLuc. IVIS imaging commenced 24h post i.c. challenge and continued until 168h post i.c. Primed mice were able to clear the virus and survived the i.c. challenge, whereas the mock primed mice showed intense VSV replication in the head with subsequent spread to the spinal cord. One mock primed mouse developed HLP by 120h post i.c. and the remaining 2 showed HLP by 168h post i.c. challenge. The scale bar shown on the right indicates the total amount of photon flux emitted from the mice according to the colour scheme.

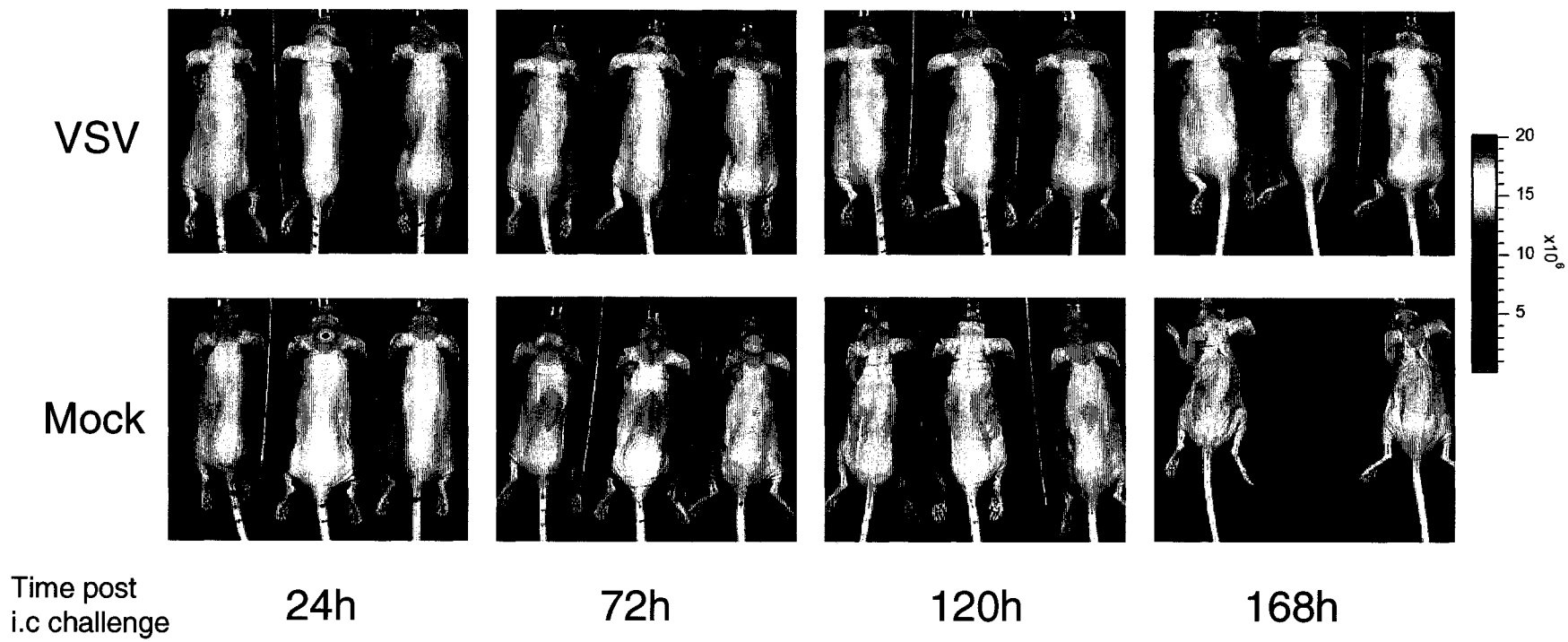
VSV
Mock
20
15
10
5
x10⁶
Time post
i.c challenge
24h
72h
120h
168h

Signal was still present in two of the three mice at 168h post challenge, but the mice were active and maintained a healthy weight. All primed nude mice survived the i.c. challenge and lived past 15 days. Mock primed mice showed significantly more signal at 24h post challenge in comparison to the primed mice. By 72h after challenge, VSV was detected in the spine of the mock primed mice and they had also lost a significant amount of weight. The mice with the most signal at 24h (middle) was the first to develop HLP and did not survive past 5 days post challenge and by 7 days after challenge, the remaining 2 mice were dragging both hind legs. The significant weight loss that occurred when mice were mock primed was more evident in nude mice. At the fifth day post i.c. challenge, all mock primed mice had extensive wrinkly skin due to the extreme weight loss and their hunched spinal cords were visible. Primed mice initially lost some weight in the first couple of days after challenge but quickly recovered to a healthy status.

4.4 Interferon expression in VSV infected Balb/c mice

The above results indicate that CNS protection induced by systemic priming with ΔM51-VSV did not require T-cells to propagate and sustain the priming effect. B-cells were never seen infiltrating into the brain over the course of the protective phenomenon and there were no factors in the serum within 24h after priming that are able to neutralize the virus. Combined with previous data indicating that protection commences as early as 12h post priming, it seems likely that the innate immune system is primarily involved in protection. IFN is an antiviral protein, and its rapid induction is an important host defence mechanism against most viral infections in the periphery [25]. Although treatment of mice injected i.n. with VSV with exogenous IFN-α (6.4×10^6 U/day) produced only marginal survival [32], ΔM51-VSV might be more sensitive to the antiviral effects of IFN. However, we wanted to first determine the kinetics and amount of IFN produced

in mice after an i.p. verses i.c. injection of the recombinant ΔM51 VSV. The induction of IFN α, β, and γ in the serum and CSF of primed and mock primed mice was assayed using ELISA. Samples were collected from mice 6h and 12h after i.p. or i.c. injection with ΔM51-VSV (3 mice per time point). Controls included serum and CSF collected at 6h and 12h from mice i.c. injected with PBS or UV inactivated AV1 VSV. *Figure 4.3* depicts the kinetics of induction of various IFNs after ΔM51-VSV infection. The average of three individual samples was used for serum values while only 2 samples were processed for CSF due to the minute quantities available. There was no induction of any IFNs in the serum or CSF when mice were i.c. injected with PBS or UV irradiated AV1 VSV.

Figure 4.3A shows that IFN-γ was only induced in the serum, and was not detected in the CSF. Six hours after i.p. injection with ΔM51-VSV, IFN-γ levels reached peak levels at 3166pg/ml, and by 12h levels decreased slightly to 2389 pg/ml. The opposite trend was seen when mice were i.c. injected with virus. At 6h, IFN-γ levels averaged 436pg/ml but rose to 2136pg/ml by 12h post i.c. injection. Although significantly more IFN-α was induced in the blood, the same trend was observed. Serum levels of IFN-α reached a peak at 6h post i.p. injection with VSV (149 022pg/ml) and decreased by 12 h post i.p. (35 473 pg/ml) (*figure 4.3 B*) whereas when i.c. injected, levels started off low (1558.1 pg/ml) but rose by 12h (10 548 pg/ml). IFN-α was detected in the CSF following the same trend seen in the blood when i.p. injected. IFN-α was not detected in the CSF using our techniques when mice were i.c. injected. IFN-β values were detected in the serum when VSV is delivered both i.p. and i.c. but only in the CSF when VSV was delivered i.c. (*figure 4.3C*). Following the pattern seen with the other two IFNs, within 6h of i.p. injection, serum levels of IFN-β reached 23 234 pg/ml and then decreased to 1067.2 pg/ml.

Figure 4.3: Induction of interferon after various routes of infection with ΔM51-VSV

Mice were i.p. primed with ΔM51-VSV-GFP and blood and CSF was collected at 6h (n=3) and 12h (n=3) after infection. Another set of mice were i.c. challenged with either ΔM51-VSV-GFP, UV inactivated AV1 or PBS and blood and CSF were collected at 6 and 12h after infection (n=3 for all groups). ELISA was carried out on all samples to analyze levels of IFN-γ (A) IFN- α (B) and IFN-β (C). No detectable levels of any IFN was seen when mice were i.c. challenged with PBS or UV irradiated AV1. All values are shown in pg/ml of blood or CSF. The average of three data points are shown for blood IFN levels but only the average of two values are shown for the CSF.

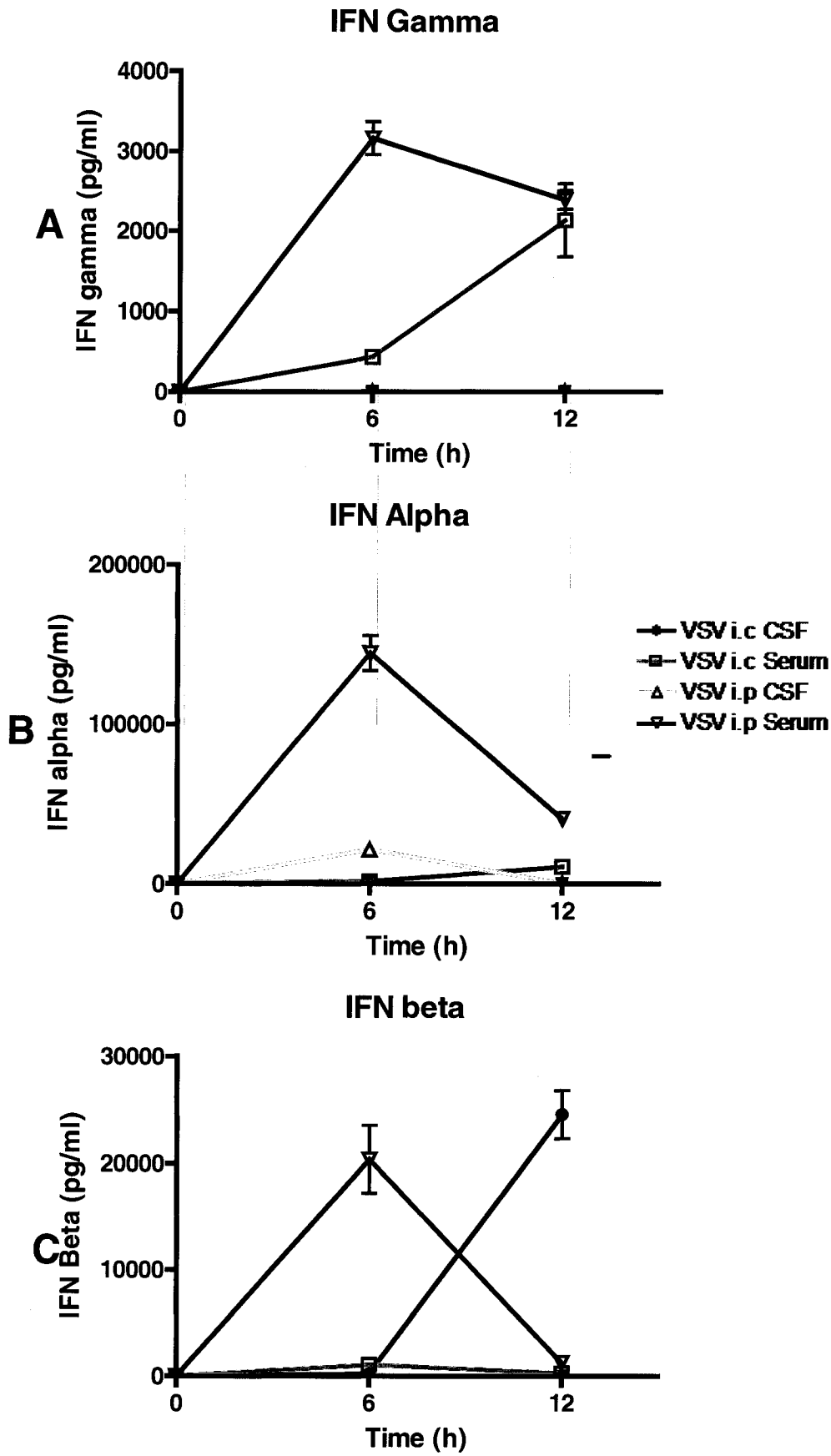
IFN Gamma
A
IFN gamma (pg/ml)
4000
3000
2000
1000
0
0
6
12
Time (h)
IFN Alpha
B
IFN alpha (pg/ml)
200000
100000
0
0
6
12
Time (h)
VSV i.c CSF
VSV i.c Serum
VSV i.p CSF
VSV i.p Serum
IFN beta
C
IFN Beta (pg/ml)
30000
20000
10000
0
0
6
12
Time (h)

However, when i.c. injected, serum levels start at 1052.2 pg/ml and continue to decrease (271pg/ml). In the CSF, a vast amount of IFN-β was induced when mice were i.c. injected. At 6h, the value in the CSF was only 123 pg/ml but climbs to 24 560 pg/ml by 12h. IFN-β was not detected in the CSF when virus was i.p. injected.

4.5 The role of interferon in protecting Balb/c mice from a VSV brain infection

Upon priming, serum IFN-α elevates to high levels within 6 hours and starts to decline afterwards and the same trend was detected for IFN-α in the CSF. To test if the protection induced by priming was strictly an IFN-α antiviral response that started in the blood and then diffused into the brain, exogenous human recombinant IFN-α (universal type I IFN) was used to treat mice prior to an i.c. challenge with ΔM51 VSV-GFP-FLuc. Two different attempts were made to pre-treat the mice with IFN-α. In the first preliminary experiment (IFN low group), Balb/c mice were i.p. injected with 20,000 U of IFN-α or PBS 24h prior to receiving an i.c. injection of the standard challenge dose of ΔM51 VSV-GFP-FLuc. On the day of challenge, 10,000 U of IFN-α was also administered i.p. just prior to the i.c. challenge with virus. Control mice were dosed with PBS. 24h post i.c. injection; the mice were again given 10,000 U of IFN α or 100ul PBS and then were imaged that same day. Positive control mice were given the regular dose of ΔM51 VSV-GFP 24h prior to the i.c. injection. The results of this experiment are presented in *figure 4.4* in the form of a survival curve. In the IFN treated group, one mouse died 4 days after the i.c. challenge and the other developed HLP at day 5 after the challenge. In the mock treated group, one mouse was dead at day 5 while the remaining mouse had developed HLP (data not shown). The positive control ΔM51-VSV primed mice all survived the i.c. challenge. The

experiment was repeated but this time more mice were treated with IFN α at a higher dose. This group (IFN high group) received 20,000 U of IFN α for all three i.p. treatment injections. A PBS treated negative control group, and a ΔM51-VSV primed positive control group were again used. These mice were not imaged and were only assessed based on survival. *Figure 4.4* shows that by day 6, one of the IFN treated mice reached endpoint and the remaining three succumbed by day 7. All PBS treated mice died while the VSV primed mice survived.

The exogenous treatment with IFN-α did not provide any protection against ΔM51-VSV infection of the brain. To confirm this result, mice were primed with a virus that is known to provide a robust IFN-α response, Respiratory Enteritic Orphan virus (Reovirus) [108, 109]. In mice, i.n. inoculation of Reovirus (Type 3 Dearing) is the most effective route of entry that results in a productive infection (personal communication); therefore mice were primed with 1 x 10^7 pfu/50ul by i.n. inoculation. At this dose and route, Reovirus is not pathogenic in mice. The i.c. challenge with ΔM51-VSV was given 48h after priming with Reovirus. Control mice were primed with PBS or ΔM51-VSV via the i.p. route and challenged 48h later. The survival data in *figure 4.4* show that by day 4 post i.c., one mouse primed with Reovirus reached endpoint, another died at day 5 and by day 6, the last mouse had developed HLP. The mock primed mice all died while the VSV primed mice survived (data not shown). To eliminate the possibility that the i.n. route could lead to Reovirus leaking into the brain and thus aggravated the ΔM51-VSV i.c. infection, mice were again primed with Reovirus but via the i.p. route. 1x 10^8 pfu/100ul of Reovirus was administered i.p. into Balb/c mice. We had previously determined by ELISA that this dose of Reovirus produces approximately 20 000 pg/ml of IFN-α within 6h of i.p. injection.

Figure 4.4: IFN treatment does not protect mice from i.c. challenge with VSV

A) Survival data from experiments in which exogenous IFN was delivered to mice prior to i.c. challenge. Low dose IFN-α group was i.p. dosed with 20,000 U 24h prior to i.c. challenge then 10,000 U was administered the day of and 24h after challenge whereas the IFN-α high dose group was always dosed with 20,000 U. None of these mice survived and neither did the mock primed control mice. Mice were also treated with either 10,000 U of IFN-β or 50,000 U of IFN-γ by local i.c. delivery 6h prior to i.c. challenge with ΔM51-VSV-GFP-Fluc. All IFN-β treated mice developed HLP while all IFN-γ treated mice survived. Virus primed mice used as positive controls also all survived.

B) Reovirus (Type 3 Dearing) was used to induce IFN-α endogenously and $1x10^8$ pfu/100ul was injected i.p. 24h or 48h prior to the i.c. challenge with ΔM51-VSV-GFP-Fluc. $1x10^7$ pfu/50ul Reovirus was also administered via the i.n. route and challenged with ΔM51-VSV-GFP-Fluc 48h after. None of the Reovirus primed mice survived. Therefore, endogenous levels of IFN-α were not enough to induce CNS protection.

A

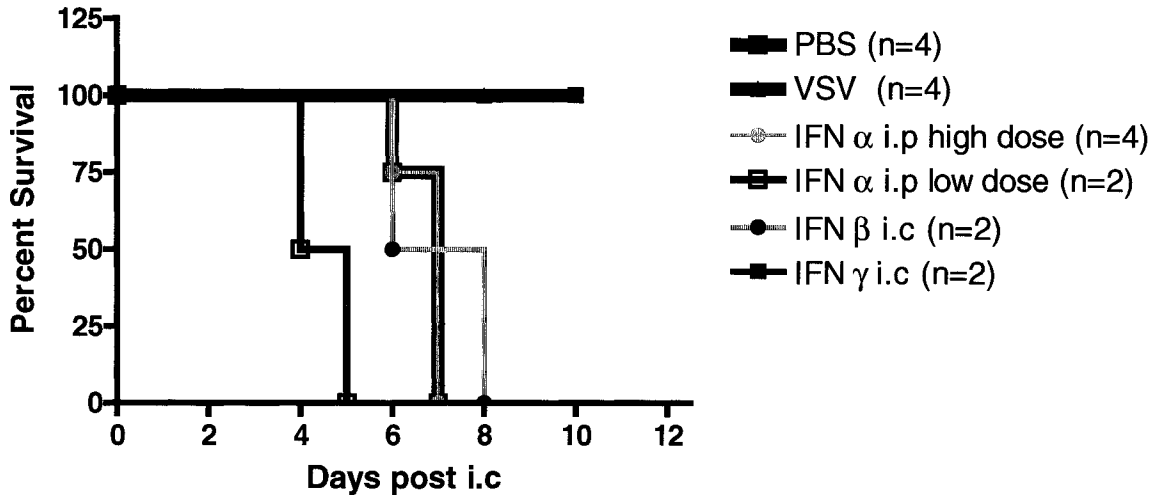
125
100
75
50
25
0
Percent Survival
0
2
4
6
8
10
12
Days post i.c
PBS (n=4)
VSV (n=4)
IFN α i.p high dose (n=4)
IFN α i.p low dose (n=2)
IFN β i.c (n=2)
IFN γ i.c (n=2)

B

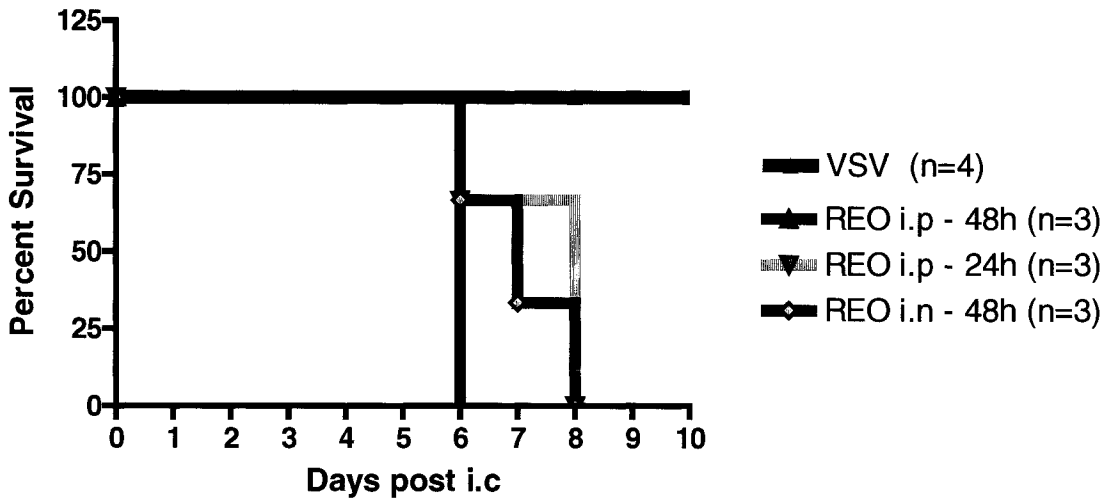
125
100
75
50
25
0
Percent Survival
0
1
2
3
4
5
6
7
8
9
10
Days post i.c
VSV (n=4)
REO i.p - 48h (n=3)
REO i.p - 24h (n=3)
REO i.n - 48h (n=3)

Figure 4.5: IFN-γ is not involved in VSV induced CNS protection

IFN-γ ligand knock-out mice were primed with ΔM51-VSV-GFP or PBS and then i.c. challenged with ΔM51-VSV-GFP-Fluc 24h later. Normal Balb/c mice were also primed and challenged as positive controls. IVIS imaging was carried out 24h after challenge and continued for 5 days. (A) The graph shows the average photon values quantified from the head of all challenged mice. The average of three mice is shown for all points. Primed mice survived whereas all mock primed mice developed HLP by day 5 after challenge (B).

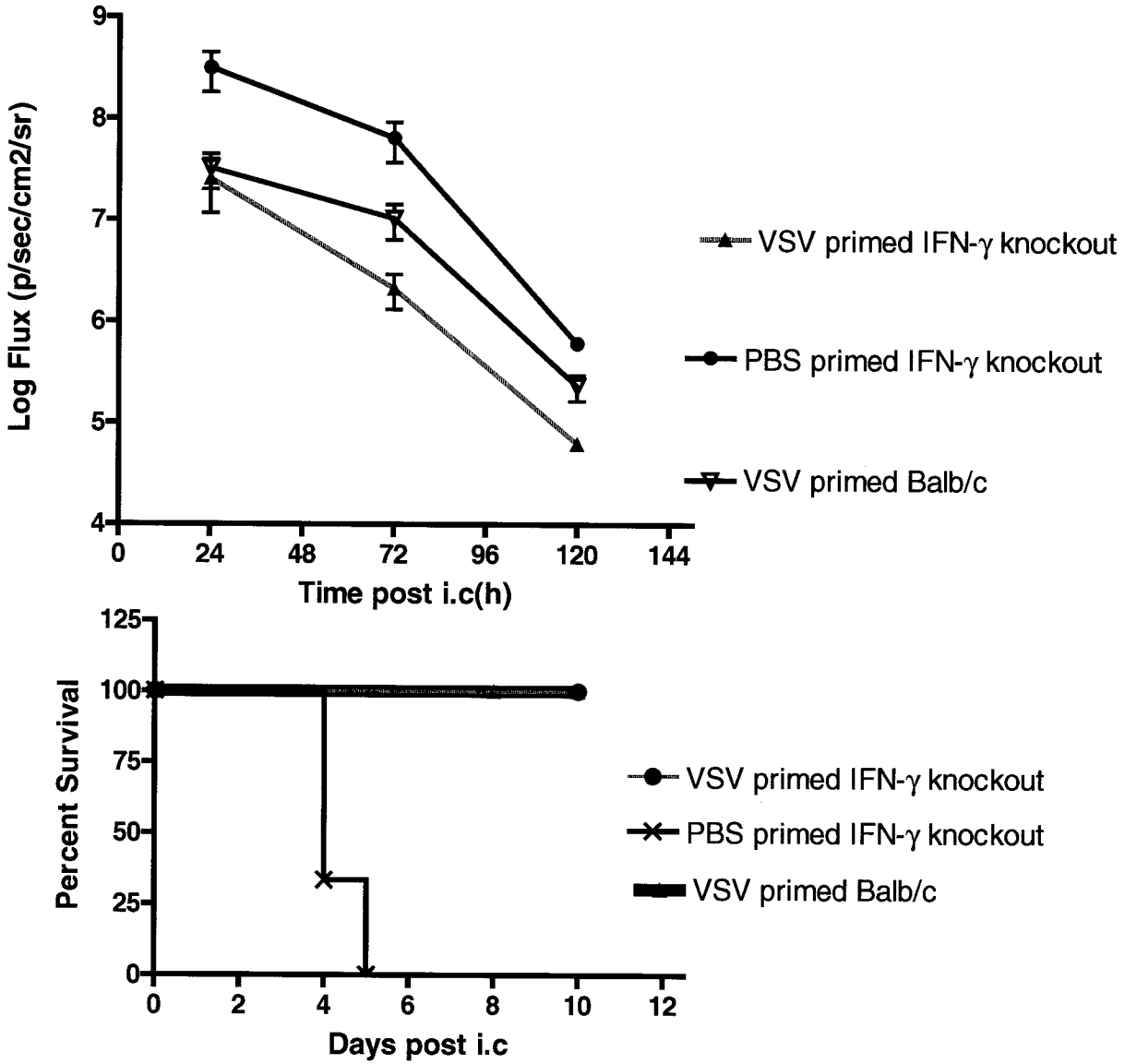
Log Flux (p/sec/cm2/sr)
9
8
7
6
5
4
0
24
48
72
96
120
144
Time post i.c(h)
VSV primed IFN-γ knockout
PBS primed IFN-γ knockout
VSV primed Balb/c
Percent Survival
125
100
75
50
25
0
0
2
4
6
8
10
12
Days post i.c
VSV primed IFN-γ knockout
PBS primed IFN-γ knockout
VSV primed Balb/c

Half of the Reovirus primed mice were i.c. challenged with ΔM51-VSV-GFP-Luc at 24h post priming, and the other set was challenged at 48h post priming. The mice were assessed everyday and from *figure 4.4* it can be seen that mice challenged at either time points eventually developed paralysis. Although Reovirus elicited an IFN-α response, it was not ineffective in protecting these mice from the VSV i.c. challenge.

From our ELISA data, we know that serum levels of IFN-γ rise at 6h after priming but decline by 12h. Although exogenous IFN-γ has been shown to have some protective effects in experimental i.n. infections with VSV, it was proven to be biologically redundant [43]. This also holds true in our priming model. We had conducted preliminary experiments where mice (n= 2) were primed locally in the brain with 50,000 units of exogenous IFN-γ 6h prior to virus challenge. In comparison to PBS primed controls, IFN-γ treated mice survived the subsequent virus challenge (*Figure 4.4*). However, when we carried out the priming experiments in male FVB/N IFN-γ ligand knock-out mice, IFN-γ was shown to be irrelevant. Three knock-out mice were primed i.p. with the standard priming virus while another group of three knock-out mice were mock primed. Mice were challenged 24h later i.c. and imaged commencing 24h post i.c. challenge. Two of the mock primed knock-out mice developed HLP by day 4 after challenge and the remaining mouse was dragging its hind limbs by day 5 (*figure 4.5*). VSV primed mice all survived the i.c. challenge verifying that IFN γ is not the crucial factor involved in providing model of infection.

CHAPTER 5: DISCUSSION

Previous studies have characterized the destructive nature of VSV to the CNS when mice are infected by i.c. or i.n. routes. VSV is fatal fifty percent of the time when administered systemically or i.n. to adult mice, [97] whereas direct i.c. infection is virtually all lethal [110]. The ΔM51 mutant strain of VSV, although shown to be safe when administered systemically, maintains its neurotoxicity when delivered to the CNS and at first does not appear to be a safe treatment for cancers of the brain. ΔM51-VSV expressing GFP was used to treat implanted human gliomas in immunodeficient nude mice and although administered i.v., VSV was able to travel to the site of the glioma. Replication was only seen in the tumour cell, whereas normal brain tissue escaped unscathed (unpublished data). Entry into the brain from within the host was somehow able to limit viral replication in normal healthy brain tissue. However, the lack of any extensive damage to normal tissue may have been due to minute amounts of virus that found its way into normal tissue. We tested whether protection could be induced against a higher dose of virus and found that mice were able to survive an i.c. challenge as high as 2×10^7 pfu of ΔM51-VSV. This protective phenomenon was reproducible in various strains of adult mice as well as in both sexes. Naïve unprimed mice were not able to survive the i.c. challenge at this dose and developed HLP or in some instances died due to extensive viral replication and spread within the CNS.

5.1 IVIS imaging techniques indicate that ΔM51-VSV replication in the CNS is restricted when mice are primed as early as 12h before i.c. challenge

Live imaging technology allowed us to quantify the amount of replication taking place in the CNS in a primed versus mock primed scenario. This technique enabled us to see that priming reduced the initial amount of replication in the brain by 1 to 2 log when compared to mock primed mice and also resulted in accelerated clearance of the virus from the CNS. In contrast, mock primed mice maintained high levels of viral replication in the CNS until experimental endpoints were reached. Imaging also allowed us to visualize the pathway taken by the virus within the CNS of the same animal over the time-course of infection. Priming limited virus spread from the brain to the spine and in cases where the virus did manage to leak into the spine, host responses were able to clear the infection and the animal survived. Mock primed animals always ended up with extensive viral infection of the spine leading to HLP within 5-6 days post challenge.

Previous studies have shown that a robust IgG host response against VSV commences by day 6 after peripheral infection [38]. The priming induced protection that we characterized occurred at a time prior to the induction of neutralizing antibodies against VSV. We thus assessed the initiation of protection at time points before a robust IgG antibody response against VSV began. Protection was induced in the CNS against the i.c. challenge dose of ΔM51-VSV as early as 12hrs post priming. Although viral replication was very high when mice were challenged 12h after priming and was eventually detected in the spine, all experimental mice cleared the virus and survived the challenge. Complete survival was also seen with all mice challenged at later time points (24h-96h).

Quantification of the amount of luminescence detected in the head indicated that the longer the challenge dose was delayed after priming, the less viral replication took place in the

head and the spread to the spine was limited. Although protection was measurable within 12h, the effect may only reach an optimal stage at later time points. Also, if protection was due to a concerted effort of different factors, these additive effects may not be in place until after a specific time-point after priming. Regardless of what time-point the mice were challenged i.c., the greatest drop in replication in the head always occurred at 120h (5 days) post priming. This was most evident when comparing signal detected from mice challenged 96h after priming. In this group, luminescence detected 24h after i.c. challenge (120h post prime) is almost 2-fold less than all other signal detected at this day of imaging (*figure 3.4*). Studies with the i.n. infection route in mouse model indicate that breakdown of the BBB is not detected until 6 days post infection [97]. However, since we injected directly into the cranium, it is possible that at 120h, there was full BBB permeability significantly earlier than with the i.n. model. If this was the case, then neutralizing IgM antibodies that normally have poor access to the CNS and the minute amounts of IgG antibodies that start to be produced at later times after infection, would have had unrestricted admission into the CNS. When mice are challenged after VSV specific antibody starts to cross into the brain (96-120h post prime), maximal protection is available and virus is neutralized before it can start to cause excessive damage. Future experiments testing the CSF for neutralizing antibodies over the length of our experiment will confirm this hypothesis.

5.2 Priming limits but does not restrict ΔM51-VSV infection of neurons

Like many other viruses that target the CNS, VSV has a specific affinity for neurons and HLP and/or death of the host is assumed to be due to widespread neuronal damage [49]. VSV infection through the i.n. route specifically infected olfactory bulb neurons and if not rapidly cleared, the infection spread trans-synaptically to other neurons within the brain [19-21]. In an i.c.

infection, VSV spreads in the CNS by targeting specific type of neurons (i.e. hippocampal) in certain regions of the brain [110]. Our IHC images indicated that priming did not initially restrict the areas infected but rather acted to restrict replication and spread within the targeted region (*figure 3.6*). VSV-specific staining indicated that VSV infects cells of the ventricles (ependymal, endothelial, choroid plexus) at first and then makes its way to the parenchyma. From the LV, VSV displayed an affinity for the hippocampal region and in the absence of priming, infected this entire region. Priming restricted infection to specific regions of the hippocampus and spread through the ventricle system was limited. However, the restriction in replication and spreading of VSV seen in the CNS of primed mice is not a result of preventing infection of neurons. Neurons of primed mice were also key targets of a VSV infection and overall survival of the host was not due to altering VSV's neurotropism.

5.3 Priming sensitizes surrounding CNS cells to undergo apoptosis in response to ΔM51-VSV infection

In an attempt to understand how priming enables host survival even though neurons continue to be infected, we assessed the extent of apoptosis in the CNS. *In vitro* studies have previously shown that VSV induced death of neuronal cell lines is due to apoptosis [15]. I.n. VSV infection of mice and subsequent neuropathology seen *in vivo* are a result of neuronal apoptosis [48, 49, 111]. Here, we also showed that apoptosis occurred in brain tissue as a result of an i.c. challenge with ΔM51-VSV (*figures 3.9, 3.10*). Mock i.c. infected brains did not display apoptotic cells, indicating that cell death occurred in response to viral infection and not the injection procedure. At 24h post i.c., primed mice showed very little viral antigen and even less apoptosis whereas mock primed mice had apoptotic cells in and around the ventricles. The number of apoptotic cells

was significantly less than the number of infected cells and minimal overlap was seen between TUNEL positive cells and VSV infected cells. As the infection proceeded, primed brains showed an increase in the number of apoptotic cells and apoptotic cells started to outnumber infected cells. These dead cells were not only evident in the ventricular region, but were also seen in the parenchyma around areas of VSV infection. This was not the case when mice were mock primed. Apoptosis was still predominately seen in and around the ventricles and there were fewer apoptotic bodies than VSV infected cells. In both cases, there was also still very minimal overlap between dying and infected cells. Our data therefore indicated that priming sensitized CNS cells to rapidly undergo apoptosis in response to VSV infection. Although unlikely, it is possible that apoptotic cells have lost expression of viral antigen. The sum of current literature and our current results favour the notion that apoptotic signals from nearby infected cells induced surrounding cells to trigger cell death in an attempt to limit VSV's path of destruction. Previous experiments have shown that apoptosis occurs around areas of infection but VSV RNA positive cells did not TUNEL stain [49]. Moreover, it was also found that although in some areas of infection there were equal numbers of infected cells and apoptotic cells, infected cells frequently and significantly outnumbered dying cells [49].

A similar mechanism of spread has been reported with Rabies virus infection of the CNS. Rabies virus (Rhabdoviridae, genus Lysavirus) also selectively infects neurons but preserves neuronal integrity so that it maintains a route of spread and propagation while inducing apoptosis in cells attempting to eliminate the virus (T-cells) [48, 70]. Less pathogenic strains of rabies results only in paralysis and not death of the host because viral spread to the brain is limited due to the induction of apoptosis [111]. The host-virus paradigm established with Rabies virus thus appears to be mimicked by VSV. However, we were unable to conclusively determine the cell type that in the CNS that was sensitized to die. GFAP (marker of astrocytes/ependymal cells), RCA-1

(endothelial/microglial cells), and NeuN (neurons) positive cells did not consistently overlap with TUNEL positive cells. Two of these proteins are cytoskeletal (GFAP) or membrane bound (RCA-1) markers and is unlikely that their expression would be lost when a cell undergoes apoptosis. NeuN is a nuclear protein and it is possible that its expression is lost or becomes faint when apoptosis occurs. In a similar manner, hoechst, the fluorescent counter-stain used to label DNA also became faint or non-existent in apoptotic positive cells. This suggests that nuclear markers may not be ideal when characterizing apoptotic cells and alternative approaches such as Fluorescence activated cell sorting (FACS) analysis may be more conclusive.

Sur et al have decisively shown using ultrastructural studies that when mice are infected i.n. with VSV, apoptosis was evident in neurons. This is most likely similar in our case. In primed brains, apoptosis is seen in the parenchyma, in areas where neurons are the predominant cell type (hippocampal formation). In contrast, apoptotic cells in the mock primed brains were found in the ventricle regions, areas where neurons are not normally located. In our infection model, we have established that VSV enters the parenchyma from the CSF by infecting cells of the ventricles. The cells found here are renewable and may be easily persuaded to undergo apoptosis to allow for viral progeny to infect nearby neurons. When mock primed, VSV strategically travels from the neuronal cell body down the axon and dendrites (as seen by spotted VSV staining on tissue sections resembling neuronal processes) to the next targeted neuron while preserving neuronal integrity. In the absence of the priming signal, apoptosis is delayed or minimized until VSV has a chance to spread rapidly through the brain neurons eventually making its way to the spine. When the virus has completely exhausted its resources, eventual cell death of infected or bystander CNS neurons results in the host's demise. Priming is a protective mechanism that sensitizes local neurons around the site of infection to induce apoptosis rapidly,

thereby cutting off VSV's route of travel through the neuronal network. Although neuronal loss may lead to host dysfunction, a few localized dead neurons are more beneficial to host survival.

5.4 Priming induced CNS protection does not involve the adaptive immune system and is most likely independent of the IFN-α antiviral response.

We have thus far confirmed that priming is able to protect the CNS from subsequent VSV i.c. infection and protection commences as early as 12h. At this early time, it seemed unlikely that the adaptive immune system can respond so quickly to defend the brain, but might be important for long term survival. Previous studies indicate that T cells are essential for preventing spread of VSV to the CNS in immunocompetent mice [38] and in promoting recovery of mice once the virus has invaded the CNS [112, 113]. By far the most significant source of CNS protection is the IgG neutralizing antibodies produced by the adaptive arm of the immune system [38, 51]. However, IgG is only capable of preventing encephalitis in mice if it is present prior to CNS infection and is not effective against an established CNS infection. Antibody alone is also insufficient for long term survival, as IgG serum transfer to nude mice does not prevent VSV infection of neural tissue and subsequent death [38].

To test whether priming induced CNS protection is dependent on the cell-mediated immunity, we first looked for the presence of T and B cells in brain tissue of primed versus mock primed mice. IHC studies over the time course of our experiment (24h post i.c. until 120-144h post i.c.) indicate that T cells are only evident 5 days after the i.c. infection in both primed and mock primed brains. At this time, the mice have either succumbed to paralysis or have cleared the virus. It is possible that the infiltrating T-cells are important for clearing up residual

virus and ensuring life-long survival as shown in previous models with wt VSV [38]. However, we had subsequently shown that priming induced protection is possible in nude mice. As seen with Balb/c mice, i.p. primed nude mice challenged 48h later survived the VSV brain infection. Initially, very little viral replication was detected in the heads of primed mice and although there was some increase, there was never any viral spread to the spine and the signal eventually cleared. In mock primed mice, there was extensive viral replication in the head and was evident in the spine two days after challenge. All mock primed mice died due to paralysis. I.v. delivery of wt VSV to nude mice resulted in fatality in over half the mice infected in the long run, but our experiments indicated that the attenuated ΔM51-VSV had no discernable toxic effects when delivered systematically since all primed mice lived past 15 days. Priming induced protection of the CNS in nude mice corroborated our IHC studies in showing that T-cells are not involved in mediating protection.

Bi et al have shown that B-cells are only seen in the brains of i.n. infected mice 14 days after VSV infection, therefore as expected, we were not able to detect infiltrating B-cells by 6 days after i.c. challenge in both primed and mock primed brains. However, others have established the importance of neutralizing antibody action against VSV in limiting infection and spread to the CNS. Our plaque reduction assay of primed or normal serum indicate that there were also no factors present in the blood that were capable of neutralizing VSV when mice were challenged 24h after priming. Although some neutralizing effect is seen 48h after priming, it has already been established that antibody formed after CNS invasion by VSV is ineffective as a means of protection. Furthermore, the same level of neutralization is seen in blood taken 48h after challenge from mice mock primed yet we have already established that mock primed never survive the i.c. challenge. Early production of IgM in the serum cannot establish neutralizing effects in the

CNS since IgM (the only type produced at this early time), cannot cross the BBB. Although it can be argued that we have breached the BBB due to the i.c. injection, IgM has been shown to be less effective than IgG antibodies in neutralizing VSV [51, 112]. The final outcome of these experiments indicates that neutralizing factors begin to form in the blood 48h after virus is detected in the host regardless of route of inoculation (i.p. vs. i.c.). Since our positive control serum indicates that by 10 days post i.p. priming, complete neutralization of VSV is possible *in vitro*, antibody produced at the early challenge time points is also an unlikely mechanism mediating priming induced CNS protection.

Since there was no definitive role for the adaptive immune system in priming induced CNS protection, we focused our attention on early innate responses to viral infection. VSV is known to be exquisitely sensitive to the antiviral effects of IFN and its therapeutic use as a potential oncolytic virus stems from the fact that the virus will preferentially replicate in cells defective in producing or responding to IFN. The ΔM51 mutant virus was created to increase the therapeutic window in order to limit infection of healthy cells with a functionally intact IFN system. Since the virus we assessed in this study is a potent biological inducer of IFN, a key antiviral factor, we started our assessment of innate immunity with this family of cytokines. Our ELISA data showed that within 6hrs of priming, a robust IFN-α response was induced in the blood of primed mice, and some was also seen in the CSF. By 12h, IFN-α levels significantly decreased in the blood and were undetectable in the CSF. IFN-α was not present when mice were injected with PBS or with UV-inactivated virus, indicating that VSV replication was necessary to activate an anti-viral state. When directly i.c. challenged, levels of IFN-α started to form in the blood but was not seen in the CSF, indicating that the IFN-α detected in the CSF (when i.p. primed) was most likely derived from the serum rather than produced locally. It has

already been established that IFNs can cross the BBB and can exert effects in the CNS although they are mainly produced in the periphery[86]. Thus far, there is no evidence of local IFN-α production in the CNS and most likely does not occur especially in light of the fact that IFN-α has potential neuro-toxic effects [68]. Armed with this knowledge, we primed mice with exogenous IFN-α 24h prior to challenge, at time of challenge, and 24h after virus infection of the brain. Despite rigorous dosing, IFN-α was ineffective at preventing fatality. Earlier attempts at treating mice already infected i.n. with VSV with exogenous IFN-α proved to be most effective when IFN-α was induced endogenously using poly i.c. [32]. However, our experiments using Reovirus to stimulate endogenous IFN-α was not able to protect mice from VSV infection of the CNS. Reovirus induction of IFN-α in serum was previously assayed and high levels of this IFN were detected *in vivo*.

Although the kinetics of IFN-β induction were very similar to those of IFN-α, the absolute levels of proteins were much lower. Furthermore, IFN-β appeared in the CSF 6h post i.c. injection, a phenomenon not seen with IFN-α. At the time of induction of IFN-β in the CSF, only minute quantities were detected in the serum indicating that this cytokine was being produced locally in the brain. IFN-β is not detected in the CSF when VSV is administered i.p. or when UV inactivated VSV is injected i.c.. Others have shown that neurons secrete IFN-β, but not IFN-α in response to a viral infection [68, 69]. Rabies virus, as well as the unrelated Theiler's and La Crosse viruses induce IFN-β production in neurons *in vitro* as well as *in vivo* [84, 85]. Due to the lack of induction of IFN-β in the brain when VSV is detected in the periphery and the surge when VSV is detected locally within the CNS, IFN-β may act as a compensatory mechanism in the CNS in a futile attempt to protect itself from excessive viral insult. It is plausible that if IFN-β is present locally before VSV is detected, neuro-protection might be achieved. Given that our preliminary

priming attempts to administer exogenous IFN-β locally (10,000 U via i.c. injection) had failed, we tentatively came to the conclusion that even though IFN-β is produced locally and its expression seems to increase over the course of an i.c. infection, IFN-β is not protective when delivered locally. The possibility also exists that IFN-β, made in the brain as an antiviral tactic by neurons when virus is detected, may in fact be a contributing factor in virus induced lethality.

As described previously, studies with Rabies virus indicate that the attenuated strain of Rabies limits the disease to just paralysis due to induction of apoptosis in neurons of the spinal cord [111]. The pathogenic strain is able to replicate freely within the spine and travel to the brain by preventing surrounding neurons from dying. Our data showed similar results, in that priming induces greater amounts of apoptosis around sites of VSV infection when compared to mock primed mice. IFN-β may play a key role in this observation since it has been reported that neurons produce IFN-β in response to Rabies virus infection[85]. The induction of IFN-β in the CSF as seen only after direct i.c. infection with ΔM51-VSV may serve to protect neurons as occurs with Rabies, and in doing so enables the virus to spread quickly. Priming may act to warn the CNS of an oncoming attack by a neurotropic virus and desensitizes neurons to the neuroprotective effects of IFN-β, allowing individual uninfected neurons to commit suicide in an attempt to preserve the entire organism. To conclusively show that neuroprotection might in fact be harmful in terms of a VSV brain infection, experiments depleting IFN-β using anti-IFN-β antibodies might prove fruitful. Type 1 IFN knock-out mice or peripheral IFN-β depletion will not be useful since type I IFNs are necessary to keep VSV infection in check outside of the CNS [98, 99]. Therefore we can attempt to create organ specific knock-out mice that lack IFN-β receptors only in the CNS to determine if IFN-β possesses neuroprotective properties that contributes to fatality by preventing the induction of apoptosis in mock primed mice.

Assuming that the IFN response necessary to protect the host from widespread VSV infection of the periphery is not applicable to the CNS, the search continues for the CNS protective factors that are induced upon priming. Our current data point towards the innate immune system and most likely a soluble factor secreted by cells important to this early arm of immunity - macrophages and dendritic cells. Natural killer (NK) cells are also key players in innate immunity and secrete IFN-γ, but NK cell depletion experiments carried out by our group (data not shown) and the IFN-γ knock-out mice studies indicate that these factors are not necessary for protection. Others have shown through macrophage and dendritic cell deletion that a subset of these cells is more critical than IFN-α in providing protection from VSV dissemination to the CNS and subsequent mortality [35]. Although these cell types are capable of migrating to the CNS, the rapid protective response we show here points to the importance of fast acting soluble factors.

Preliminary data from adoptive transfer experiments indicate that soluble factors in the blood that may be vital to CNS protection. Thus far, it seems that transfer of plasma extracted from mice that were primed 6h earlier with ΔM51-VSV provides partial protection against ΔM51-VSV brain challenge. Protection decreases when mice were primed with 24h plasma or with splenocytes. We have also started to profile specific factors in the blood using cytokine array technology (RayBio Cytokine Antibody Array II, RayBiotech Inc.). In a preliminary array, the chemokine MCP-1 was shown to be up-regulated in the plasma of mice within 6h of infection with ΔM51-VSV. Others have shown that VSV infection of macrophages *in vitro* also up-regulates MCP-1 as well as IP-10[115]. MCP-1 is implicated in increasing permeability of the BBB and is not only secreted by macrophages but also by astrocytes in order to recruit blood monocytes into the CNS during viral insult [77, 96, 115]. Further experimentation is underway to verify these results and hopefully solidify our ground-work.

CHAPTER 6: CONCLUSIONS AND FUTURE DIRECTIONS

Direct infection of the CNS with VSV or the "IFN inducing" ΔM51 VSV is lethal in mice. However, we have established here that systemic delivery or "priming" with ΔM51-VSV prior to an i.c. injection of the same virus affords complete CNS protection. Using current *in vivo* imaging techniques allowed us to track viral replication from within a living animal and also enabled us to quantify the amount of replication taking place over time. Using imaging, we saw that priming did not prevent VSV from infecting and actively replicating in the brain, but decreased the extent of initial infection by 1-2 logs in comparison to mock primed mice. Mock primed mice showed increased viral replication in the head and eventual spread to the spine. However, not all mock primed mice showed intense viral replication in the brain and spine on the last day. Most animals showed intense signal 1-2 days prior to developing paralysis and were clear of any signal on the day they were fully dragging their hind limbs. This is indicative of VSV reaching the end of its replication capacity because of the lack of new cells to infect or host defences catching up with viral infection.

Although we know that complete clearance and life-long protection against VSV is likely due to an antibody response, we have shown that protection is initiated as early as 12h after a priming event. At this time, the adaptive immune system is not active and others have shown that immune serum against VSV is not protective once the virus has already gained access into the CNS [38]. Our plaque reduction studies also indicated that in our priming model there was no neutralizing factors present in the blood until 48h after virus infection. Therefore, we conclude that priming induced protection commences as early as 12h post infection due to an unknown mechanism or factor(s) and continues to protect the brain from subsequent VSV challenge past this time point. 96h after priming, the initial protective factor(s) subsides and switches to an

antibody response or works in concert with a VSV specific antibody response to completely eliminate any residual pathogen remaining in the CNS and provide life-long immunity. Future experiments will attempt to determine at what point after priming the IgM response switches to an IgG antibody response and at what time antibody is present in the CSF or brain tissue.

Although VSV is extremely sensitive to the antiviral effects of type 1 IFN and we are using an engineered virus that does not prevent the induction of IFN within the host, thus far it does not seem that IFN is the key protective factor induced upon priming. IFN-α is not reported to be made locally in the CNS, but neurons have been reported to produce IFN-β in response to viral infection as a neuro-protective measure [84, 85]. This is interesting in light of the fact that we had detected induction of IFN-β in the CSF within 6h after mice where challenged i.c.. Local production of IFN-β in the brain was not seen when mice were primed i.p.. We had established that priming restricts infection and spread of VSV in neurons by rapidly inducing apoptosis in surrounding cells at the site of infection. Although we have not definitively proved that neurons are undergoing cell death, the areas where apoptosis is seen when mice are primed and what has been seen by others with VSV infection and the related Rabies virus indicates that it may in fact be neurons that are primed to die. In our i.c. infection model, the protective nature of IFN-β might work against the host by promoting viral infection and spread. Priming inhibits the production of IFN-β by neurons, potentially as a means to sensitize neurons to die upon viral infection. Future experiments will look the anti-apoptotic neuroprotective properties of IFN-β within the CNS and assess whether this contributed to ΔM51-VSV's ability to spread uncontrollably within the neuronal network.

Our work has raised new questions as to how counteraction to VSV infection of the CNS occurs that allows for host survival. We are leaning towards a soluble factor(s) in the blood that acts in the CNS or turns on important protective elements in the CNS. There are many potent

cytokines that have been implicated to function in the CNS. TNF-α, IFN-γ, IL-1a, IL-2, IL-6 mRNA can be detected soon after several neurotropic viral infections [68, 69, 82, 83, 91, 93]. Our goal now is to show that protection can be passed on to other animals by transferring VSV-depleted primed serum and if this proves to be valid, we will embark on a series of DNA micro-arrays of brain tissue and cytokine arrays of the serum and CSF to find the elements that link systemic priming with CNS protection.

REFERENCES

1. **HANSON, R. P.** 1952. The natural history of vesicular stomatitis. Bacteriol. Rev. **16:**179-204.

2. **Letchworth, G. J., L. L. Rodriguez, and J. Del cbarrera.** 1999. Vesicular stomatitis. Vet. J. **157:**239-260.

3. **BRANDLY, C. A. and R. P. HANSON.** 1957. Epizootiology of vesicular stomatitis. Am. J. Public Health **47:**205-209.

4. **SORENSEN, D. K., T. L. CHOW, T. KOWALCZYK, R. P. HANSON, and C. A. BRANDLY.** 1958. Persistence in cattle of serum-neutralizing antibodies of vesicular stomatitis virus. Am. J. Vet. Res. **19:**74-77.

5. **Rodriguez, L. L.** 2002. Emergence and re-emergence of vesicular stomatitis in the United States. Virus Res. **85:**211-219.

6. **Schlegel, R., T. S. Tralka, M. C. Willingham, and I. Pastan.** 1983. Inhibition of VSV binding and infectivity by phosphatidylserine: is phosphatidylserine a VSV-binding site? Cell **32:**639-646.

7. **Seganti, L., F. Superti, C. Girmenia, L. Melucci, and N. Orsi.** 1986. Study of receptors for vesicular stomatitis virus in vertebrate and invertebrate cells. Microbiologica **9:**259-267.

8. **Superti, F., L. Seganti, F. M. Ruggeri, A. Tinari, G. Donelli, and N. Orsi.** 1987. Entry pathway of vesicular stomatitis virus into different host cells. J. Gen. Virol. **68 (Pt 2):**387-399.

9. **Rose, J. K. and L. Iverson.** 1979. Nucleotide sequences from the 3'-ends of vesicular stomatitis virus mRNA's as determined from cloned DNA. J. Virol. **32:**404-411.

10. **Gallione, C. J., J. R. Greene, L. E. Iverson, and J. K. Rose.** 1981. Nucleotide sequences of the mRNA's encoding the vesicular stomatitis virus N and NS proteins. J. Virol. **39:**529-535.

11. **Ahmed, M. and D. S. Lyles.** 1998. Effect of vesicular stomatitis virus matrix protein on transcription directed by host RNA polymerases I, II, and III. J. Virol. **72:**8413-8419.

12. **Petersen, J. M., L. S. Her, V. Varvel, E. Lund, and J. E. Dahlberg.** 2000. The matrix protein of vesicular stomatitis virus inhibits nucleocytoplasmic transport when it is in the nucleus and associated with nuclear pore complexes. Mol. Cell. Biol. **20:**8590-8601.

13. **Connor, J. H. and D. S. Lyles.** 2002. Vesicular stomatitis virus infection alters the eIF4F translation initiation complex and causes dephosphorylation of the eIF4E binding protein 4E-BP1. J. Virol. **76:**10177-10187.

14. **Connor, J. H. and D. S. Lyles.** 2005. Inhibition of host and viral translation during vesicular stomatitis virus infection. eIF2 is responsible for the inhibition of viral but not host translation. J. Biol. Chem. **280:**13512-13519.

15. **Gaddy, D. F. and D. S. Lyles.** 2005. Vesicular stomatitis viruses expressing wild-type or mutant M proteins activate apoptosis through distinct pathways. J. Virol. **79:**4170-4179.

16. **Connor, J. H., M. O. McKenzie, and D. S. Lyles.** 2006. Role of residues 121 to 124 of vesicular stomatitis virus matrix protein in virus assembly and virus-host interaction. J. Virol. **80:**3701-3711.

17. **Rabinowitz, S. G., T. C. Johnson, and M. C. Dal Canto.** 1977. The uncoupled relationship between the temperature-sensitivity and neurovirulence in mice of mutants of vesicular stomatitis virus. J. Gen. Virol. **35:**237-249.

18. **Fultz, P. N. and J. J. Holland.** 1985. Differing responses of hamsters to infection by vesicular stomatitis virus Indiana and New Jersey serotypes. Virus Res. **3:**129-140.

19. **Huneycutt, B. S., I. V. Plakhov, Z. Shusterman, S. M. Bartido, A. Huang, C. S. Reiss, and C. Aoki.** 1994. Distribution of vesicular stomatitis virus proteins in the brains of BALB/c mice following intranasal inoculation: an immunohistochemical analysis. Brain Res. **635:**81-95.

20. **Plakhov, I. V., E. E. Arlund, C. Aoki, and C. S. Reiss.** 1995. The earliest events in vesicular stomatitis virus infection of the murine olfactory neuroepithelium and entry of the central nervous system. Virology **209:**257-262.

21. **Reiss, C. S., I. V. Plakhov, and T. Komatsu.** 1998. Viral replication in olfactory receptor neurons and entry into the olfactory bulb and brain. Ann. N. Y. Acad. Sci. **855:**751-761.

22. **Forger, J. M.,3rd, R. T. Bronson, A. S. Huang, and C. S. Reiss.** 1991. Murine infection by vesicular stomatitis virus: initial characterization of the H-2d system. J. Virol. **65:**4950-4958.

23. **Young, H. A.** 1996. Regulation of interferon-gamma gene expression. J. Interferon Cytokine Res. **16:**563-568.

24. **Bach, E. A., M. Aguet, and R. D. Schreiber.** 1997. The IFN gamma receptor: a paradigm for cytokine receptor signaling. Annu. Rev. Immunol. **15:**563-591.

25. **Samuel, C. E.** 2001. Antiviral actions of interferons. Clin. Microbiol. Rev. **14:**778-809, table of contents.

26. **Vogel, S. N. and D. Fertsch.** 1987. Macrophages from endotoxin-hyporesponsive (Lpsd) C3H/HeJ mice are permissive for vesicular stomatitis virus because of reduced levels of endogenous interferon: possible mechanism for natural resistance to virus infection. J. Virol. **61:**812-818.

27. **Belardelli, F., F. Vignaux, E. Proietti, and I. Gresser.** 1984. Injection of mice with antibody to interferon renders peritoneal macrophages permissive for vesicular stomatitis virus and encephalomyocarditis virus. Proc. Natl. Acad. Sci. U. S. A. **81:**602-606.

28. **Proietti, E., S. Gessani, F. Belardelli, and I. Gresser.** 1986. Mouse peritoneal cells confer an antiviral state on mouse cell monolayers: role of interferon. J. Virol. **57:**456-463.

29. **Muller, U., U. Steinhoff, L. F. Reis, S. Hemmi, J. Pavlovic, R. M. Zinkernagel, and M. Aguet.** 1994. Functional role of type I and type II interferons in antiviral defense. Science **264:**1918-1921.

30. **Stojdl, D. F., N. Abraham, S. Knowles, R. Marius, A. Brasey, B. D. Lichty, E. G. Brown, N. Sonenberg, and J. C. Bell.** 2000. The murine double-stranded RNA-dependent protein kinase PKR is required for resistance to vesicular stomatitis virus. J. Virol. **74:**9580-9585.

31. **Clemens, M. J. and A. Elia.** 1997. The double-stranded RNA-dependent protein kinase PKR: structure and function. J. Interferon Cytokine Res. **17:**503-524.

32. **De Clercq, E. and P. De Somer.** 1971. Comparative study of the efficacy of different forms of interferon therapy in the treatment of mice challenged intranassaly with vesicular stomatitis virus (VSV). Proc. Soc. Exp. Biol. Med. **138:**301-307.

33. **Gresser, I., M. G. Tovey, and C. Bourali-Maury.** 1975. Efficacy of exogenous interferon treatment initiated after onset of multiplication of vesicular stomatitis virus in the brains of mice. J. Gen. Virol. **27:**395-398.

34. **Ito, Y., H. Aoki, Y. Kimura, M. Takano, K. Shimokata, and K. Maeno.** 1981. Natural interferon-producing cells in mice. Infect. Immun. **31:**519-523.

35. **Ciavarra, R. P., L. Taylor, A. R. Greene, N. Yousefieh, D. Horeth, N. van Rooijen, C. Steel, B. Gregory, M. Birkenbach, and M. Sekellick.** 2005. Impact of macrophage and dendritic cell subset elimination on antiviral immunity, viral clearance and production of type 1 interferon. Virology **342:**177-189.

36. **Kundig, T. M., H. Hengartner, and R. M. Zinkernagel.** 1993. T cell-dependent IFN-gamma exerts an antiviral effect in the central nervous system but not in peripheral solid organs. J. Immunol. **150:**2316-2321.

37. **Bi, Z., P. Quandt, T. Komatsu, M. Barna, and C. S. Reiss.** 1995. IL-12 promotes enhanced recovery from vesicular stomatitis virus infection of the central nervous system. J. Immunol. **155:**5684-5689.

38. **Thomsen, A. R., A. Nansen, C. Andersen, J. Johansen, O. Marker, and J. P. Christensen.** 1997. Cooperation of B cells and T cells is required for survival of mice infected with vesicular stomatitis virus. Int. Immunol. **9:**1757-1766.

39. **Griffith, O. W. and D. J. Stuehr.** 1995. Nitric oxide synthases: properties and catalytic mechanism. Annu. Rev. Physiol. **57:**707-736.

40. **Corradin, S. B., N. Fasel, Y. Buchmuller-Rouiller, A. Ransijn, J. Smith, and J. Mauel.** 1993. Induction of macrophage nitric oxide production by interferon-gamma and tumor necrosis factor-alpha is enhanced by interleukin-10. Eur. J. Immunol. **23:**2045-2048.

41. **Corradin, S. B., J. Mauel, S. D. Donini, E. Quattrocchi, and P. Ricciardi-Castagnoli.** 1993. Inducible nitric oxide synthase activity of cloned murine microglial cells. Glia **7:**255-262.

42. **Bi, Z. and C. S. Reiss.** 1995. Inhibition of vesicular stomatitis virus infection by nitric oxide. J. Virol. **69:**2208-2213.

43. **Komatsu, T., D. D. Ireland, N. Chen, and C. S. Reiss.** 1999. Neuronal expression of NOS-1 is required for host recovery from viral encephalitis. Virology **258:**389-395.

44. **Wyllie, A. H.** 1987. Apoptosis: cell death in tissue regulation. J. Pathol. **153:**313-316.

45. **Hobbs, J. A., G. Hommel-Berrey, and Z. Brahmi.** 2003. Requirement of caspase-3 for efficient apoptosis induction and caspase-7 activation but not viral replication or cell rounding in cells infected with vesicular stomatitis virus. Hum. Immunol. **64:**82-92.

46. **Balachandran, S., P. C. Roberts, T. Kipperman, K. N. Bhalla, R. W. Compans, D. R. Archer, and G. N. Barber.** 2000. Alpha/beta interferons potentiate virus-induced apoptosis through activation of the FADD/Caspase-8 death signaling pathway. J. Virol. **74:**1513-1523.

47. **Griffin, D. E.** 2005. Neuronal cell death in alphavirus encephalomyelitis. Curr. Top. Microbiol. Immunol. **289:**57-77.

48. **Licata, J. M. and R. N. Harty.** 2003. Rhabdoviruses and apoptosis. Int. Rev. Immunol. **22:**451-476.

49. **Sur, J. H., R. Allende, and A. R. Doster.** 2003. Vesicular stomatitis virus infection and neuropathogenesis in the murine model are associated with apoptosis. Vet. Pathol. **40:**512-520.

50. **Charan, S., A. W. Huegin, A. Cerny, H. Hengartner, and R. M. Zinkernagel.** 1986. Effects of cyclosporin A on humoral immune response and resistance against vesicular stomatitis virus in mice. J. Virol. **57:**1139-1144.

51. **Steinhoff, U., U. Muller, A. Schertler, H. Hengartner, M. Aguet, and R. M. Zinkernagel.** 1995. Antiviral protection by vesicular stomatitis virus-specific antibodies in alpha/beta interferon receptor-deficient mice. J. Virol. **69:**2153-2158.

52. **Ishitsuka, H., Y. Nomura, and K. Takano.** 1977. A simple and efficient microassay method for titration of interferon. Microbiol. Immunol. **21:**583-591.

53. **Bell, J. C., K. A. Garson, B. D. Lichty, and D. F. Stojdl.** 2002. Oncolytic viruses: programmable tumour hunters. Curr. Gene Ther. **2:**243-254.

54. **Grander, D. and S. Einhorn.** 1998. Interferon and malignant disease—how does it work and why doesn't it always? Acta Oncol. **37:**331-338.

55. **Stojdl, D. F., B. Lichty, S. Knowles, R. Marius, H. Atkins, N. Sonenberg, and J. C. Bell.** 2000. Exploiting tumor-specific defects in the interferon pathway with a previously unknown oncolytic virus. Nat. Med. **6:**821-825.

56. **Stojdl, D. F., B. D. Lichty, B. R. tenOever, J. M. Paterson, A. T. Power, S. Knowles, R. Marius, J. Reynard, L. Poliquin, H. Atkins, E. G. Brown, R. K. Durbin, J. E. Durbin, J. Hiscott, and J. C. Bell.** 2003. VSV strains with defects in their ability to shutdown innate immunity are potent systemic anti-cancer agents. Cancer. Cell. **4:**263-275.

57. **Lichty, B. D., A. T. Power, D. F. Stojdl, and J. C. Bell.** 2004. Vesicular stomatitis virus: re-inventing the bullet. Trends Mol. Med. **10:**210-216.

58. **Greenlee, R. T., M. B. Hill-Harmon, T. Murray, and M. Thun.** 2001. Cancer statistics, 2001. CA Cancer. J. Clin. **51:**15-36.

59. **Cao, Y., V. Nagesh, D. Hamstra, C. I. Tsien, B. D. Ross, T. L. Chenevert, L. Junck, and T. S. Lawrence.** 2006. The extent and severity of vascular leakage as evidence of tumor aggressiveness in high-grade gliomas. Cancer Res. **66:**8912-8917.

60. **Schwartzbaum, J. A., J. L. Fisher, K. D. Aldape, and M. Wrensch.** 2006. Epidemiology and molecular pathology of glioma. Nat. Clin. Pract. Neurol. **2:**494-503; quiz 1 p following 516.

61. **Duntsch, C. D., Q. Zhou, H. R. Jayakar, J. D. Weimar, J. H. Robertson, L. M. Pfeffer, L. Wang, Z. Xiang, and M. A. Whitt.** 2004. Recombinant vesicular stomatitis virus vectors as oncolytic agents in the treatment of high-grade gliomas in an organotypic brain tissue slice-glioma coculture model. J. Neurosurg. **100:**1049-1059.

62. **Wollmann, G., P. Tattersall, and A. N. van den Pol.** 2005. Targeting human glioblastoma cells: comparison of nine viruses with oncolytic potential. J. Virol. **79:**6005-6022.

63. **Cserr, H. F. and P. M. Knopf.** 1992. Cervical lymphatics, the blood-brain barrier and the immunoreactivity of the brain: a new view. Immunol. Today **13:**507-512.

64. **McGavern, D. B.** 2005. The role of bystander T cells in CNS pathology and pathogen clearance. Crit. Rev. Immunol. **25:**289-303.

65. **Hickey, W. F.** 1999. Leukocyte traffic in the central nervous system: the participants and their roles. Semin. Immunol. **11:**125-137.

66. **McGavern, D. B., D. Homann, and M. B. Oldstone.** 2002. T cells in the central nervous system: the delicate balance between viral clearance and disease. J. Infect. Dis. **186 Suppl 2:**S145-51.

67. **Binder, G. K. and D. E. Griffin.** 2003. Immune-mediated clearance of virus from the central nervous system. Microbes Infect. **5:**439-448.

68. **Griffin, D. E.** 2003. Immune responses to RNA-virus infections of the CNS. Nat. Rev. Immunol. **3:**493-502.

69. **Griffin, D. E. and J. M. Hardwick.** 1999. Perspective: virus infections and the death of neurons. Trends Microbiol. **7:**155-160.

70. **Rutherford, M. and A. C. Jackson.** 2004. Neuronal apoptosis in immunodeficient mice infected with the challenge virus standard strain of rabies virus by intracerebral inoculation. J. Neurovirol. **10:**409-413.

71. **Shrestha, B., D. Gottlieb, and M. S. Diamond.** 2003. Infection and injury of neurons by West Nile encephalitis virus. J. Virol. **77:**13203-13213.

72. **Prikhod'ko, G. G., E. A. Prikhod'ko, A. G. Pletnev, and J. I. Cohen.** 2002. Langat flavivirus protease NS3 binds caspase-8 and induces apoptosis. J. Virol. **76:**5701-5710.

73. **Couderc, T., F. Guivel-Benhassine, V. Calaora, A. S. Gosselin, and B. Blondel.** 2002. An ex vivo murine model to study poliovirus-induced apoptosis in nerve cells. J. Gen. Virol. **83:**1925-1930.

74. **Girard, S., T. Couderc, J. Destombes, D. Thiesson, F. Delpeyroux, and B. Blondel.** 1999. Poliovirus induces apoptosis in the mouse central nervous system. J. Virol. **73:**6066-6072.

75. **Bauer, J., T. Sminia, F. G. Wouterlood, and C. D. Dijkstra.** 1994. Phagocytic activity of macrophages and microglial cells during the course of acute and chronic relapsing experimental autoimmune encephalomyelitis. J. Neurosci. Res. **38:**365-375.

76. **Flugel, A., M. Bradl, G. W. Kreutzberg, and M. B. Graeber.** 2001. Transformation of donor-derived bone marrow precursors into host microglia during autoimmune CNS inflammation and during the retrograde response to axotomy. J. Neurosci. Res. **66:**74-82.

77. **Flugel, A., G. Hager, A. Horvat, C. Spitzer, G. M. Singer, M. B. Graeber, G. W. Kreutzberg, and F. W. Schwaiger.** 2001. Neuronal MCP-1 expression in response to remote nerve injury. J. Cereb. Blood Flow Metab. **21:**69-76.

78. **Weiss, J. M., S. A. Downie, W. D. Lyman, and J. W. Berman.** 1998. Astrocyte-derived monocyte-chemoattractant protein-1 directs the transmigration of leukocytes across a model of the human blood-brain barrier. J. Immunol. **161:**6896-6903.

79. **Aloisi, F., R. De Simone, S. Columba-Cabezas, G. Penna, and L. Adorini.** 2000. Functional maturation of adult mouse resting microglia into an APC is promoted by granulocyte-macrophage colony-stimulating factor and interaction with Th1 cells. J. Immunol. **164:**1705-1712.

80. **Matyszak, M. K.** 1998. Inflammation in the CNS: balance between immunological privilege and immune responses. Prog. Neurobiol. **56:**19-35.

81. **Aloisi, F.** 2001. Immune function of microglia. Glia **36:**165-179.

82. **Stoll, G., S. Jander, and M. Schroeter.** 2000. Cytokines in CNS disorders: neurotoxicity versus neuroprotection. J. Neural Transm. Suppl. **59:**81-89.

83. **Komatsu, T., N. Srivastava, M. Revzin, D. D. Ireland, D. Chesler, and C. Shoshkes Reiss.** 1999. Mechanisms of cytokine-mediated inhibition of viral replication. Virology **259:**334-341.

84. **Delhaye, S., S. Paul, G. Blakqori, M. Minet, F. Weber, P. Staeheli, and T. Michiels.** 2006. Neurons produce type I interferon during viral encephalitis. Proc. Natl. Acad. Sci. U. S. A. **103:**7835-7840.

85. **Prehaud, C., F. Megret, M. Lafage, and M. Lafon.** 2005. Virus infection switches TLR-3-positive human neurons to become strong producers of beta interferon. J. Virol. **79:**12893-12904.

86. **Pan, W., W. A. Banks, and A. J. Kastin.** 1997. Permeability of the blood-brain and blood-spinal cord barriers to interferons. J. Neuroimmunol. **76:**105-111.

87. **Chabot, S. and V. W. Yong.** 2000. Interferon beta-1b increases interleukin-10 in a model of T cell-microglia interaction: relevance to MS. Neurology **55:**1497-1505.

88. **Wang, J., R. D. Schreiber, and I. L. Campbell.** 2002. STAT1 deficiency unexpectedly and markedly exacerbates the pathophysiological actions of IFN-alpha in the central nervous system. Proc. Natl. Acad. Sci. U. S. A. **99:**16209-16214.

89. **Chesler, D. A. and C. S. Reiss.** 2002. The role of IFN-gamma in immune responses to viral infections of the central nervous system. Cytokine Growth Factor Rev. **13:**441-454.

90. **Boehm, U., T. Klamp, M. Groot, and J. C. Howard.** 1997. Cellular responses to interferon-gamma. Annu. Rev. Immunol. **15:**749-795.

91. **Benveniste, E. N.** 1992. Inflammatory cytokines within the central nervous system: sources, function, and mechanism of action. Am. J. Physiol. **263:**C1-16.

92. **Lee, S. J., J. Y. Park, J. Hou, and E. N. Benveniste.** 1999. Transcriptional regulation of the intercellular adhesion molecule-1 gene by proinflammatory cytokines in human astrocytes. Glia **25:**21-32.

93. **Benveniste, E. N.** 1998. Cytokine actions in the central nervous system. Cytokine Growth Factor Rev. **9:**259-275.

94. **Sharif, S. F., R. J. Hariri, V. A. Chang, P. S. Barie, R. S. Wang, and J. B. Ghajar.** 1993. Human astrocyte production of tumour necrosis factor-alpha, interleukin-1 beta, and interleukin-6 following exposure to lipopolysaccharide endotoxin. Neurol. Res. **15:**109-112.

95. **Unsicker, K. and K. Krieglstein.** 2002. TGF-betas and their roles in the regulation of neuron survival. Adv. Exp. Med. Biol. **513:**353-374.

96. **Mahad, D. J. and R. M. Ransohoff.** 2003. The role of MCP-1 (CCL2) and CCR2 in multiple sclerosis and experimental autoimmune encephalomyelitis (EAE). Semin. Immunol. **15:**23-32.

97. **Bi, Z., M. Barna, T. Komatsu, and C. S. Reiss.** 1995. Vesicular stomatitis virus infection of the central nervous system activates both innate and acquired immunity. J. Virol. **69:**6466-6472.

98. **Lam, V., K. A. Duca, and J. Yin.** 2005. Arrested spread of vesicular stomatitis virus infections in vitro depends on interferon-mediated antiviral activity. Biotechnol. Bioeng. **90:**793-804.

99. **Trottier, M. D.,Jr, B. M. Palian, and C. Shoshkes Reiss.** 2005. VSV replication in neurons is inhibited by type I IFN at multiple stages of infection. Virology **333:**215-225.

100. **Ireland, D. D., B. M. Palian, and C. S. Reiss.** 2005. Interleukin (IL)-12 receptor beta1 or IL-12 receptor beta 2 deficiency in mice indicates that IL-12 and IL-23 are not essential for host recovery from viral encephalitis. Viral Immunol. **18:**397-402.

101. **Chesler, D. A., J. A. McCutcheon, and C. S. Reiss.** 2004. Posttranscriptional regulation of neuronal nitric oxide synthase expression by IFN-gamma. J. Interferon Cytokine Res. **24:**141-149.

102. **Chesler, D. A. and C. S. Reiss.** 2002. IL-12, while beneficial, is not essential for the host response to VSV encephalitis. J. Neuroimmunol. **131:**92-97.

103. **Komatsu, T. and C. S. Reiss.** 1997. IFN-gamma is not required in the IL-12 response to vesicular stomatitis virus infection of the olfactory bulb. J. Immunol. **159:**3444-3452.

104. **Sekellick, M. J. and P. I. Marcus.** 1979. Persistent infection. II. Interferon-inducing temperature-sensitive mutants as mediators of cell sparing: possible role in persistent infection by vesicular stomatitis virus. Virology **95:**36-47.

105. **Kennedy, P. G.** 1982. Neural cell markers and their applications to neurology. J. Neuroimmunol. **2:**35-53.

106. **Hewicker-Trautwein, M., G. Schultheis, and G. Trautwein.** 1996. Demonstration of amoeboid and ramified microglial cells in pre- and postnatal bovine brains by lectin histochemistry. Ann. Anat. **178:**25-31.

107. **Pelleitier, M. and S. Montplaisir.** 1975. The nude mouse: a model of deficient T-cell function. Methods Achiev. Exp. Pathol. **7:**149-166.

108. **Steele, T. A. and C. C. Hauser.** 2005. The role of interferon-alpha in a successful murine tumor therapy. Exp. Biol. Med. (Maywood) **230:**487-493.

109. **Sherry, B., J. Torres, and M. A. Blum.** 1998. Reovirus induction of and sensitivity to beta interferon in cardiac myocyte cultures correlate with induction of myocarditis and are determined by viral core proteins. J. Virol. **72:**1314-1323.

110. **van den Pol, A. N., K. P. Dalton, and J. K. Rose.** 2002. Relative neurotropism of a recombinant rhabdovirus expressing a green fluorescent envelope glycoprotein. J. Virol. **76:**1309-1327.

111. **Baloul, L. and M. Lafon.** 2003. Apoptosis and rabies virus neuroinvasion. Biochimie **85:**777-788.

112. **Fehr, T., M. F. Bachmann, H. Bluethmann, H. Kikutani, H. Hengartner, and R. M. Zinkernagel.** 1996. T-independent activation of B cells by vesicular stomatitis virus: no evidence for the need of a second signal. Cell. Immunol. **168:**184-192.

113. **Huneycutt, B. S., Z. Bi, C. J. Aoki, and C. S. Reiss.** 1993. Central neuropathogenesis of vesicular stomatitis virus infection of immunodeficient mice. J. Virol. **67:**6698-6706.

114. **Maloy, K. J., B. Odermatt, H. Hengartner, and R. M. Zinkernagel.** 1998. Interferon gamma-producing gammadelta T cell-dependent antibody isotype switching in the absence of germinal center formation during virus infection. Proc. Natl. Acad. Sci. U. S. A. **95:**1160-1165.

115. **Bussfeld, D., M. Nain, P. Hofmann, D. Gemsa, and H. Sprenger.** 2000. Selective induction of the monocyte-attracting chemokines MCP-1 and IP-10 in vesicular stomatitis virus-infected human monocytes. J. Interferon Cytokine Res. **20:**615-621.

Curriculum Vitae

Curriculum Vitae

LUKXMI BALATHASAN
4441 Ashley Ave
Mississauga, ON L5R 2A3
(905) 890-3443
Email: lukxmib@hotmail.com

EDUCATION

M.Sc., Microbiology and Immunology ***Sept. 04 – Present***
University of Ottawa – Ottawa, ON

- Thesis: Characterizing the CNS protection induced by systemic administration of the "interferon inducing" mutant virus ΔM51-VSV.
- Supervisors: David F. Stojdl; Robert G. Korneluk

B.Sc., Honours Biochemistry Co-op Program ***Class of 2004***
McMaster University - Hamilton, ON

- Undergraduate Honours thesis: Interactions between mammalian transcription factor E2F1 and HCF-1
- Deans Honours List 2002-2004

Ontario Secondary School Diploma ***Class of 1999***
The Woodlands School - Mississauga, ON

- Graduated as an Ontario Scholar
- Honour Roll from 1995 to1999

EMPLOYMENT

Teaching Assistant ***Sept 05 – Dec. 05***
3rd Year Biochemistry Undergraduate Laboratory
University of Ottawa – Ottawa, ON

Research Assistant – Summer Student ***May 04 – Aug. 04***
Mammalian Genetics
Biotechnology Research Institute (NRC) – Montreal, QC

- Worked with optimizing small interfering RNA cell culture assays

Research Assistant – Co-op ***Sept. 03 – Dec. 03***
Cancer Endocrinology
BC Cancer Centre – Vancouver, BC

- Characterized SHIP knockout mice to determine SHIP's role in dendritic cell development using FACS analysis

Research Assistant – Co-op ***May 03 – Sept. 03***
Cancer Biology Department
Shire Biochem Inc. – Laval, QC

- Conducted inhibition assays as well as competition assays for specific tubulin inhibitors

Research Assistant – Co-op ***Jan. 02 – Sept. 02***
Biological Sciences Department
Boehringer Ingelheim (Canada) Ltd. - Laval, QC

- Evaluated inhibitors of polymerase activity of the Hepatitis C virus NS5B protein using scintillation proximity assay

CONFERENCES AND POSTER PRESENTATION

The 2nd International Meeting on Oncolytic Viruses asCancer therapeutics (2005)
Rimrock Hotel – Banff, AB
"Intervenous priming with VSV confers protection to subsequent intracranial VSV Infection in mice" L. Balathasan and David F. Stojdl